# Wnt/β-catenin signaling induces MLL to create epigenetic changes in salivary gland tumors

**Peter Wend[1,7], Liang Fang[1], Qionghua Zhu[1], Jörg H. Schipper[2], Christoph Loddenkemper[3], Frauke Kosel[1], Volker Brinkmann[4], Klaus Eckert[1], Simone Hindersin[2], Jane D. Holland[1], Stephan Lehr[5], Michael Kahn[6], Ulrike Ziebold[1,*], Walter Birchmeier[1,*]**

[1]Max-Delbrueck Center for Molecular Medicine, Robert-Rössle-Str. 10, 13125 Berlin, Germany

[2]Department of Otorhinolaryngology, University Hospital Düsseldorf, Moorenstr. 5, 40225 Düsseldorf, Germany

[3]Institute of Pathology, Charité-UKBF, Hindenburgdamm 30, 12200 Berlin, Germany

[4]Max Planck Institute for Infection Biology, Schumannstr. 20, 10117 Berlin, Germany

[5]Baxter Innovations GmbH, Wagramer Str. 17-19, 1220 Vienna, Austria

[6]Eli and Edythe Broad Center for Regenerative Medicine and Stem Cell Research, University of Southern California, Los Angeles, CA 90033, USA

[7]Present address: David Geffen School of Medicine and Jonsson Comprehensive Cancer Center, University of California at Los Angeles, CA 90095, USA

*These senior authors contributed equally to this work.

Contact: wbirch@mdc-berlin.de, phone: +49-30-9406-3800, fax: +49-30-9406-2656

Running title: β-catenin and MLL drive salivary gland tumors

Characters (including spaces): 52,604

**Abstract**

We show that activation of Wnt/β-catenin and attenuation of Bmp signals, by combined gain- and loss-of-function mutations of β-catenin and Bmpr1a, respectively, results in rapidly growing, aggressive squamous cell carcinomas (SCC) in the salivary glands of mice. Tumors contain transplantable and hyper-proliferative tumor propagating cells, which can be enriched by FACS. Single mutations stimulate stem cells, but tumors are not formed. We show that β-catenin, CBP and Mll promote self-renewal and H3K4 tri-methylation in tumor propagating cells. Blocking β-catenin-CBP interaction with the small molecule ICG-001 and siRNAs against β-catenin, CBP or Mll abrogate hyper-proliferation and H3K4 tri-methylation, and induce differentiation of cultured tumor propagating cells into acini-like structures. ICG-001 decreases H3K4me3 at promoters of stem cell-associated genes in vitro and reduces tumor growth in vivo. Remarkably, high Wnt/β-catenin and low Bmp signaling also characterize human salivary gland SCC and head and neck SCC in general. Our work defines mechanisms by which β-catenin signals remodel chromatin and control induction and maintenance of tumor propagating cells. Further, it supports new strategies for the therapy of solid tumors.

## Introduction

Tumor propagating cells or cancer stem cells exhibit stem cell- or progenitor-like properties, i.e. they are able to either self-renew or to differentiate into multiple cell types (Barker et al, 2009; Ben-Porath et al, 2008; Sneddon & Werb, 2007). Understanding molecular mechanisms that regulate tumor propagating cells may help to develop rational therapies. Canonical Wnt signaling maintains many embryonic and adult stem cell types; this signaling system also contributes to the generation of tumor propagating cells (Clevers, 2006; Grigoryan et al, 2008; Malanchi et al, 2008; Wend et al, 2010). Conversely, Bmp signaling inhibits the tumorigenic potential of cancer stem cells of the brain (Piccirillo et al, 2006).

Wnt/β-catenin signals control transcription and gene expression through Wnt response elements (WRE) that are recognized by the β-catenin-LEF/TCF complex, and modulate chromatin structure (Behrens et al, 1996; Molenaar et al, 1996; Mosimann et al, 2009). Hallmarks of chromatin states are modifications on the tails of core histones: tri-methylation of lysines 4, 9 and 27 of histone H3 (H3K4me3, H3K9me3 and H3K27me3) are associated with active chromatin, heterochromatin, and repressed chromatin, respectively (Albert & Peters, 2009; Goldberg et al, 2007). Various chromatin modifiers are recruited to the C-terminus of β-catenin (Mosimann et al, 2009). In *Drosophila*, β-catenin recruits CBP; the histone acetyltransferase (HAT) activity of CBP acetylates chromatin over wide regions surrounding particular WRE (Parker et al, 2008). β-Catenin also interacts with histone methyltransferase MLL that promotes H3K4 tri-methylation (Sierra et al, 2006).

The developing salivary glands of human and mice are complex secretory organs, which in mice begin to develop from a simple epithelial bud around embryonic day (E)11.5-12.5 (Tucker, 2007). The mature glands include luminal ductal, acinar and intercalated duct cells that intermingle with stem cells, which express CD24 and CD29 surface markers (Hisatomi et al, 2004; Nanduri et al, 2011). Salivary gland stem cells contribute to maintenance and regeneration of the adult salivary glands in rodents and can amend the function of irradiated salivary glands after stem cell transplantation (Lombaert et al, 2008; Man et al, 2001; Nanduri et al, 2011). Regeneration of mouse salivary glands was recently found to depend on Wnt/β-catenin signals (Hai et al, 2010).

Head and neck carcinomas in humans amount to 6% of all cancers (Stewart & Kleihues, 2003), the majority being squamous cell carcinomas (SCC). SCC may originate from epithelial stem or progenitor cells of the epidermis or the mucous membranes. Subpopulations of cells from human head and neck SCC with tumor propagating cell properties have recently been isolated, based on the markers CD44 and ALDH (Clay et al, 2010; Prince et al, 2007). Salivary gland carcinomas constitute only a fraction of head and neck cancers, and 8% are SCC, which often arise in the glandula parotis (Speight & Barrett, 2002). Salivary gland SCC are aggressive, produce early lymphogenic metastases, and have a poor prognosis (Ying et al, 2006).

This study demonstrates that high-grade salivary gland SCC and head and neck SCC in general rely on high Wnt/β-catenin and low Bmp signaling for proliferation and self-renewal. In SCC, tumor propagating cells depend on the β-catenin-CBP complex but also MLL for the generation of an open chromatin state and the induction of a

stem cell-associated gene signature. Knowing that specific Wnt/β-catenin inhibition can revert the chromatin state and lead to differentiation and tumor remission in vivo provides a step to safely eradicate tumor propagating cells.

**Results**

*Head and neck squamous cell carcinomas in humans and mice display high Wnt/β-catenin and attenuated Bmp signals*

18 human salivary gland SCC and 29 other head and neck cancer of the SCC subtype were examined for Wnt/β-catenin and Bmp signaling activity (Supplementary Table 1). The majority of tumors exhibited nuclear β-catenin, a hallmark of high canonical Wnt signals (Behrens et al, 1996; Grigoryan et al, 2008), and were negative for nuclear p-Smad 1/5/8 (Whitman, 1998), indicating that Bmp signals were low (Fig. 1A). Nuclear β-catenin accumulated at tumor fronts (arrows on the left) (Fodde & Brabletz, 2007), whereas nuclear p-Smad persisted in differentiated central areas (arrow in inset on the right). 75% of grade 3 salivary gland SCC (SG-SCC), the most aggressive cancers, displayed nuclear β-catenin and were negative for p-Smad, whereas only 25% of grade 2 tumors displayed these characteristics (Fig. 1B, upper left; tumor grading criteria were as defined in (Barnes et al, 2005)). Similarly, two thirds of grade 3 head and neck SCC (HN-SCC) showed high nuclear β-catenin and low p-Smad staining (Fig. 1B, upper right). Cells with nuclear β-catenin at the tumor fronts also co-expressed cytokeratin (CK)10, which is a marker for squamous cell carcinoma (Chu & Weiss, 2002) (Supplementary Figure 1A). A subset of nuclear β-catenin-positive cells from human SG-SCC and HN-SCC co-expressed the marker CD24 (Fig. 1A*,C, left; quantifications are shown in B, lower panels, percentages

refer to all tumor cells) (Monroe et al, 2011; Visvader & Lindeman, 2008) and the marker CD44, which is specific for tumor propagating cells in HN-SCC (Fig. 1C, right; quantifications for grade 2 and grade 3 tumors are depicted in yellow letters below insets) (Prince et al, 2007; Visvader & Lindeman, 2008).

To gain mechanistic insights into the relevance of β-catenin and BMP signals in tumor formation of salivary gland SCC, we created a mouse model. Combined β-catenin gain-of-function (β-cat$^{GOF}$) and Bmp receptor 1a loss-of-function (Bmpr1a$^{LOF}$) mutations were introduced by Cre recombinase driven by the Keratin 14 gene, referred to as double mutants (Harada et al, 1999; Huelsken et al, 2001; Mishina et al, 2002) (see breeding scheme in Supplementary Fig. 1F). K14-Cre activity was confirmed by using a LacZ indicator mouse line; recombination occurred in ductal cells of the salivary glands (Supplementary Fig. 1B-E,G). Aggressive tumors appeared rapidly in the salivary glands of the double mutants (Fig. 1D, a schematic view of the normal mouse salivary glands is provided on http://www.informatics.jax.org/cookbook/figures/figure45.shtml). Kaplan-Meier plots show that double mutants succumbed to tumors rapidly, dying between postnatal day (P)75 and P90 (Fig. 1E). After full necroscopy, a pathologist (C.L.) determined that these tumors exclusively arose from the submandibular salivary glands. The tumors were classified as SG-SCC by histopathological criteria, contained keratin pearls and expressed high levels of CK10 (Supplementary Fig. 2A, right, see also inset) (Barnes et al, 2005; Chu & Weiss, 2002). Moreover, consistent with the human tumors, mouse SG-SCC also showed high Wnt/β-catenin and low Bmp signals, as determined by staining for β-catenin, the Wnt target gene Axin2 and pSmad1/5/8 (Supplementary Fig. 2B). Neither single β-cat$^{GOF}$ nor Bmpr1a$^{LOF}$ mutant mice did develop tumors

(Fig. 1E, Supplementary Fig. 2A, middle panels). Gene expression profiling and gene set enrichment analysis at P1 and P90 revealed that in double mutant salivary glands, genes associated with proliferation as *c-myc* and differentiation/apoptosis as *Loricrin* or *Fas* were up-regulated and down-regulated, respectively, when compared to β-cat$^{GOF}$ tissues (Supplementary Fig. 2C, Supplementary Tables 2 and 3, see also below). Other K14-expressing tissues of double mutants did not develop tumors; while epithelia of the esophagus and forestomach showed no significant histological changes, we observed excessive supernumerary hair follicles in the skin, when compared to wildtype mice (Supplementary Fig. 2D). Taken together, the fast accumulation of salivary gland SCC in the double mutant mice was the net result of strong proliferation and reduced differentiation and apoptosis.

*Wnt/β-catenin and Bmp signals control tumor propagating cells in salivary gland SCC*

In order to characterize cells that are specific and essential for tumor formation in double mutant salivary glands, we isolated CD24$^{+}$CD29$^{+}$ cells by fluorescence activated cell sorting (FACS) from glands of the different genotypes; these surface markers have been previously used to enrich for stem cells of salivary glands (Hisatomi et al, 2004; Nanduri et al, 2011; Visvader & Lindeman, 2008). The proportion of CD24$^{+}$CD29$^{+}$ cells increased 3-fold and 10-fold in single and double mutants, respectively, compared to controls (Fig. 2A, Supplementary Figure 3A-C). Enrichment of CD24$^{+}$ cells could be confirmed by immunofluorescence analysis (Fig. 2B). Isolated CD24$^{+}$CD29$^{+}$ cells were collected by cytospin and their proliferation was assessed using Ki67 antibody staining (Fig. 2C). CD24$^{+}$CD29$^{+}$ cells from double mutant salivary glands were hyper-proliferative: over 80% were Ki67$^{+}$ (Fig. 2D),

compared to 13% non-sorted cells (Fig. 2E). High proliferation was confirmed by FACS for Ki67, which showed that over 90% of $CD24^{+}CD29^{+}$ cells were highly proliferating (P1 cells in Supplementary Fig. 4A,B). Another strongly proliferative $CD24^{-}$ subpopulation (up to 40% $Ki67^{+}$) was identified, but these were not epithelial cells and instead expressed stromal markers (P4 cells, Supplementary Fig. 4A,B, and data not shown). The salivary gland tumors stained weakly for Sca-1 or c-kit (not shown) (Hisatomi et al, 2004), and the $CD24^{+}CD29^{+}$ subpopulation co-expressed the marker CD44 only at low levels (Supplementary Figure 3D,E). To examine the tumor-propagating potential, $CD24^{+}CD29^{+}$ cells of double mutants and various control cell populations were injected into the back skin of NOD/SCID mice (Fig. 2F) (Visvader & Lindeman, 2008). As few as 500 $CD24^{+}CD29^{+}$ cells from double mutant glands produced fast-growing tumors, while cells that expressed only high CD24 or CD29 did not produce fast-growing tumors (Fig. 2F,G, Supplementary Figure 4C). Unsorted cells from double mutant glands were only moderately tumorigenic, at $10^{5}$ but not $10^{4}$ injected cells (Fig. 2F). Tumors arising from transplanted cells co-expressed the SCC markers CK10 and CK14, and contained differentiated and undifferentiated areas (Supplementary Figure 4D,E). Transplanted tumors maintained stable subpopulations of $CD24^{+}CD29^{+}$ cells in serial transplantations that retained high tumor propagating potential (Supplementary Figure 4F,G). From these results, we conclude that $CD24^{+}CD29^{+}$ cells from double mutant salivary gland SCC are highly enriched for tumor propagating cells.

*Salivary gland tumor propagating cells are characterized by a stem cell-associated gene signature and specific chromatin marks*

To elucidate mechanisms that potentiate the self-renewal of tumor propagating cells, we examined stem cell-associated genes that were co-expressed with activated Wnt/β-catenin (Ben-Porath et al, 2008; Wend et al, 2010). Remarkably, tumor propagating cells of double mutants expressed embryonic-type $SSEA1^+$ (Fig. 3A) (Read et al, ,2009). The SSEA1 expression specifically characterized cells with high Wnt/β-catenin signals since >90% of the $CD24^+CD29^+SSEA1^+$ triple-sorted cells exhibited nuclear β-catenin, which was not found in other subpopulations (Fig. 3B, and data not shown). $CD24^+CD29^+$ cells were also characterized by low pSmad1/5/8 intensity, as compared to unsorted tumor cells (Supplementary Figure 5A,B). Gene expression profiling of $CD24^+CD29^+$ cells revealed that a number of genes associated with the pluripotent state were highly expressed (Supplementary Fig. 5C,D, Supplementary Table 4). Among those were Nr5a2, which can replace Oct4 in reprogramming of iPS cells (Heng et al, 2010), the ES-cell associated Snf2-like helicase Hells (Xi et al, 2009), the stem cell marker Dppa5 (Ware et al, 2009) and the stem cell-associated chromatin modifiers Ash2, Mll (Dou et al, 2005) and Rnf2 (de Napoles et al, 2004). A GSEA analysis confirmed that genes important for pluripotent stages in organism development were enriched in double-mutant tumor propagating cells (Supplementary Table 3). Treatment for 24 hours with ICG-001, an inhibitor of canonical Wnt signaling that blocks β-catenin-CBP interaction (Emami et al, 2004), and siRNA-mediated down-regulation of β-catenin significantly suppressed these genes (Fig. 3C).

Previous research has shown that the maintenance of pluripotency is linked to the epigenetic state of cells (Albert & Peters, 2009; Surani et al, 2007; Wend et al, 2010). Remarkably, sorted $CD24^+CD29^+$ tumor propagating cells from double mutant salivary glands showed a marked increase of H3K4me3, as assessed by

immunohistological analysis of cytospins, which was low in $CD24^+CD29^+$ cells from wildtype and single mutant tissue (Fig. 3D, quantified in E). H3K4me3 generally characterizes transcriptionally active promoters, but high enrichment is also indicative of stem cell promoters (Albert & Peters, 2009; Gaspar-Maia et al, 2011; Wend et al, 2010). In contrast, $CD24^+CD29^+$ cells from double mutants showed a low level of H3K27me3, compared to $CD24^+CD29^+$ cells from wildtype and single mutants (Fig. 3D,E), whereas the H3K9me3 levels were similar in all genotypes (Fig. 3E, Supplementary Fig. 5E). These epigenetic marks in $CD24^+CD29^+$ cells from double mutants require high Wnt/β-catenin: after 24 hrs of ICG-001 treatment, the numbers of H3K4me3-positive cells declined by more than 60% (Fig. 3F). Similar changes in H3K4me3 and H3K27me3, but not H3K9me3, were also observed by Western blot analysis of extracts from salivary glands of control and mutant mice, and in tumors that arose from transplanted cells (Supplementary Fig. 5F). Thus, the specific alterations in chromatin-associated histone marks suggest that the overall epigenetic makeup has changed in the tumor propagating cells of the salivary glands. Further, tumor propagating cells are distinguished by the expression of a gene signature that is associated with pluripotency.

To examine whether activated canonical Wnt signaling affects human salivary SCC in a similar manner, we assessed H3K4me3 and nuclear β-catenin levels in human tumors, which could be detected preferentially at the invasive tumor fronts (Supplementary Fig. 5G). We also investigated several tumor cell lines of human head and neck SCC. Endogenous Wnt signaling activity in these cells was variable, as assessed by the expression of the Wnt/β-catenin target gene Axin2 (Grigoryan et al, 2008; Lustig et al, 2002). Typically, cell lines with high and low Wnt activity (e.g.,

HN-SCCUM-03T and HN-SCCUM-02T) displayed opposite, i.e., low and high pSmad1/5/8 levels, respectively (Supplementary Fig. 6A). HNSCCUM-03T cells with high Wnt activity were treated with ICG-001, which down-regulated the expression of stem cell-associated signature genes *NR5A2, ABCB1B, LRRC34, DNAJC6* and of the genes encoding chromatin modifiers *HELLS, MLL and ASH2* (Supplementary Fig. 6B). Conversely, CHIR 99021, a Wnt activator (Ring et al, 2003), up-regulated the expression of these genes in HNSCCUM-02T cells that display low endogenous Wnt signals (Supplementary Fig. 6B). Interestingly, a large number of HNSCCUM-03T cells with high Wnt co-expressed CD44, a stem cell marker of human SCC tumors, as well as CD24, whereas HNSCCUM-02T cells with low Wnt only co-expressed CD24 and CD44 after Wnt activation, i.e., 48 hrs exposure to CHIR 99021 (Supplementary Fig. 6A,C) (Monroe et al, 2011). Collectively, mouse salivary gland and human head and neck SCC cells depend on high canonical Wnt signals to create a permissive epigenetic environment that allows the expression of a stem cell-associated gene signature. This includes the human-specific stem cell marker CD44 (Gires, 2011).

*ICG-001 treatment leads to tumor remission and reprograms salispheres to form differentiated acini-like structures*

$CD24^{+}CD29^{+}$ tumor propagating cells from the tumors of double mutant salivary glands were cultured. Remarkably, the canonical Wnt inhibitor ICG-001 strongly blocked proliferation of the $CD24^{+}CD29^{+}$ cells (Fig. 4A). We then performed a therapy experiment in NOD/SCID mice, which were transplanted with $CD24^{+}CD29^{+}$ tumor propagating cells that were forming tumors (see Fig. 2F): ICG-001 significantly reduced the size of the growing tumors (Fig. 4B).

Stem cells from organs and tumors can often be expanded as non-adherent, sphere-like aggregates, which reflects their self-renewal capacity (Lombaert et al, 2008; Monroe et al, 2011; Visvader & Lindeman, 2008). Whereas $CD24^{+}CD29^{+}$ salivary gland cells from wildtype or single mutant mice did not grow as spheres, $CD24^{+}CD29^{+}$ cells from double mutants could be propagated as salispheres in the presence of hepatocyte growth factor, HGF (Fig. 4C, left panel) (Brinkmann et al, 1995). In such salispheres, cells formed loose, net-like aggregates, i.e., displayed undifferentiated structures (Fig. 4D, left, see also below). Remarkably, in the presence of ICG-001, salispheres formed instead glandular structures that resemble salivary gland acini (Fig. 4C, second panel, Fig. 4D, right, the quantification of differentiation is in E). Light and electron microscopy demonstrated the formation of lumen, secretory granules and tight junctions in the acini-like structures but not in the undifferentiated salispheres (Supplementary Fig. 6E,F, and data not shown). ICG-001 treatment also up-regulated the expression of the gene encoding Amylase 1, an enzyme of differentiated salivary glands (Supplementary Fig. 6G). Thus, $CD24^{+}CD29^{+}$ tumor propagating cells from salivary gland tumors of double mutant mice exhibit unrestricted self-renewal in salisphere culture that depends on canonical Wnt signaling. We next analyzed the effect of the HDAC inhibitor Valproic acid (VPA) and the DNA methylation inhibitor 5-azacytidine (Aza) (Ware et al, 2009) on ICG-001-elicited responses in salispheres. Inhibition of proliferation by ICG-001 was not seen in the presence of VPA or Aza, but differentiation was blocked (Fig. 4C, right panels, quantitation in Fig. 4E, Supplementary Fig. 6H). Furthermore, ICG-001 treatment of human HNSCCUM-03T cells with high endogenous Wnt strongly reduced their ability to form spheres (Supplementary Fig. 6D). ICG-001 has been shown to inhibit the growth of Wnt/β-catenin-dependent human tumor cells (Emami

et al, 2004; Wend et al, 2013). Conversely, CHIR 99021 enhanced the capacity of HNSCCUM-02T cells with low endogenous Wnt to form spheres (Supplementary Fig. 6D). Thus, unrestricted self-renewal of tumor propagating cells of mouse salivary glands and of human SCC tumor cell lines in sphere culture depends on continuous Wnt signaling and on the maintenance of their specific epigenetic state.

*Wnt/β-catenin signals exploit MLL-dependent H3K4 histone methylation activity to establish and maintain salivary gland tumor propagating cells*

To learn about the significance of Wnt/β-catenin-dependent epigenetic regulation, we examined whether blocking β-catenin-CBP by ICG-001 leads to changes of histone modifications at gene promoters of stem cell-associated genes. Chromatin immunoprecipitation (ChIP) using anti-H3K4me3 antibodies was performed with $CD24^{+}CD29^{+}$ cells from mouse salivary gland tumors and with human HNSCCUM-03T tumor cells that display high Wnt activity. We detected high enrichments of H3K4me3 at sequences, which are in close proximity to the promoters of *Mll, Hells, Ash2* and *c-myc* genes, but not at promoter-far sequences in the mouse and human cells (Fig. 5A,B). ICG-001 significantly decreased the enrichment of H3K4me3 at promoter-proximal sequences. We also examined the sequential order of changes in H3K4me3 and in gene expression of mouse $CD24^{+}CD29^{+}$ tumor propagating cells that depend on ICG-001. H3K4me3 down-regulation could be detected 12h after ICG-001 treatment (Fig. 5C). In contrast, expression changes of genes of the stem cell-associated gene signature or of the differentiation marker Amylase occur later, 24h after ICG-001 treatment (Figure 5D). These data show that the β-catenin-CBP-interfering substance ICG-001 elicits changes in H3K4me3 at target promoters, and that the epigenetic changes precede transcriptional changes.

We next addressed the question of how abrogation of Wnt/β-catenin signals might produce the shift of epigenetic marks. Remarkably, treating $CD24^{+}CD29^{+}$ cells from double mutant tumors with ICG-001 resulted in a significant translocation of β-catenin out of the nucleus and in cytoplasmic accumulation (Fig. 6A, protein quantifications are shown above the blots). Concomitantly, Mll, a known binding partner of nuclear β-catenin with histone methyltransferase towards H3K4 (Sierra et al, 2006), disappeared from the nuclear fraction (Fig. 6B). Two protein products of the stem cell signature, Hells and Nr5a2, were also downregulated (Supplementary Fig. 7A). Conversely, activating Wnt/β-catenin with CHIR 99021 lead to an increase of nuclear β-catenin and nuclear Mll (Figure 6A,B). The increase of β-catenin might be due to the product of the remaining wildtype allele in the double mutant mice (see Supplementary Figure 1F,G). Nuclear exclusion of β-catenin by inhibiting with ICG-001 could also be detected in the human high Wnt HNSCCUM-03T cells (Supplementary Fig. 7B). Collectively, these data show that nuclear Mll and the expression of the stem cell-associated gene signature are dependent on the presence of high Wnt/β-catenin signals.

We next examined the potential role of Mll in the $CD24^{+}CD29^{+}$ cells of salivary gland tumors by performing siRNA-mediated down-regulation of β-catenin, CBP and Mll. These treatments resulted in a strong reduction of the numbers of $H3K4me3^{+}$ and $Ki67^{+}$ cells (Fig. 6C, Supplementary Fig. 7C). Down-regulation of another histone methyltransferase, Ash1, had no effect on H3K4me3 and Ki67 levels. ICG-treatment and siRNA against Mll or β-catenin also profoundly reduced the proliferation of tumor propagating cells, while siRNA against Dppa5 had no effect (Fig. 6D) (Kim et

al, 2005). Mll is strongly expressed in the tumor propagating cells of salivary glands; nuclear Mll was found to be associated with the rare $CD24^+$ cells (Supplementary Fig. 7E, arrows). Remarkably, knockdown of β-catenin and Mll by siRNA treatment resulted in acini formation in sphere culture, i.e., forced a large fraction of $CD24^+CD29^+$ cells into differentiation, whereas Ash1 siRNA had no effect (Fig. 6E). siRNA treatments did not affect all cells, in contrast to ICG-001, possibly due to incomplete transfection efficacy (Fig. 6C-E, Supplementary Fig. 7D). In order to show that β-catenin and MLL are relevant in human salivary gland tumors, we evaluated the association of the gene products in the collection of 13 human SG-SCC specimens: nuclear β-catenin was associated with nuclear MLL, and both products significantly correlated with high grade tumors (Fig 6F,G, Supplementary Fig. 7F,G; n=13). This may also lead to an up-regulation of other stem cell-associated genes, as exemplified for NR5A2 (Supplementary Fig. 7H). These data show that the association of nuclear β-catenin with nuclear MLL is of clinical relevance in human SG-SCC. Collectively, our data suggest that in both, murine and human tumors, the β-catenin/CBP/MLL axis drives self-renewal and fends off differentiation of tumor propagating cells via epigenetic mechanisms.

**Discussion**

Here we report that mice with increased Wnt/β-catenin and attenuated Bmp signaling in Keratin 14-expressing tissues rapidly develop salivary gland SCC, from which we can enrich tumor propagating cells by FACS. The importance of canonical Wnt signaling in tumor propagating cells is known (Barker et al, 2009; Malanchi et al, 2008; Wend et al, 2010). We provide evidence that β-catenin activation leads to an

induction and stabilization of MLL, and that β-catenin, CBP and MLL are required to trigger H3K4 trimethylation at promoters of self-renewal genes in tumor propagating cells (Summary scheme in Fig. 7A).

Tumor propagating cells from salivary gland SCC of double mutants were enriched by FACS using high expression of the CD24 and CD29 surface antigens as markers, and 500 of sorted cells produced tumors upon serial transplantation in immune-compromised mice. Such serial transplantation experiments with low numbers of injected cells define tumor propagating cells, also called cancer stem cells (Gires, 2011; Nanduri et al, 2011; Prince et al, 2007; Visvader & Lindeman, 2012). The tumor propagating cells of salivary gland SCC retained the capacity to differentiate following transplantation, akin to cancer stem cells (Visvader & Lindeman, 2008). In our hands, other markers and marker combinations failed to isolate cells that could be used to generate tumors at this low number of injected cells. We also compared the tumor propagating cells from the double mutants with $CD24^{+}CD29^{+}$ cells of wildtype and single mutant salivary glands; this revealed that proliferation was significantly higher in double mutant cells than in cells obtained from single mutants or control mice. Remarkably, 13% of the unsorted cells of tumors but 80-90% of the $CD24^{+}CD29^{+}$ cells were Ki67-positive in the double mutant tissue. In conclusion, constitutive activation of Wnt/β-catenin signals strongly increase self-renewal of tumor propagating cells, while repression of BMP signals inhibits apoptosis, which in combination leads to permanently hyper-proliferating salivary gland tumor cells.

β-Catenin and CBP can tether MLL to promoters, where histone methyltransferase activity toward H3K4 is promoted (Arai et al, 2010; Dou et al, 2006; Emami et al,

2004; Mosimann et al, 2009; Taki et al, 1997). The trithorax-related MLL has been linked with gene activation and confers stem cell-like properties to hematopoietic cancer cells (Krivtsov & Armstrong, 2007; Schuettengruber et al, 2011; Visvader & Lindeman, 2008). Similarly, specific mutations of β-catenin bestow self-renewal properties to chronic myeloid leukemia cells (Jamieson et al, 2004). MLL can exist in high molecular weight complexes with other methyltransferase components such as ASH2, which can enhance the activity of the MLL core complex (Southall et al, 2009). We found that high levels of nuclear β-catenin increase not only MLL, but also ASH2 levels in tumor propagating cells. Likewise, HELLS is up-regulated in a Wnt/β-catenin-dependent manner in $CD24^{+}CD29^{+}$ tumor propagating cells. It is noteworthy that MLL expression depends on HELLS in prostate cancers (von Eyss et al, 2011). This suggests that the expression of a network of chromatin-associated proteins might be amplified by a feed-forward mechanism, ensuring that β-catenin-CBP-MLL has ample trithorax-related activity to maintain high H3K4me3 levels at target promoters. Further, differentiation of $CD24^{+}CD29^{+}$ tumor propagating cells is restored by down-regulation of canonical Wnt signaling, i.e., by ICG-001 or siRNA-mediated down-regulation of β-catenin, CBP or MLL (scheme in Fig. 7B). The temporal coordination of epigenetic reshaping and target gene expression in the differentiation of salivary gland tumor propagating cells supports the hypothesis that the tumor cells depend on Wnt/β-catenin-MLL-mediated epigenetic changes to suppress salivary gland differentiation. Finally, ICG-001-mediated differentiation of $CD24^{+}CD29^{+}$ tumor propagating cells cannot occur in the presence of the HDAC-inhibitor valproic acid or the DNA methylation inhibitor 5-azacytidine, indicating that chromatin remodeling is also critical for differentiation (scheme in Fig. 7B).

The strong effects of ICG-001 on tumor propagating cells might support new strategies for the development of rational therapies of solid tumors. Wnt/β–catenin signaling inhibitors eliminated stem cells in non-solid tumors, and ICG-001 eradicated drug-resistant leukemic cancer stem cells *in vitro* and *in vivo* (Takahashi-Yanaga & Kahn, 2010). We show here that ICG-001 enforces differentiation of salivary gland tumor propagating cells in the mouse model, providing an efficient approach to target salivary gland cancer and potentially head and neck cancer in general. High Wnt/β-catenin and low Bmp signaling also correlate with the aggressiveness of human head and neck cancer and with the potential of the human tumor cells to self-renew. Moreover, the data with human cancers illustrate that nuclear β-catenin is significantly correlated with nuclear MLL and high tumor grade. It will be important to test whether human head and neck cancers also respond to Wnt/β-catenin inhibitors.

## Materials and methods

*Mouse strains*

*K14Cre*(Δneo), *β-catenin*$^{floxEx3}$, *Bmpr1a*$^{flox}$ alleles and Cre-inducible lacZ reporter mice have been described, and mutant mice were analyzed for genotype and recombination by PCR (Harada et al, 1999; Huelsken et al, 2001; Mishina et al, 2002; Thorey et al, 1998). The conditional gain-of-function mutation of β-catenin was produced by crossing homozygous mice carrying the β-*catenin*$^{lox(ex3)}$ allele to *K14-cre* mice. The loss-of function mutation of *Bmpr1a* was produced by crossing homozygous mice carrying *Bmpr1a*$^{flox}$ alleles to *K14-cre* mice that were homozygous for the *BmpRIA*$^{flox}$ allele. To obtain the compound mutants, homozygous mice

carrying the β-*catenin*$^{lox(ex3)}$ gain-of-function and the *BmpRIA*$^{flox}$ loss-of-function allele were crossed with *K14-Cre* mice that were homozygous for the *Bmpr1a*$^{flox}$ allele (a breeding scheme is shown in Supplementary Fig. 1F). Animal experiments were performed according to the EU and national institutional regulations.

*Immunodetection and other stainings*

Immunohistochemistry, immunofluorescence and H&E staining were performed on frozen or formalin-fixed paraffin-embedded tissue sections as described (Huelsken et al, 2001). Human tumor samples were obtained from the Institute of Pathology, Charité-UKBF Berlin, Germany, and from the Department of Otorhinolaryngology, University Hospital Düsseldorf, Düsseldorf, Germany (for patient data see Supplementary Table 1). Immunoblotting of Westerns was performed using standard protocols: cells were lysed in HNTG buffer (20 mM HEPES pH 7.5, 150 mM NaCl, 1% (w/v) Triton X-10, 10% (w/v) glycerol). Histone extraction was performed according to the technical instructions from Abcam. Protein lysates were subjected to SDS-PAGE and transferred to PVDF membranes. Membranes were incubated with specific antibodies, and Western blots were developed using the chemiluminescence method (PerkinElmer). The following primary antibodies were used for immunodetection: mouse-anti β-catenin (from BD Transduction Laboratories), rabbit-anti phospho-Smad1/5/8, rabbit-anti cleaved caspase-3, mouse-anti CD44, rabbit-anti Axin2, rabbit-anti tri-methyl histone H3 (Lys4) (Cell Signaling), mouse-anti CK10 and rabbit-anti CK14 (Covance), Phycoerythrin (PE)-conjugated rat-anti CD24 (BD Pharmingen), biotinylated goat-anti CD29 (R&D Systems), rabbit-anti phospho-histone H3 (Upstate), rabbit-anti tri-methyl histone H3 (Lys9; Abcam), rabbit-anti tri-

methyl histone H3 (Lys27) (Millipore), rabbit-anti MLL1 (Bethyl), rabbit-anti Lamin (Santa Cruz) and mouse-anti α-Tubulin (Sigma).

*Quantitative real-time PCR and microarray profiling*

Isolation of total RNA, cDNA synthesis and qRT PCR were performed using standard protocols: briefly, total RNA of tissue samples was isolated using Trizol (Invitrogen), and 5 μg total RNA was reverse-transcribed using MMLV reverse transcriptase (Promega) according to the instructions by the manufacturers. qRT PCR was performed using the iCycler IQTM 5 multicolor real-time detection system (Bio-Rad) with absolute SYBR green fluorescein (ABgene). PCR was carried out following a standard protocol: primer sequences used for qRT PCR can be found in Supplemental Table 5. Microarray profiling was performed using GeneChip Mouse Genome 430 2.0 arrays (Affymetrix), following the protocol of the manufacturer. Profiling experiments are from salivary gland tissues of three mice in each group for the analysis at P1 and for the analysis of $CD24^{+}CD29^{+}$ stem cells at P90 (each n=3). Processing and statistical analysis of microarray data was performed using Genespring software.

*Bioinformatics and gene set enrichment analysis of gene expression data and mouse survival statistics*

Analysis of Affymetrix array data conformed to MIAME structure (http://www.mged.org). Log of ratio normalized expression data were analyzed using a cross-gene error model and normalized according to the manufacture protocol (GeneSpring software, Agilent). Assessment of differential expression was based on the highest achieved fold change and the lowest achieved p-value (Welch's t-test) and

1-way-ANOVA with p-value cutoff of 0.05. No assumption of equality of variance was made, and Benjamini and Hochberg false discovery rates were used. A cut-off of 1.5-fold or greater expression difference was set to compare samples. Gene set enrichment analysis (GSEA) was performed following the authors guidelines (Subramanian et al, 2005). We made use of gene sets representing biological pathways or gene ontology categories for biological processes, molecular functions, and cellular compartments (http://www. broadinstitute.org/gsea/msigdb/). Each gene set was converted from human to mouse using the orthology mapping from The Jackson Laboratory (http://bioinf.wehi.edu.au/software/MSigDB). Kaplan-Meier survival curves of mice were calculated using SPSS 12.0 software (SPSS, Chicago), and differences in survival were assessed by the log rank test. Survival analysis curves are representative of at least 21 mice for each genotype.

*Cell preparation and FACS analysis*

Salivary glands and primary tumor samples were collected, minced, and incubated for 90 min at 37°C with digestion buffer containing DMEM/F12 1:1 (Invitrogen), 1.67 mg/ml collagenase (Invitrogen) and 1.33 mg/ml hyaluronidase (Sigma). The partly digested tissues were further treated for 60 minutes at 37°C with dispersion buffer containing DMEM/F12 (Invitrogen) and 1.67 mg/ml dispase (Invitrogen). Cell suspensions were passed through a stainless filter (70 μm) and centrifuged at 900g for 5 minutes at 4°C. Pellets were suspended in 10 ml Dulbecco's modified Eagle/F12 1:1 medium and washed three times with PBS containing 10% fetal bovine serum (Invitrogen). After lysis of red blood cells in ice-cold 0.8% NH4Cl (PBS), cells were washed three times with staining buffer (1% FBS/PBS) and incubated for 20 minutes with Fc receptor antibody (anti-mouse CD16/CD32; BD Pharmingen). Cells were

washed three times with staining buffer and incubated with surface antigen antibodies for 45 minutes at 4°C. Primary antibodies were Phycoerythrin (PE)-conjugated rat-anti CD24 (BD Pharmingen), biotinylated goat-anti CD29 (R&D Systems), Allophycocyanin (APC) conjugated CD29 (R&D Systems), mouse-anti CD44 (Cell Signaling), and mouse-anti SSEA-1 antibody (R&D Systems). Samples were washed and incubated for 30 minutes at 4°C with secondary antibody, streptavidin-APC (Invitrogen) or Cy5 (BD Pharmingen). Cells were sorted using FACS Aria (BD Biosciences), and surface antigens of cells were analyzed using a FACS caliber (BD Biosciences). Data were analyzed using CELLQuest (BD Biosciences). Apoptotic cells were excluded by elimination of Dapi-positive cells. Gates were set to exclude 99.9% of cells labelled with isoform-matched control antibodies conjugated with the corresponding fluorochromes. Cytocentrifuge preparations were fixed in 4% formaldehyde and stained.

*Xenograft and regeneration experiments*

$CD24^{+}CD29^{+}$-sorted and unsorted cells were transplanted at different dilutions subcutaneously into the back skin of NOD/SCID mice. Inhibition by ICG-001 in the NOD/SCID mouse xenograft model was investigated (each group n=3) as described (Emami et al, 2004).

*Cell culture*

Mouse cells were cultured in DMEM/F12 medium supplemented with 20% KSR, nonessential minimal amino acids, penicillin/streptomycin, L-glutamine and β-mercaptoethanol (Invitrogen). Human head and neck carcinoma cell lines HNSCCUM-02T and HNSCCUM-03T were cultured as described (Welkoborsky et

al, 2003). Cell proliferation was determined using the WST-1 cell proliferation assay (Roche) according to the instructions of the manufacturers. To test for non-adherent salisphere formation, cells were cultivated in a three-dimensional Matrigel (Invitrogen) layer for 24 hours with culture medium and HGF at a concentration of 100 U/ml. Recombinant HGF was prepared as described (Brinkmann et al, 1995). After 24 hours, cells were treated with ICG-001 (Emami et al, 2004), Valproic acid (Enzo Life Sciences), 5-azacytidine (Sigma-Aldrich) or CHIR 99021 (Axon Medchem). For siRNA treatments, 30 pmol of various small interfering RNA (siRNA) (Dharmacon) were transfected by Lipofectamin (Invitrogen) according to the manufacture's protocol. Cells were used for further experiments 48 hours after transfection. All siRNA oligonucleotides were purchased from Dharmacon and used as pools of four specific oligos (SMARTpool). RNAi oligonucleotide sequences are provided in Supplemental Table 6.

*Time course experiment*

Salivary gland tumor propagating cells were plated at day 0. Starting from day 1, 25 µM of ICG-001 was added into culture medium at different time points allowing cells at different time points to be collected together and subjected to RT-PCR and Western blot analysis. Cells at 0, 6, 12 and 24 h were incubated with equivalent concentration of compound vehicle (DMSO, 1:1000) before treated with ICG-001 to exclude the impact of vehicle on the cells.

*Chromatin-immunoprecipitation (ChIP)*

$10^6$ cells were lysed and nuclear extracts prepared. These were incubated with 5 µg of antibody (rabbit-anti tri-methyl histone H3 [Lys4; Cell Signaling] and 20 µl Protein A

Sepharose beads (Invitrogen) in 500 µl PBS, 5 mg/ml BSA over night at 4°C. The beads were re-suspended in 100 µl PBS and 5 mg BSA per ml chromatin, and the chromatin was incubated at 4°C on a rotating wheel. The beads were washed successively with 1 ml sonication buffer (50 mM Hepes pH 7.9, 140 mM NaCl, 1 mM EDTA, 1% Triton X-100, 0.1% Na-deoxycholate, 0.1% SDS, 0.25 mM PMSF and protease inhibitor cocktail (Roche), with 1 ml high salt buffer (same as sonication buffer except 500 mM NaCl) and with 1 ml LiCl wash buffer (20 mM Tris, pH 8.0, 1 mM EDTA, 250 mM LiCl, 0.5% NP-40, 0.5% Na-deoxycholate, 0.25 mM PMSF, protease inhibitor cocktail. All washing steps were repeated twice and performed on a rotating wheel at 4°C. The chromatin was eluted with 50 mM Tris, pH 8.0, 1 mM EDTA, 1% SDS, 50 mM NaHCO3 at 65°C for 30 min. Primer sequences used for qRT PCR of ChIP samples are provided in Supplemental Table 7.

*Ultrastructural analysis of cells by electron microscopy.* Cells were fixed with 4% formaldehyde, post-fixed with 1% OsO4 for 45 min and contrasted with tannic acid and uranyl acetate. Specimens were dehydrated in a graduated ethanol series and embedded in PolyBed (Polysciences Europe GmbH). After polymerization, blocks were cut at 60–80 nm, contrasted with lead citrate and analyzed in a LEO 906E TEM (Zeiss SMT) equipped with a Morada camera (SIS).

**Acknowledgements**

We thank Dr. C. Birchmeier and R. Hodge (MDC) for helpful discussion and critical reading of the manuscript, Dr. H.-P. Rahn (MDC) for support with FACS and D. Gerhard (MDC) for advice on animal experiments. We are indebted to R.R. Behringer

for providing the Bmpr1a$^{lox}$ mice, to M.M. Taketo for the β-catenin$^{loxEx3}$ mice, and to R.H. Stauber for the HNSCCUM-02T and HNSCCUM-03T cell lines. P.W. was funded in part by the German Cancer Aid (Deutsche Krebshilfe). U.Z. was funded by a Marie Curie Excellence Grant.

**Author contributions:**

PW and LF designed and performed experiments and analyzed the data. QZ, FK, KE, VB, and JDH performed experiments. JHS, CL, and SH graded and screened human tumors. JHS, CL, and MK provided material. JHS was involved in manuscript preparation. The biostatistics analysis for clinical relevance studies was conducted by SL. UZ and WB supervised the project, designed experiments, and analyzed the data. This manuscript was written by PW, UZ, and WB. All authors reviewed the manuscript.

**Conflict of interest**

Financial Disclosure: Dr. Michael Kahn is a consultant, and equity holder in Prism Pharmaceuticals, which is developing the CBP/beta-catenin antagonist PRI-724.

**References:**

Albert M, Peters AH (2009) Genetic and epigenetic control of early mouse development. *Current opinion in genetics & development* **19:** 113-121

Arai M, Dyson HJ, Wright PE (2010) Leu628 of the KIX domain of CBP is a key residue for the interaction with the MLL transactivation domain. *FEBS letters* **584:** 4500-4504

Barker N, Ridgway RA, van Es JH, van de Wetering M, Begthel H, van den Born M, Danenberg E, Clarke AR, Sansom OJ, Clevers H (2009) Crypt stem cells as the cells-of-origin of intestinal cancer. *Nature* **457:** 608-611

Barnes L, Eveson JW, Reichart P, Sidransky D (2005) World Health Organization Classification of Tumours, Pathology & Genetics of Head and Neck Tumours. *IARC Press, Lyon*

Behrens J, von Kries JP, Kuhl M, Bruhn L, Wedlich D, Grosschedl R, Birchmeier W (1996) Functional interaction of beta-catenin with the transcription factor LEF-1. *Nature* **382:** 638-642

Ben-Porath I, Thomson MW, Carey VJ, Ge R, Bell GW, Regev A, Weinberg RA (2008) An embryonic stem cell-like gene expression signature in poorly differentiated aggressive human tumors. *Nature genetics* **40:** 499-507

Brinkmann V, Foroutan H, Sachs M, Weidner KM, Birchmeier W (1995) Hepatocyte growth factor/scatter factor induces a variety of tissue-specific morphogenic programs in epithelial cells. *The Journal of cell biology* **131:** 1573-1586

Chu PG, Weiss LM (2002) Keratin expression in human tissues and neoplasms. *Histopathology* **40:** 403-439

Clay MR, Tabor M, Owen JH, Carey TE, Bradford CR, Wolf GT, Wicha MS, Prince ME (2010) Single-marker identification of head and neck squamous cell carcinoma cancer stem cells with aldehyde dehydrogenase. *Head Neck* **32:** 1195-1201

Clevers H (2006) Wnt/beta-catenin signaling in development and disease. *Cell* **127:** 469-480

de Napoles M, Mermoud JE, Wakao R, Tang YA, Endoh M, Appanah R, Nesterova TB, Silva J, Otte AP, Vidal M, Koseki H, Brockdorff N (2004) Polycomb group proteins Ring1A/B link ubiquitylation of histone H2A to heritable gene silencing and X inactivation. *Developmental cell* **7:** 663-676

Dou Y, Milne TA, Ruthenburg AJ, Lee S, Lee JW, Verdine GL, Allis CD, Roeder RG (2006) Regulation of MLL1 H3K4 methyltransferase activity by its core components. *Nature structural & molecular biology* **13:** 713-719

Dou Y, Milne TA, Tackett AJ, Smith ER, Fukuda A, Wysocka J, Allis CD, Chait BT, Hess JL, Roeder RG (2005) Physical association and coordinate function of the H3 K4 methyltransferase MLL1 and the H4 K16 acetyltransferase MOF. *Cell* **121:** 873-885

Emami KH, Nguyen C, Ma H, Kim DH, Jeong KW, Eguchi M, Moon RT, Teo JL, Kim HY, Moon SH, Ha JR, Kahn M (2004) A small molecule inhibitor of beta-catenin/CREB-binding protein transcription [corrected]. *Proceedings of the National Academy of Sciences of the United States of America* **101:** 12682-12687

Fodde R, Brabletz T (2007) Wnt/beta-catenin signaling in cancer stemness and malignant behavior. *CurrOpinCell Biol* **19:** 150-158

Gaspar-Maia A, Alajem A, Meshorer E, Ramalho-Santos M (2011) Open chromatin in pluripotency and reprogramming. *Nature reviews Molecular cell biology* **12:** 36-47

Gires O (2011) Lessons from common markers of tumor-initiating cells in solid cancers. *Cell Mol Life Sci* **68:** 4009-4022

Goldberg AD, Allis CD, Bernstein E (2007) Epigenetics: a landscape takes shape. *Cell* **128:** 635-638

Grigoryan T, Wend P, Klaus A, Birchmeier W (2008) Deciphering the function of canonical Wnt signals in development and disease: conditional loss- and gain-of-function mutations of beta-catenin in mice. *Genes & development* **22:** 2308-2341

Hai B, Yang Z, Millar SE, Choi YS, Taketo MM, Nagy A, Liu F (2010) Wnt/beta-catenin signaling regulates postnatal development and regeneration of the salivary gland. *Stem Cells Dev* **19:** 1793-1801

Harada N, Tamai Y, Ishikawa T, Sauer B, Takaku K, Oshima M, Taketo MM (1999) Intestinal polyposis in mice with a dominant stable mutation of the beta-catenin gene. *EMBO J* **18:** 5931-5942

Heng JC, Feng B, Han J, Jiang J, Kraus P, Ng JH, Orlov YL, Huss M, Yang L, Lufkin T, Lim B, Ng HH (2010) The nuclear receptor Nr5a2 can replace Oct4 in the reprogramming of murine somatic cells to pluripotent cells. *Cell stem cell* **6:** 167-174

Hisatomi Y, Okumura K, Nakamura K, Matsumoto S, Satoh A, Nagano K, Yamamoto T, Endo F (2004) Flow cytometric isolation of endodermal progenitors from mouse salivary gland differentiate into hepatic and pancreatic lineages. *Hepatology (Baltimore, Md* **39:** 667-675

Huelsken J, Vogel R, Erdmann B, Cotsarelis G, Birchmeier W (2001) Beta-Catenin controls hair follicle morphogenesis and stem cell differentiation in the skin. *Cell* **105:** 533-545

Jamieson CH, Ailles LE, Dylla SJ, Muijtjens M, Jones C, Zehnder JL, Gotlib J, Li K, Manz MG, Keating A, Sawyers CL, Weissman IL (2004) Granulocyte-macrophage progenitors as candidate leukemic stem cells in blast-crisis CML. *The New England journal of medicine* **351:** 657-667

Kim SK, Suh MR, Yoon HS, Lee JB, Oh SK, Moon SY, Moon SH, Lee JY, Hwang JH, Cho WJ, Kim KS (2005) Identification of developmental pluripotency associated 5 expression in human pluripotent stem cells. *Stem cells (Dayton, Ohio)* **23:** 458-462

Krivtsov AV, Armstrong SA (2007) MLL translocations, histone modifications and leukaemia stem-cell development. *Nature reviews Cancer* **7:** 823-833

Lombaert IM, Brunsting JF, Wierenga PK, Faber H, Stokman MA, Kok T, Visser WH, Kampinga HH, de Haan G, Coppes RP (2008) Rescue of salivary gland function after stem cell transplantation in irradiated glands. *PLoS ONE* **3:** e2063

Lustig B, Jerchow B, Sachs M, Weiler S, Pietsch T, Karsten U, van de WM, Clevers H, Schlag PM, Birchmeier W, Behrens J (2002) Negative feedback loop of Wnt signaling through upregulation of conductin/axin2 in colorectal and liver tumors. *MolCell Biol* **22:** 1184-1193

Malanchi I, Peinado H, Kassen D, Hussenet T, Metzger D, Chambon P, Huber M, Hohl D, Cano A, Birchmeier W, Huelsken J (2008) Cutaneous cancer stem cell maintenance is dependent on beta-catenin signalling. *Nature* **452:** 650-653

Man YG, Ball WD, Marchetti L, Hand AR (2001) Contributions of intercalated duct cells to the normal parenchyma of submandibular glands of adult rats. *The Anatomical record* **263:** 202-214

Mishina Y, Hanks MC, Miura S, Tallquist MD, Behringer RR (2002) Generation of Bmpr/Alk3 conditional knockout mice. *Genesis* **32:** 69-72

Molenaar M, van de Wetering M, Oosterwegel M, Peterson-Maduro J, Godsave S, Korinek V, Roose J, Destree O, Clevers H (1996) XTcf-3 transcription factor mediates beta-catenin-induced axis formation in Xenopus embryos. *Cell* **86:** 391-399

Monroe MM, Anderson EC, Clayburgh DR, Wong MH (2011) Cancer stem cells in head and neck squamous cell carcinoma. *J Oncol* **2011:** 762780

Mosimann C, Hausmann G, Basler K (2009) Beta-catenin hits chromatin: regulation of Wnt target gene activation. *Nat Rev Mol Cell Biol* **10:** 276-286

Nanduri LS, Maimets M, Pringle SA, van der Zwaag M, van Os RP, Coppes RP (2011) Regeneration of irradiated salivary glands with stem cell marker expressing cells. *Radiother Oncol* **99:** 367-372

Parker DS, Ni YY, Chang JL, Li J, Cadigan KM (2008) Wingless signaling induces widespread chromatin remodeling of target loci. *Molecular and cellular biology* **28:** 1815-1828

Piccirillo SG, Reynolds BA, Zanetti N, Lamorte G, Binda E, Broggi G, Brem H, Olivi A, Dimeco F, Vescovi AL (2006) Bone morphogenetic proteins inhibit the tumorigenic potential of human brain tumour-initiating cells. *Nature* **444:** 761-765

Prince ME, Sivanandan R, Kaczorowski A, Wolf GT, Kaplan MJ, Dalerba P, Weissman IL, Clarke MF, Ailles LE (2007) Identification of a subpopulation of cells with cancer stem cell properties in head and neck squamous cell carcinoma.

*Proceedings of the National Academy of Sciences of the United States of America* **104:** 973-978

Read TA, Fogarty MP, Markant SL, McLendon RE, Wei Z, Ellison DW, Febbo PG, Wechsler-Reya RJ (2009) Identification of CD15 as a marker for tumor-propagating cells in a mouse model of medulloblastoma. *Cancer Cell* **15:** 135-147

Ring DB, Johnson KW, Henriksen EJ, Nuss JM, Goff D, Kinnick TR, Ma ST, Reeder JW, Samuels I, Slabiak T, Wagman AS, Hammond ME, Harrison SD (2003) Selective glycogen synthase kinase 3 inhibitors potentiate insulin activation of glucose transport and utilization in vitro and in vivo. *Diabetes* **52:** 588-595

Schuettengruber B, Martinez AM, Iovino N, Cavalli G (2011) Trithorax group proteins: switching genes on and keeping them active. *Nature reviews Molecular cell biology* **12:** 799-814

Sierra J, Yoshida T, Joazeiro CA, Jones KA (2006) The APC tumor suppressor counteracts beta-catenin activation and H3K4 methylation at Wnt target genes. *Genes & development* **20:** 586-600

Sneddon JB, Werb Z (2007) Location, location, location: the cancer stem cell niche. *Cell stem cell* **1:** 607-611

Southall SM, Wong PS, Odho Z, Roe SM, Wilson JR (2009) Structural basis for the requirement of additional factors for MLL1 SET domain activity and recognition of epigenetic marks. *Molecular cell* **33:** 181-191

Speight PM, Barrett AW (2002) Salivary gland tumours. *Oral Dis* **8:** 229-240

Stewart BW, Kleihues P (2003) World cancer report. . *World Health Organization, Lyon: IARC*

Subramanian A, Tamayo P, Mootha VK, Mukherjee S, Ebert BL, Gillette MA, Paulovich A, Pomeroy SL, Golub TR, Lander ES, Mesirov JP (2005) Gene set enrichment analysis: a knowledge-based approach for interpreting genome-wide expression profiles. *Proceedings of the National Academy of Sciences of the United States of America* **102:** 15545-15550

Surani MA, Hayashi K, Hajkova P (2007) Genetic and epigenetic regulators of pluripotency. *Cell* **128:** 747-762

Takahashi-Yanaga F, Kahn M (2010) Targeting Wnt signaling: can we safely eradicate cancer stem cells? *Clin Cancer Res* **16:** 3153-3162

Taki T, Sako M, Tsuchida M, Hayashi Y (1997) The t(11;16)(q23;p13) translocation in myelodysplastic syndrome fuses the MLL gene to the CBP gene. *Blood* **89:** 3945-3950

Thorey IS, Muth K, Russ AP, Otte J, Reffelmann A, von Melchner H (1998) Selective disruption of genes transiently induced in differentiating mouse embryonic stem cells

by using gene trap mutagenesis and site-specific recombination. *Molecular and cellular biology* **18:** 3081-3088

Tucker AS (2007) Salivary gland development. *Seminars in cell & developmental biology* **18:** 237-244

Visvader JE, Lindeman GJ (2008) Cancer stem cells in solid tumours: accumulating evidence and unresolved questions. *Nature reviews* **8:** 755-768

Visvader JE, Lindeman GJ (2012) Cancer stem cells: current status and evolving complexities. *Cell stem cell* **10:** 717-728

von Eyss B, Maaskola J, Memczak S, Mollmann K, Schuetz A, Loddenkemper C, Tanh MD, Otto A, Muegge K, Heinemann U, Rajewsky N, Ziebold U (2011) The SNF2-like helicase HELLS mediates E2F3-dependent transcription and cellular transformation. *The EMBO journal*

Ware CB, Wang L, Mecham BH, Shen L, Nelson AM, Bar M, Lamba DA, Dauphin DS, Buckingham B, Askari B, Lim R, Tewari M, Gartler SM, Issa JP, Pavlidis P, Duan Z, Blau CA (2009) Histone deacetylase inhibition elicits an evolutionarily conserved self-renewal program in embryonic stem cells. *Cell stem cell* **4:** 359-369

Welkoborsky HJ, Jacob R, Riazimand SH, Bernauer HS, Mann WJ (2003) Molecular biologic characteristics of seven new cell lines of squamous cell carcinomas of the head and neck and comparison to fresh tumor tissue. *Oncology* **65:** 60-71

Wend P, Holland JD, Ziebold U, Birchmeier W (2010) Wnt signaling in stem and cancer stem cells. *Seminars in cell & developmental biology* **21:** 855-863

Wend P, Runke S, Wend K, Anchondo B, Yesayan M, Jardon M, Hardie N, Loddenkemper C, Ulasov I, Lesniak MS, Wolsky R, Bentolila LA, Grant SG, Elashoff D, Lehr S, Latimer JJ, Bose S, Sattar H, Krum SA, Miranda-Carboni GA (2013) WNT10B/beta-catenin signalling induces HMGA2 and proliferation in metastatic triple-negative breast cancer. *EMBO Mol Med* **5:** 264-279

Whitman M (1998) Smads and early developmental signaling by the TGFbeta superfamily. *Genes & development* **12:** 2445-2462

Xi S, Geiman TM, Briones V, Guang Tao Y, Xu H, Muegge K (2009) Lsh participates in DNA methylation and silencing of stem cell genes. *Stem cells (Dayton, Ohio)* **27:** 2691-2702

Ying YL, Johnson JT, Myers EN (2006) Squamous cell carcinoma of the parotid gland. *Head Neck* **28:** 626-632

**Figure Legends**

**Figure 1.** *High Wnt/β-catenin and low Bmp signaling characterize head and neck squamous cell carcinoma of humans and mice.* **(A)** Serial sections of human salivary gland SCC, as analyzed by immunohistochemistry for β-catenin and pSmad1/5/8 or by H&E-staining; at tumor fronts, β-catenin is located in nuclei (black arrows) and at cell junctions in differentiated, central tumor areas (inset), whereas phospho-Smad1/5/8 staining is low (inset shows nuclear pSmad1/5/8 staining in tubular cells from a differentiated, central area of the same tumor, see arrow). (A*) Immunofluorescence for CD24 (in red) and β-catenin (in green, DAPI in blue); CD24 co-localizes with nuclear β-catenin. st, stroma; tu, tumor. **(B)** Upper graphs: the specific combination of nuclear β-catenin and negative pSmad 1/5/8 was detected in 75% of aggressive, grade 3 human salivary gland SCC (SG-SCC) and in 63% of grade 3 head and neck SCC (HN-SCC). **(C)** Sections of human HN-SCC, as analyzed by immunofluorescence for the stem cell markers CD24 and CD44 (in red) and β-catenin (in green, DAPI in blue). CD24 and CD44 co-localize with nuclear β-catenin in head and neck SCC (quantitation is in B, lower graph, and in C, right panel, in yellow letters for grade 2 and grade 3 tumors: the number of double positive cells for nuclear β-catenin and CD24 was up-regulated in grade 3 SG-SCC and HN-SCC; percentages refer to all tumor cells). The bars give means and standard deviations (*$p < 0.05$, Student's t-test). P values are as compared with grade 2 tumors. **(D)** Side view of control (wt) and K14Cre;β-cat$^{GOF}$:Bmpr1a$^{LOF}$ double mutant mice at P90 (arrow marks a salivary gland tumor). **(E)** Kaplan Meier survival plot of double mutant tumor mice, compared to control and single mutant mice without tumors (each group n=21). Bar, 200 μm in A and 50 μm in A*,C.

**Figure 2.** *Wnt/β-catenin and Bmp signaling control tumor propagating cells in salivary glands of mice.* **(A)** FACS analysis of control (wt) and mutant salivary gland cells. High $CD24^{+}CD29^{+}$ expressing cells are marked by squares (insets), and quantification is shown above the squares (details on isotype control staining are shown in Supplementary Fig. 3). **(B)** Sections of control and mutant salivary glands stained by immunofluorescence for CD24 (in red, DAPI in blue). **(C,D)** Identification of proliferating cells within the $CD24^{+}CD29^{+}$ salivary gland cell populations of all genotypes by immunofluorescence of cytospins for Ki67 (in red, DAPI in blue). Staining of double mutant cells is shown in C, quantification for all genotypes is shown in D (n=3). The bars give means and standard deviations (*$p < 0.05$, Student's t-test). P values are as compared with wildtype cells. Bar, 25 μm. **(E)** Quantification of proliferation in salivary gland cells of control and mutant mice, as determined by immunofluorescence for Ki67 (n=3). The bars give means and standard deviations (*$p < 0.05$, Student's t-test). P values are as compared with wildtype cells. **(F)** Tumor outgrowths produced from subcutaneous injections of different cell numbers of unsorted or sorted $CD24^{+}CD29^{+}$ cells from $\beta\text{-cat}^{GOF}$;$Bmpr1a^{LOF}$ double mutant glands into the back skin of NOD/SCID mice (each group n=3, details on serial transplantations are provided in Supplementary Fig. 4F,G). **(G)** Tumor formation capacity of other sorted subpopulations of cells of $\beta\text{-cat}^{GOF}$;$Bmpr1a^{LOF}$ double mutant glands (each group n=3). Single $CD24^{+}$ or $CD29^{+}$ or $CD24^{-}/CD29^{-}$ cells did not produce tumors.

**Figure 3.** *Salivary gland tumor propagating cells of double mutant mice are characterized by stem cell-associated gene expression and specific chromatin marks.* **(A)** FAC-sorted $CD29^{+}$ salivary gland tumor propagating cells were further sorted for

CD24 and SSEA-1 expression (high or low expressing cells are gated, insets). **(B)** Immunofluorescence of triple-sorted SSEA-1$^+$ and SSEA-1$^-$ cells for nuclear β-catenin (in red, DAPI in blue). **(C)** qRT-PCR of highly expressed genes in sorted CD24$^+$CD29$^+$ tumor propagating cells at P75-80, which were identified by Affymetrix microarray analysis (details shown in Supplementary Fig. 5B,C and Table S4), and down-regulation following treatment with the Wnt/β-catenin inhibitor ICG-001 or β-catenin siRNA (n=4). **(D)** Analysis of histone trimethylation patterns by immunofluorescence for H3K4me3 and H3K27me3 of cytospins of CD24$^+$CD29$^+$ salivary gland cells (in red, DAPI in blue, quantification is shown in E). **(E)** Histone trimethylation revealed a profound switch of chromatin marks in the double mutant tumor propagating cells. Immunofluorescence for H3K9me3 is shown in Supplementary Fig. 5D. **(F)** H3K4me3 (in red, DAPI in blue) is suppressed in tumor propagating cells upon treatment with ICG-001 at 25μM (for quantification of H3K9me3 and H3K27me3 after ICG-001 see E). The vertical bars give means and standard deviations (*$p < 0.05$, Student's t-test). P values are as compared with controls (C,F). Bars of magnifications in B, D and F; 25 μm.

**Figure 4.** *Salivary gland tumor propagating cells grow in non-adherent spheres (salispheres) and respond to Wnt/β-catenin and HDAC and DNA methylation inhibitors.* **(A)** Proliferation of tumor propagating cells and treatment with the Wnt/β-catenin inhibitor ICG-001, at 25μM in 1% DMSO (n=3). **(B)** Tumor growth of transplanted tumor propagating cells in NOD/SCID mice, and inhibition after intra-peritoneal administration of ICG-001 at 200 mg/kg (n=5). Red triangles indicate ICG-001 administration. **(C,** *left panel***)** Phase contrast images of undifferentiated salispheres in Matrigel cultures containing HGF, or differentiated cultures following

additional treatment with ICG-001. **(C,** *right panel***)** Reversion of differentiation of sphere cultures in the presence of additional valproic acid (VPA) or 5-azacytidine (Aza) (controls are shown in Supplementary Fig. 6H). **(D)** Phalloidin staining (in green; DAPI in blue) of salispheres (left) and differentiated, gland-like structures after 72 hrs treatment with ICG-001 (right). **(E)** Quantifications of differentiation of spheres from (C) at 72 hrs. In A, B and E, means and standard deviations are shown (*$p < 0.05$, Student's t-test for A,B; ANOVA for E). P values are as compared with control cells or with cells that received combined treatment. Bar in C and D; 100 μm.

**Figure 5.** *Chromatin immunoprecipitation of promoters of chromatin-modifying or Wnt/β-catenin target genes. ICG-001-induced downregulation of H3K4me3 precedes changes in gene expression in mouse tumor propagating cells and human HN-SCC tumor cells*. **(A,B)** H3K4me3 enrichment at the promoters of *Mll, Hells, Ash2, Myc*, and *GAPDH* or *actin* genes assessed by chromatin immunoprecipitation (ChIP) of mouse β-cat$^{GOF}$;Bmpr1a$^{LOF}$ tumor propagating cells and human head and neck tumor cells (HNSCCUM-03T) upon ICG-001 treatment (n=3, I+IV: amplicons from promoter-far regions; II+III: amplicons from promoter-near regions). **(C)** Western blot analysis of H3K4me3 in a time course experiment of ICG-001-treated mouse β-cat$^{GOF}$;Bmpr1a$^{LOF}$ tumor propagating cells. Protein ratios depict H3K4me3 signal intensities, normalized to H3, which served as loading control. **(D)** qRT-PCR analysis of samples from the time course experiment depicted in C. Expression changes in the differentiation-associated gene *Amy1* or *Mll, Hells, Ash2* and *Myc* (genes analyzed by ChIP in A) were quantified (n=3). In A,B,D, means and standard deviations are shown (*$p < 0.05$, Student's t-test). P values are as compared with control cells.

**Figure 6.** *Wnt/β-catenin signaling exploits a MLL-dependent H3K4 activity to establish and maintain salivary gland tumor propagating cells. Co-expression of nuclear β-catenin and nuclear MLL is associated in human salivary gland SCC.* **(A)** Western blot analysis of β-catenin in cytoplasmic and nuclear fractions from untreated (w/o), CHIR- or ICG-001-treated $CD24^{+}CD29^{+}$ salivary gland tumor propagating cells. **(B)** Western blot analysis of MLL in nuclear fractions of untreated (Ctr), CHIR- or ICG-001-treated tumor propagating cells. α-Tubulin and Lamin in A, B are the cytoplasmic or nuclear loading controls, respectively. Protein ratios in A, B depict β-catenin or MLL signal intensities, normalized to the corresponding loading controls. **(C)** Analysis of histone trimethylation pattern and proliferation by immunofluorescence for H3K4me3 (in red) and Ki67 (in green, DAPI in blue), using cytospins of tumor propagating cells upon siRNA-induced knockdown of *Mll*, *β-catenin*, *CBP* and *Ash1*, or treatment with the Wnt/β-catenin inhibitor ICG-001 at 25μM in 1% DMSO (n=3). Quantifications are shown on the right (siCtr, control siRNA). **(D)** Proliferation of tumor propagating cells upon siRNA-induced knockdown of *Dppa5a*, *Mll* and *β-catenin*, or treatment with ICG-001 (n=3). **(E)** Quantifications of differentiation of tumor propagating cells in 3D-Matrigel cultures upon siRNA-induced knockdown of *β-catenin, Mll and Ash1*, or treatment with ICG-001 (n=4). **(F)** Immunofluorescence analysis for β-catenin (green) and MLL (red, DAPI in blue) of human salivary gland SCC (n=13). Two representative tumors are shown to distinguish high $\beta\text{-catenin}^{nucl}/\text{MLL}^{nucl}$ from low $\beta\text{-catenin}^{nucl}/\text{MLL}^{nucl}$ tumors. White arrows highlight cells co-expressing nuclear β-catenin and nuclear MLL. **(G)** Nuclear β-catenin correlates with nuclear MLL expression and both markers correlate with grade 3 human salivary gland SCC. β-Catenin and MLL expression was determined by immunofluorescence analysis in 13 SG-SCC.

Associations were determined on an ordinal scale and evaluated using Kendall's Tau coefficient. P-values and patient numbers (n) are indicated. For details see Supplementary Fig. 7F,G, Supplementary Table 1 and Materials and Methods. In C-E, means and standard deviations are shown (*$p < 0.05$, Student's t-test). P values are as compared with control cells. Bar in C,F; 25 μm.

**Figure 7.** *Model of self-renewal and differentiation of tumor propagating cells in salivary gland SCC.* **(A)** Self-renewal depends on active Wnt/β-catenin signals, permissive chromatin, and expression of specific target genes, e.g., pluripotency-associated genes. Potential histone methyltransferases (HMT; MLL) and histone acetyltransferases (HAT; CBP) bound to the C-terminus of β-catenin are shown. Genetic ablation of β-catenin or siRNAs against *Mll* inhibits interaction at Wnt-responsive elements (WRE). ICG-001 blocks association of CBP with β-catenin. **(B)** In contrast, differentiated tumor propagating cells exhibit inactive Wnt/β-catenin signaling, repressive chromatin, and down-regulation of pluripotency-associated genes. Instead of β-catenin and associates, Groucho and DNMT may be bound to the WRE.

# Wend *et al.*, Fig. 1

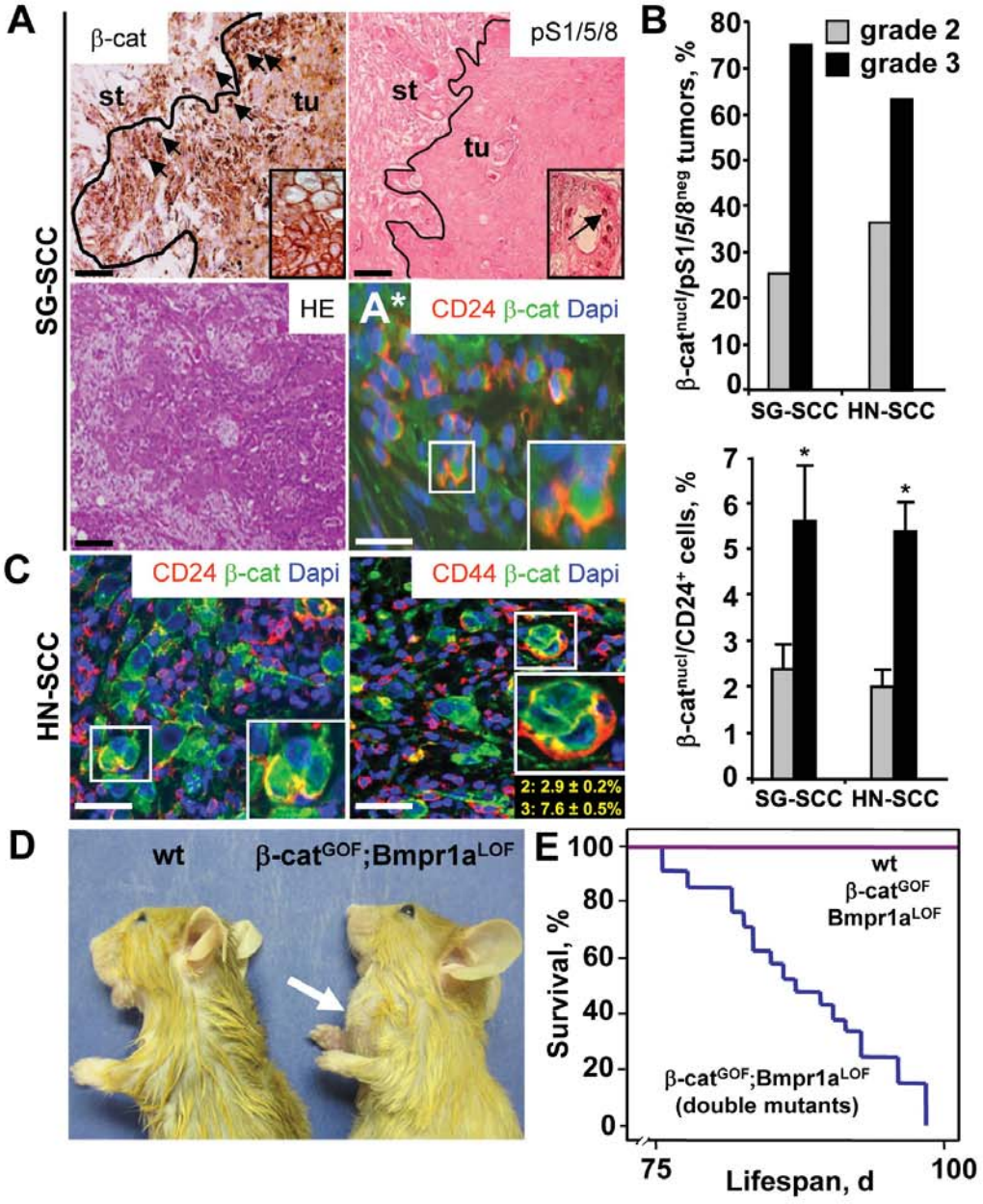

# Wend *et al.*, Fig. 2

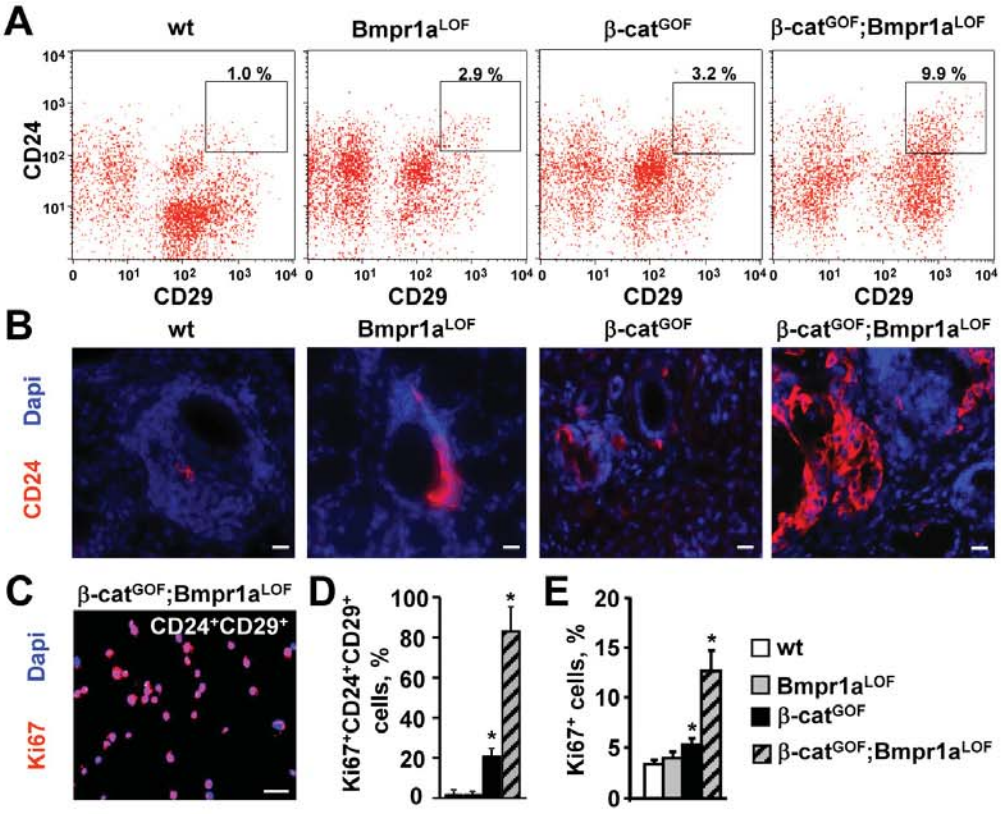


**F**

| Transplanted cells | Unsorted | $CD24^+CD29^+$ |
|---|---|---|
| 10 millions | 3/3 | 3/3 |
| 1 million | 3/3 | 3/3 |
| 100,000 | 2/3 | 3/3 |
| 10,000 | 0/3 | 3/3 |
| 1000 | 0/3 | 3/3 |
| 500 | 0/3 | 2/3 |
| 100 | 0/3 | 0/3 |

**G**

| CD24 | CD29 | Transplanted 100,000 cells | |
|---|---|---|---|
| + | + | tumor | 3/3 |
| + | - | none | 0/3 |
| - | + | none | 0/3 |
| - | - | none | 0/3 |

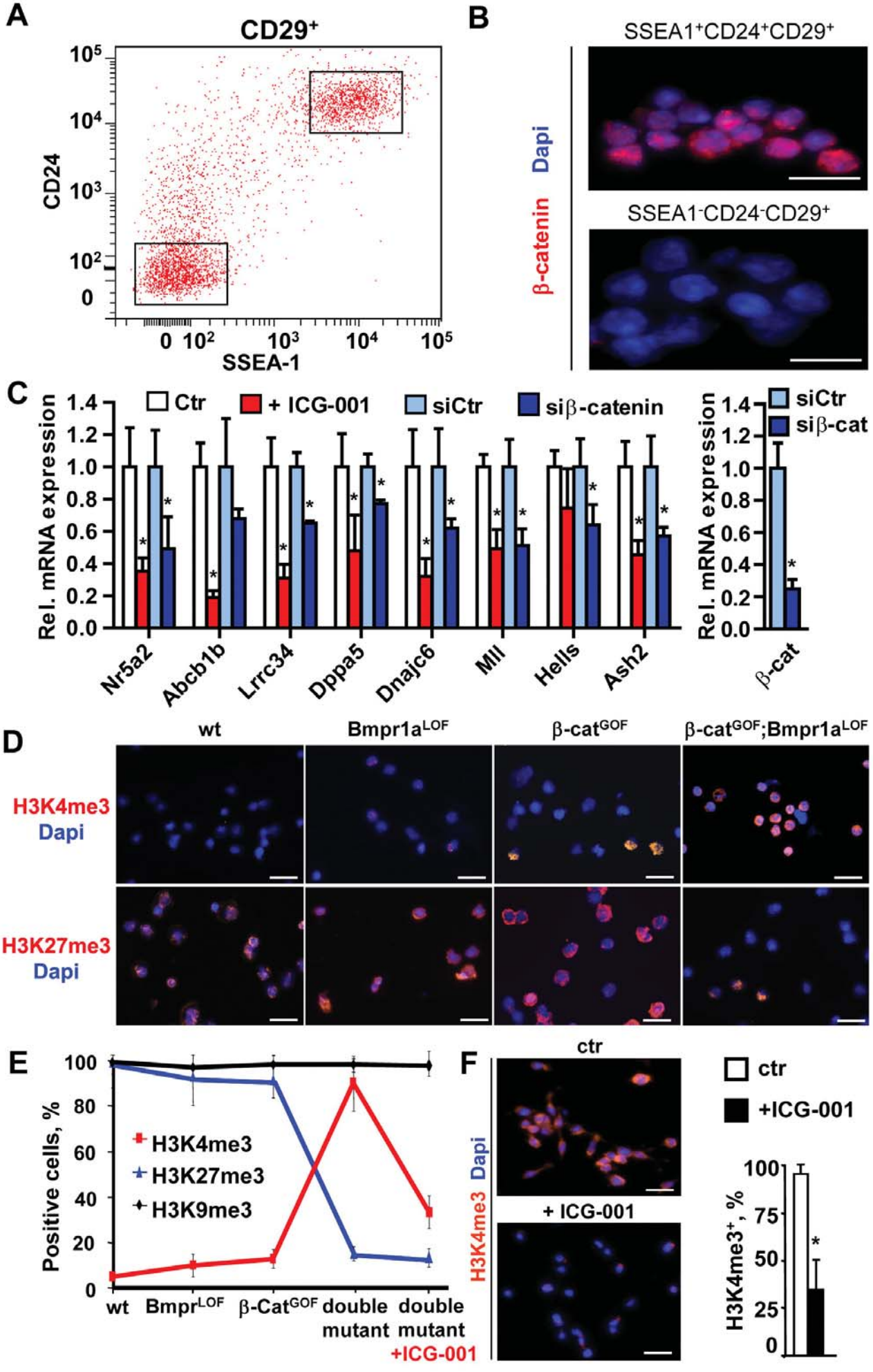
A
CD29+
CD24
SSEA-1
B
SSEA1+CD24+CD29+
SSEA1-CD24-CD29+
β-catenin
Dapi
C
Ctr
+ ICG-001
siCtr
siβ-catenin
Rel. mRNA expression
Nr5a2
Abcb1b
Lrrc34
Dppa5
Dnajc6
Mll
Hells
Ash2
siβ-cat
β-cat
D
wt
Bmpr1a^LOF
β-cat^GOF
β-cat^GOF;Bmpr1a^LOF
H3K4me3
Dapi
H3K27me3
E
Positive cells, %
H3K4me3
H3K27me3
H3K9me3
wt
Bmpr^LOF
β-Cat^GOF
double mutant
double mutant +ICG-001
F
ctr
+ ICG-001
H3K4me3
Dapi
H3K4me3+, %

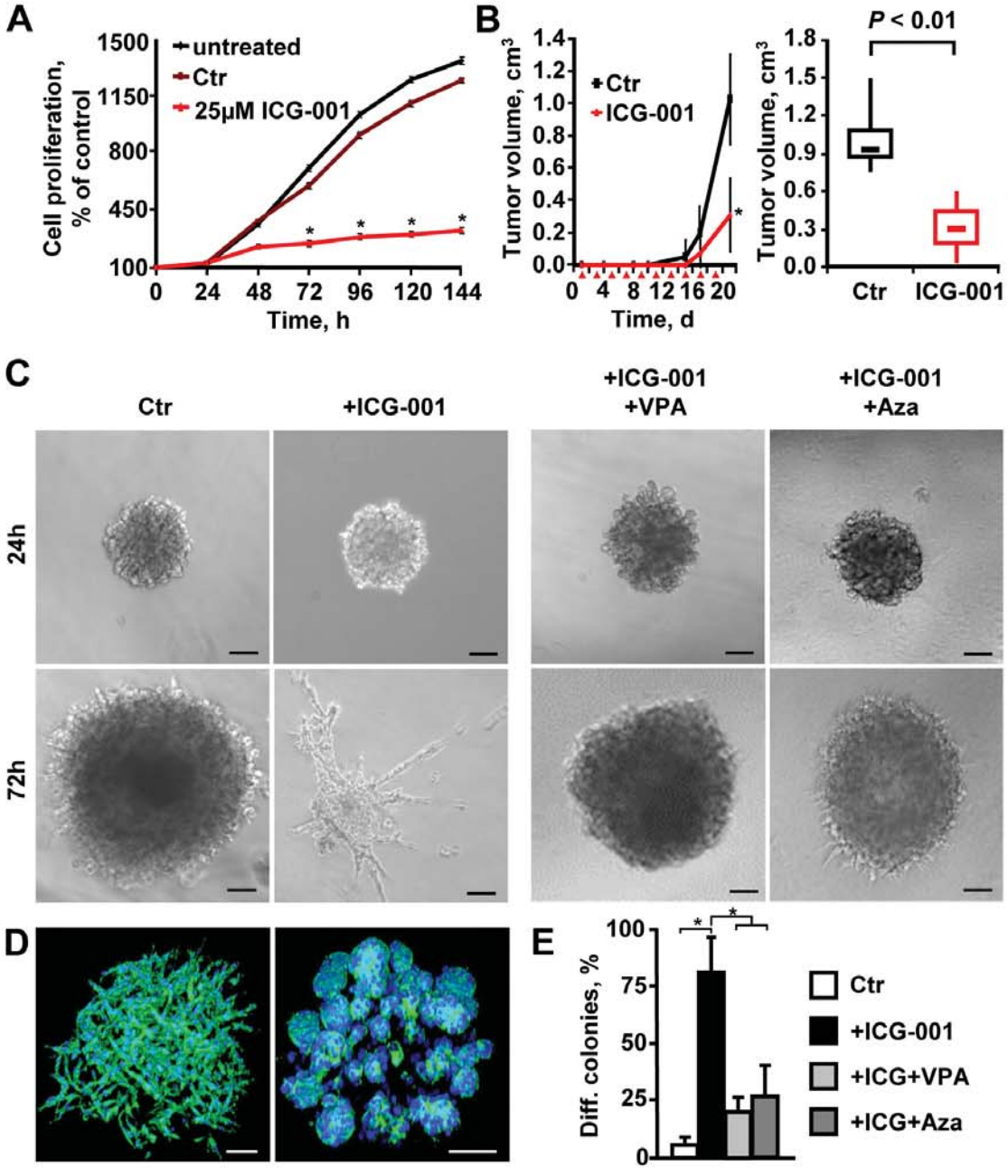
A
Cell proliferation, % of control
1500
1150
800
450
100
untreated
Ctr
25μM ICG-001
0 24 48 72 96 120 144
Time, h
B
Tumor volume, cm3
1.4
1.2
1.0
0.8
0.6
0.4
0.2
0.0
Ctr
ICG-001
0 4 8 12 16 20
Time, d
P < 0.01
1.8
1.5
1.2
0.9
0.6
0.3
0.0
Ctr ICG-001
C
Ctr
+ICG-001
+ICG-001 +VPA
+ICG-001 +Aza
24h
72h
D
E
Diff. colonies, %
100
75
50
25
0
Ctr
+ICG-001
+ICG+VPA
+ICG+Aza

# Wend *et al.*, Fig. 5

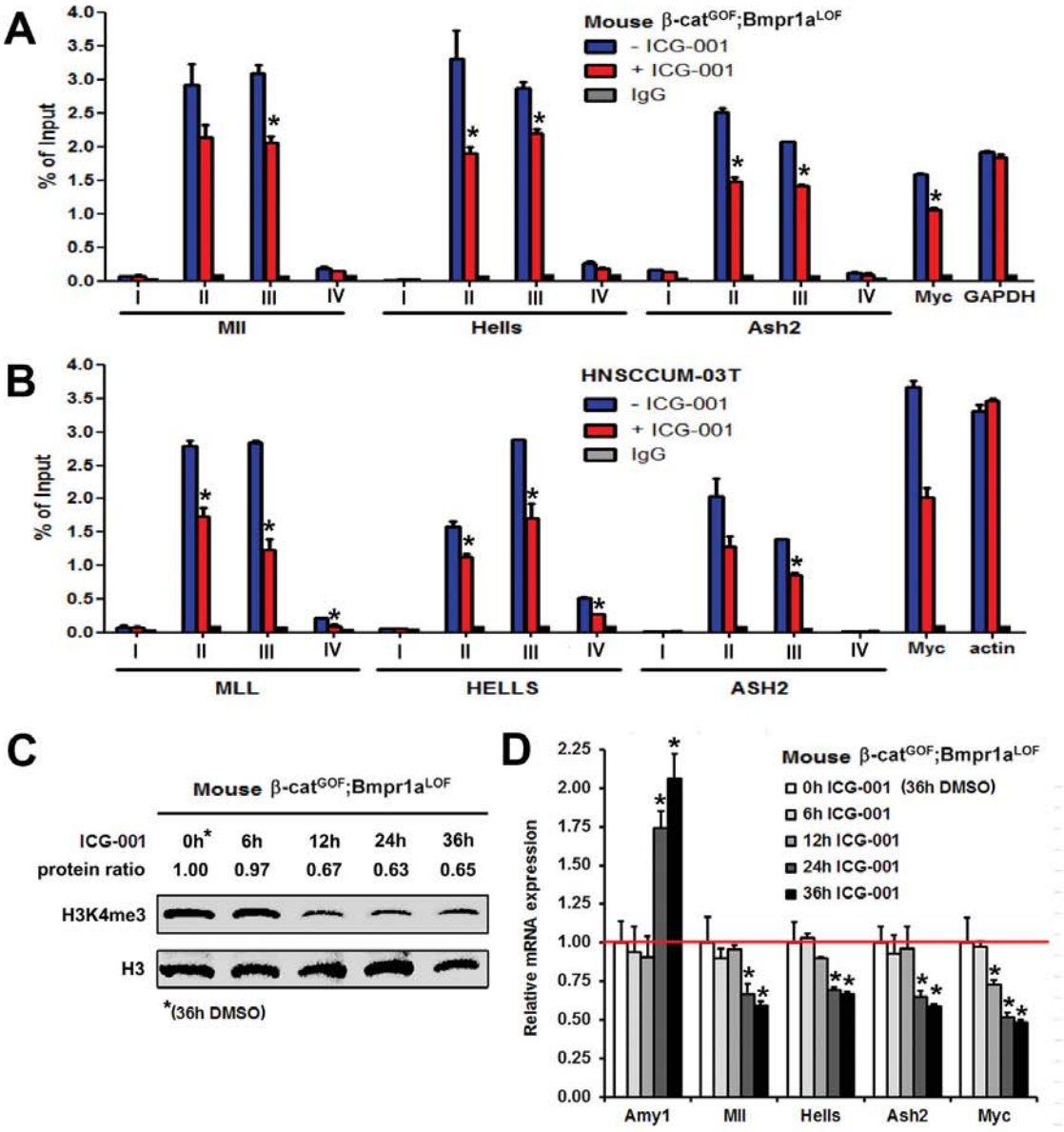

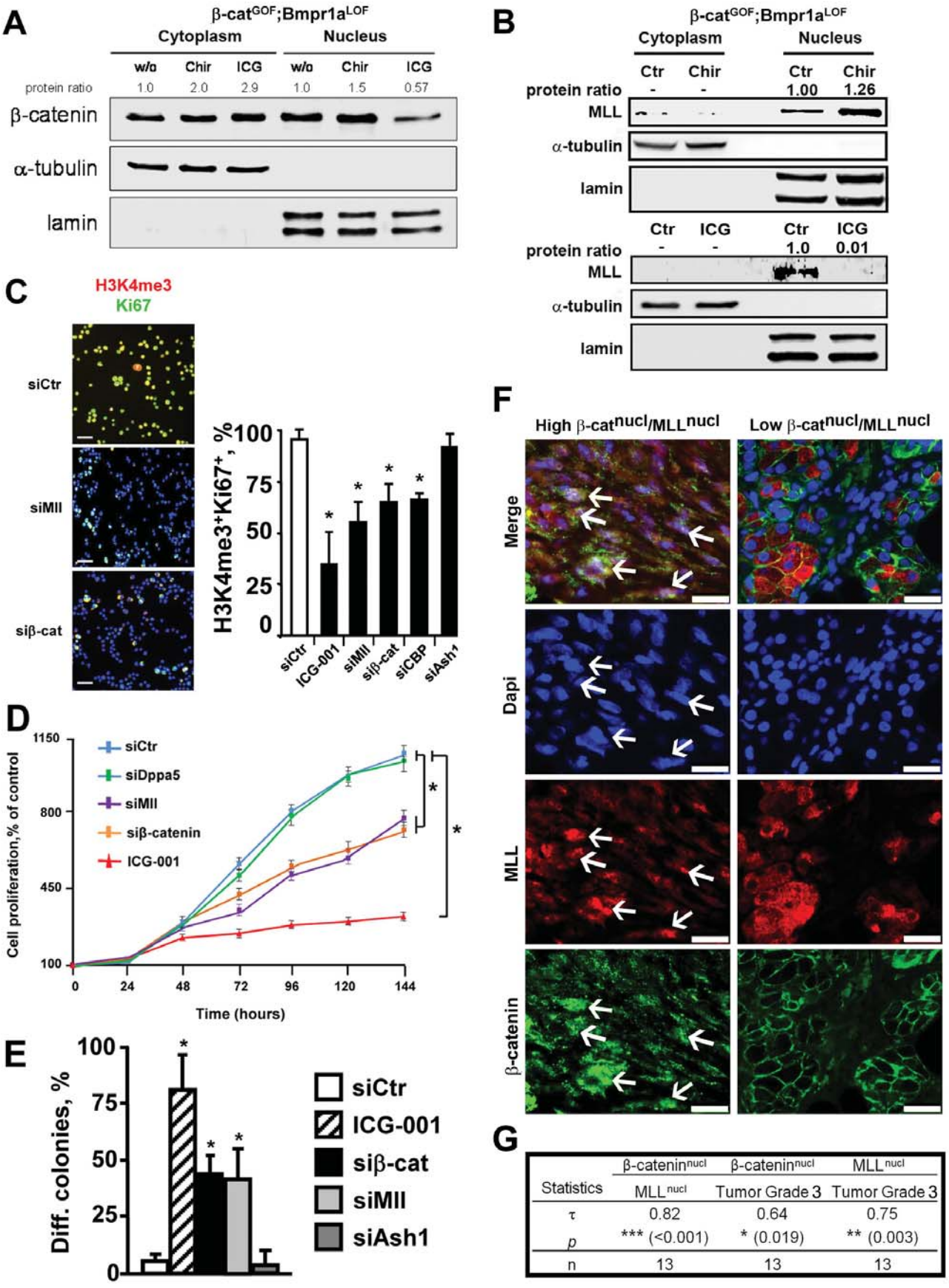


| Statistics | β-catenin$^{nucl}$ MLL$^{nucl}$ | β-catenin$^{nucl}$ Tumor Grade 3 | MLL$^{nucl}$ Tumor Grade 3 |
|---|---|---|---|
| τ | 0.82 | 0.64 | 0.75 |
| *p* | *** (<0.001) | * (0.019) | ** (0.003) |
| n | 13 | 13 | 13 |

Wend *et al.*, Fig. 7

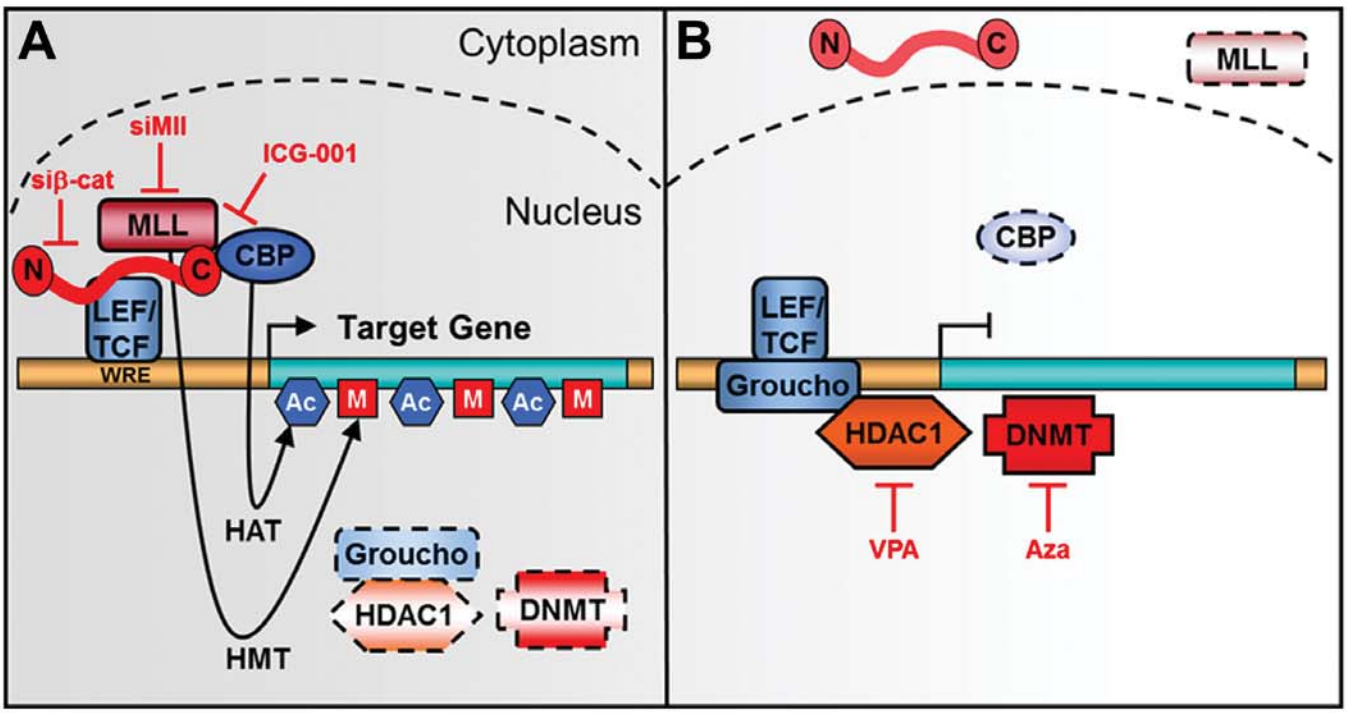


**Self-renewal** **Differentiation**

**Supplementary Information**

# "Wnt/β-catenin signaling induces MLL to create epigenetic changes in salivary gland tumors"

Peter Wend, Liang Fang, Qionghua Zhu, Jörg H. Schipper, Christoph Loddenkemper, Frauke Kosel, Volker Brinkmann, Klaus Eckert, Simone Hindersin, Jane D. Holland, Stephan Lehr, Michael Kahn, Ulrike Ziebold, Walter Birchmeier

Our **Supplementary Information** is submitted as merged pdf-file and includes:

- Seven Supplementary Figures and Legends
- Seven Supplementary Tables
- Supplemental References

## Supplemental Figure Legends

**Figure S1.** *Co-expression of Keratin 10 and nuclear β-catenin in tumor cells at the invasive front of human salivary gland tumors. Anatomy and K14-Cre activity in mouse salivary glands. Scheme of breeding and verification of gene recombination.* **(A)** Sections of representative human salivary gland tumors (Tu1, Tu2) stained by immunofluorescence for cytokeratin 10 (in red) and β-catenin (in green, DAPI in blue). White dashed lines indicate tumor fronts. White arrow highlight cells co-expressing CK10 and nuclear β-catenin; white stars highlight $CK10^{negative}$/nuclear β-catenin cells. st; stroma, tu; tumor. **(B)** Structure of the salivary gland (AC; acinar cells, MEC; myoepithelial cells, IDC; intercalated duct cells, DC; ductal cells). **(C)** Keratin14-Cre-mediated expression of LacZ can be detected in ductal but not in acinar cells of the mouse salivary gland at P1. **(D,E)** Verification of K14 expression in salivary gland ducts by *in situ* hybridization. **(F)** Breeding scheme for the generation of compound mutant mice. **(G)** K14-Cre-mediated recombination of the BmpR1a and β-catenin genes was evaluated by recombination-specific PCR in wildtype, single mutant and double mutant (tumor) cells. Bars in A; 50 μm. Bars in C,D 200 μm.

**Figure S2.** *Wnt/β-catenin and Bmp signaling in the regulation of proliferation, apoptosis, and differentiation in mouse salivary glands at P90. Phenotypes in other K14-expressing tissues, and cytokeratin 10 expression in transplanted tumors.* **(A)** Histological analysis of wildtype, single (K14Cre;$Bmpr1a^{LOF}$ or K14Cre;β-$cat^{GOF}$) and tumorigenic double mutant (K14Cre;β-$cat^{GOF}$:$Bmpr1a^{LOF}$) salivary glands as revealed by H&E staining and immunohistochemistry for cytokeratin 10 (marker for squamous cell carcinoma; insets) (Chu and Weiss, 2002). Bars; 250 μm. **(B)** Serial sections of double mutant mouse SG-SCC, as analyzed by immunohistochemistry for β-catenin (i) and pSmad1/5/8 (iii) and *in situ* hybridization for the Wnt/β-catenin target gene Axin2 (ii). Bars; 100 μm. At tumor fronts, β-catenin is located in nuclei and at cell junctions in central differentiated tumor areas (inset);

whereas phospho-Smad1/5/8 staining is low (inset shows nuclear pSmad1/5/8 staining in tubular cells from a differentiated, central area of the same tumor). **(C)** Left: quantification of apoptosis in salivary glands of wildtype and mutant mice, as determined by immunofluorescence for cleaved caspase 3. Middle and right: quantitative real-time PCR for the expression of genes important for proliferation (*c-myc* and *CK6*), apoptosis (*Fas*), and differentiation (*Loricrin*). Means and the standard deviations are shown (n=3, *p < 0.05, Student's t-test). P values are as compared with wildtype cells. **(D)** Sections of skin, esophagus and forestomach of wildtype and double mutant mice at P90, as analyzed by H&E staining. Bars; 250 μm.

**Figure S3.** *Characterization of expression patterns of CD24, CD29 and CD44 in salivary gland cells.* **(A,B)** FACS of wt and mutant salivary gland cells for the expression of CD24 (A) and CD29 (B), as indicated by the open histograms and the corresponding isotype controls (filled histograms). **(C)** Overlay of CD24 and CD29 signal intensities of wt and mutant salivary gland cells, as analyzed by FACS (single staining are shown in A,B). **(D,E)** FACS of CD44 expression in double mutant $CD24^{+}CD29^{+}$ tumor propagating cells. Note that $CD24^{+}CD29^{+}$ cells weakly express CD44. CT26 cells (a mouse colon carcinoma cell line) served as positive control for high CD44 expression.

**Figure S4.** *Proliferative activity in different subpopulations of double mutant salivary gland tumor cells, growth kinetics and cytokeratin expressions in transplanted tumors, and tumor propagating cells in secondary and tertiary tumor transplants.* **(A)** Freshly isolated tumor cells from double mutant mice were analyzed by FACS for the expression of CD24 and CD29 (profiles shown in black) and the proliferation marker Ki67 (profile indicated in red). **(B)** Quantification of proliferation in different CD24/CD29 subpopulations of double mutant tumor cells (of samples shown in A). Note that proliferation is highest in the high

$CD24^+CD29^+$ expressing tumor propagating cell population (P1) and in $CD24^{low}CD29^+$ cells (P4). **(C)** Tumor growth kinetics of transplants generated from different numbers of unsorted or sorted $CD24^+CD29^+$ salivary gland tumor cells after subcutaneous injection in the back skin of NOD/SCID mice (n=3). **(D)** Sections of tumors generated by injection of $CD24^+CD29^+$ tumor propagating cells of the salivary gland of double mutant mice into back skin of NOD/SCID mice. Cytokeratin 10 was highly expressed in differentiated but not in dedifferentiated parts of the tumors, as revealed by immunofluorescence analysis (CK10 in red, DAPI nuclei staining in blue). **(E)** Sections of tumors generated by injection of $CD24^+CD29^+$ tumor propagating cells of the salivary gland of double mutant mice into back skin of NOD/SCID mice. CK10 and CK14 are co-expressed by the tumor cells as revealed by immunofluorescence analysis (CK10 in red, CK14 in green, DAPI nuclear staining in blue). **(F)** FACS of salivary gland tumor cells from double mutant mice from secondary ($2^{nd}$) and tertiary ($3^{rd}$) transplanted tumors. High $CD24^+CD29^+$ expressing cells are marked by squares (insets), and quantification is shown above the squares (details on isotype control staining are shown in Supplementary Fig. 3). **(G)** Tumor outgrowths produced from subcutaneous injections of different cell numbers of unsorted or sorted $CD24^+CD29^+$ cells from secondary and tertiary tumors from double mutant glands into the back skin of NOD/SCID mice (each group n=3). Bar in D,E; 100 μm.

**Figure S5.** *Salivary gland $CD24^+CD29^+$ tumor propagating cells show increased expression of genes associated with maintenance of pluripotency and exhibit an increase in permissive and a decrease in repressive chromatin marks.* **(A)** Determination of active Bmp signaling by immunofluorescence for phospho-Smad 1/5/8 (in red; DAPI in blue) of cytospins of unsorted and $CD24^+CD29^+$ double-mutant mouse salivary gland squamous cell carcinoma cells (SG-SCC). Images from the analysis of two representative SG-SCC are shown. Quantifications are shown in **(B)**. Means and the standard deviations are shown and the P value is depicted (n=3,

Student's t-test). **(C)** qRT-PCR of sorted $CD24^{+}CD29^{+}$ salivary gland cells from single mutant and double mutant mice at P80 to validate the salivary gland tumor propagating cell gene signature shown in Fig. 3C, which was identified by Affymetrix microarray analysis (n=3, *p < 0.05, ANOVA, P values are as indicated by brackets, details shown in Supplementary Fig. 5D and Table S4). **(D)** Gene signature enriched in salivary gland tumor propagating cells of double mutant mice as determined by microarray profiling. Detailed expression is shown in Tables S2 and S4. **(E)** Immunofluorescence analysis for H3K9me3 of $CD24^{+}CD29^{+}$ salivary gland cells (red, DAPI in blue) from wt, single mutant (*Bmpr1a*$^{LOF}$ or *β-cat*$^{GOF}$) and double mutant mice. **(F)** Western blot analyses of tri-methylated H3K4, H3K27 and H3K9 from wt, single and double mutant mice (dm1, dm2) and from transplanted tumors (T1, T2). Histone 3 (H3) served as loading control. **(G)** Section of human salivary gland squamous cell carcinoma (SG-SCC) stained by immunofluorescence for H3K4me3 (in red) and β-catenin (in green, DAPI in blue). H3K4me3 co-localizes with nuclear β-catenin at the tumor fronts (white dotted line). Bars in A,D,F; 50 μm.

**Figure S6.** *The impact of high Wnt/β-catenin and low Bmp signaling on the expression of stem cell markers and self-renewal in human head and neck cancer. Salispheres of mouse tumor propagating cells respond to Wnt/β-catenin, HDAC and DNA methylation inhibitors.* **(A)** Human head and neck SCC cells (HNSCCUM-03T and HNSCCUM-02T) were analyzed by Western blotting for the expression of Axin2, pSmad1/5/8 and CD44. α-Tubulin served as a loading control. **(B)** Confirmation of the salivary gland tumor propagating cell-gene signature in human head and neck cancer cells, and effects on gene expression following treatment with either the Wnt/β-catenin activator CHIR or with the inhibitor ICG-001, as determined by qRT PCR. **(C)** Quantification of $CD24^{+}CD44^{+}$ cell populations in 03T and 02T cells treated with ICG-001 or CHIR, as determined by FACS. **(D)** Quantification of sphere formation of 03T and 02T cells treated with ICG-001 or CHIR. **(E)** H&E staining of a

differentiated salisphere; inset shows magnified duct-like structures. **(F)** Differentiated salispheres show lumen formation in electron microscopy. The magnification highlights secretory granules (asterisk) and tight junctions (arrow). **(G)** Induction of *Amylase 1* (*Amy1*) expression in differentiated salispheres, as detected by qRT PCR (n=3). **(H)** Phase-contrast images of salispheres in Matrigel cultures treated with valproic acid (VPA) and 5-azacytidine (Aza). In B,C,D and G, the means and the standard deviations are shown (n=3, *$p < 0.05$, Student's t-test). P values are as compared with controls. Bars in E,H; 100 µm, in F; 5 µm.

**Figure S7.** *High Wnt/β-catenin signals correlate with increased expression of HELLS, NR5A2 and MLL in both salivary gland tumor propagating cells of double-mutant mice and high grade human head and neck tumors.* **(A)** Western blot analyses of HELLS and NR5A2 from salivary gland tumor propagating cells from double mutant mice after treatment with ICG-001. Tubulin served as loading control. **(B)** Human head and neck SCC cells (03T and 02T) were analyzed by immunofluorescence for nuclear β-catenin (in green, DAPI in blue) and changes in β-catenin localization were determined upon treatment with the Wnt/β-catenin inhibitor ICG-001 at 25µM. **(C)** Quantification of H3K4me3-positive tumor propagating cells upon siRNA-induced knockdown of *Mll*, *β-catenin, CBP* and *Ash1* or treatment with the Wnt/β-catenin inhibitor ICG-001 at 25µM, as analyzed by immunofluorescence in Figure 6C. The means and the standard deviations (SD) are specified (n=3). **(D)** siRNA efficacy in double mutant ($\beta\text{-}cat^{GOF};Bmpr1a^{LOF}$) salivary gland tumor propagating cells. The effect of transiently transfected siRNA pools was analyzed by qPCR. Results are normalized for β-actin. **(E)** Immunofluorescence analysis for CD24 (in green) and MLL (in red, DAPI in blue) in salivary glands from wt, single mutant ($Bmpr1a^{LOF}$ or $\beta\text{-}cat^{GOF}$) and double mutant mice. High power insets and separate channels are shown. **(F,G)** Associations between nuclear β-catenin, nuclear MLL and the clinical parameter "tumor grade" were measured on an ordinal scale and evaluated using Kendall's Tau (for τ and p-values see Figure 6F,G, further details

are shown in Supplementary Table 1 and Materials and Methods). β-catenin and MLL expressions were determined by immunofluorescence analysis of human SG-SCC (n=13). **(H)** Quantification of NR5A2 expression in human head and neck cancer revealed increased levels in high grade tumors, as determined by immunohistochemistry (n=29, and data not shown). The bars give the means and standard deviations (***p <0.001, *p < 0.05, Student's t-test). P values are as compared with siCtr-transfected cells (D) or grade 2 tumors (H). Bars in B, E; 25 μm.

## Supplemental Reference

Chu, P. G., and Weiss, L. M. (2002). Keratin expression in human tissues and neoplasms. Histopathology 40, 403-439.

# Wend *et al.*, Suppl. Fig. 1

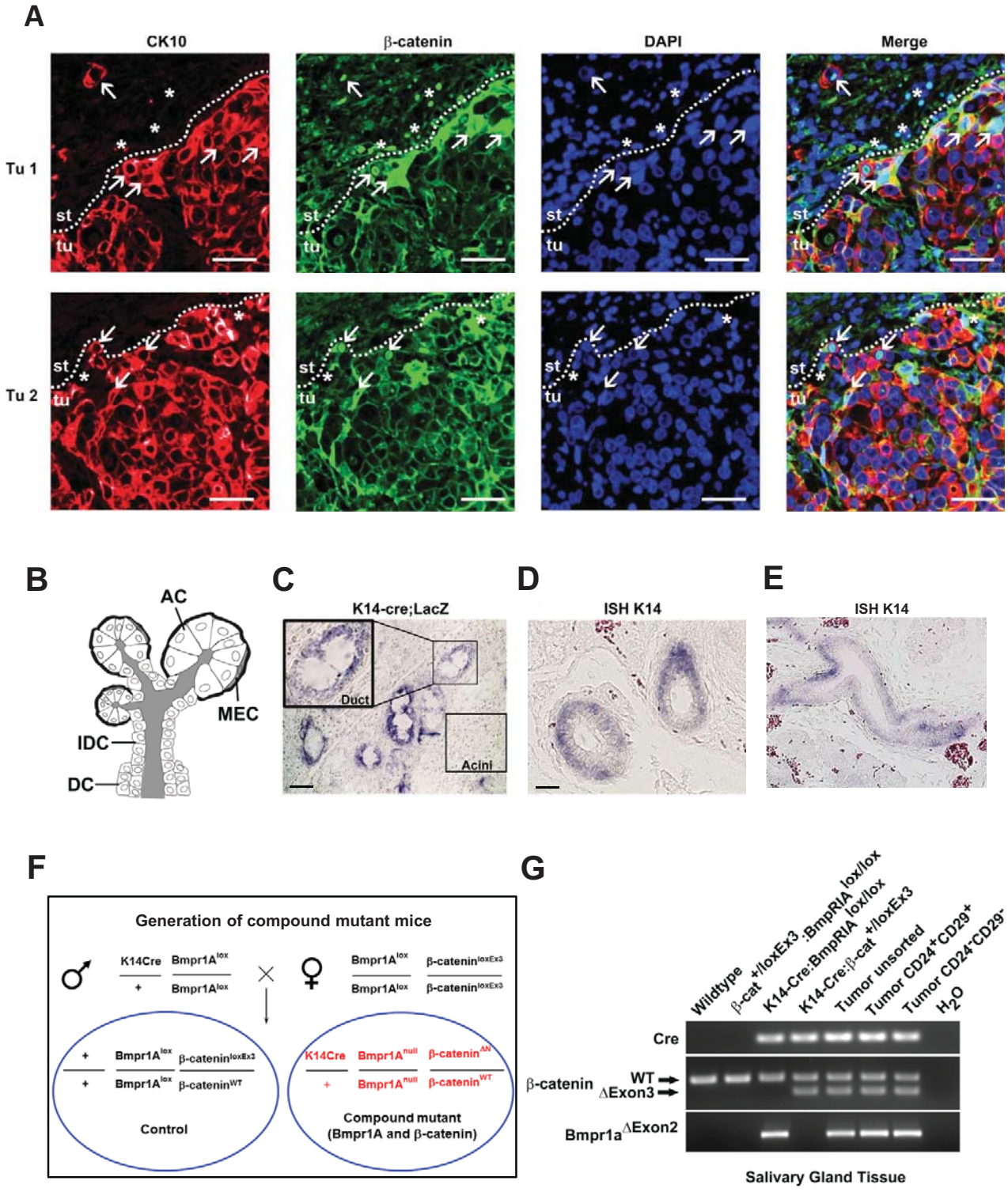

Wend *et al.*, Suppl. Fig. 2

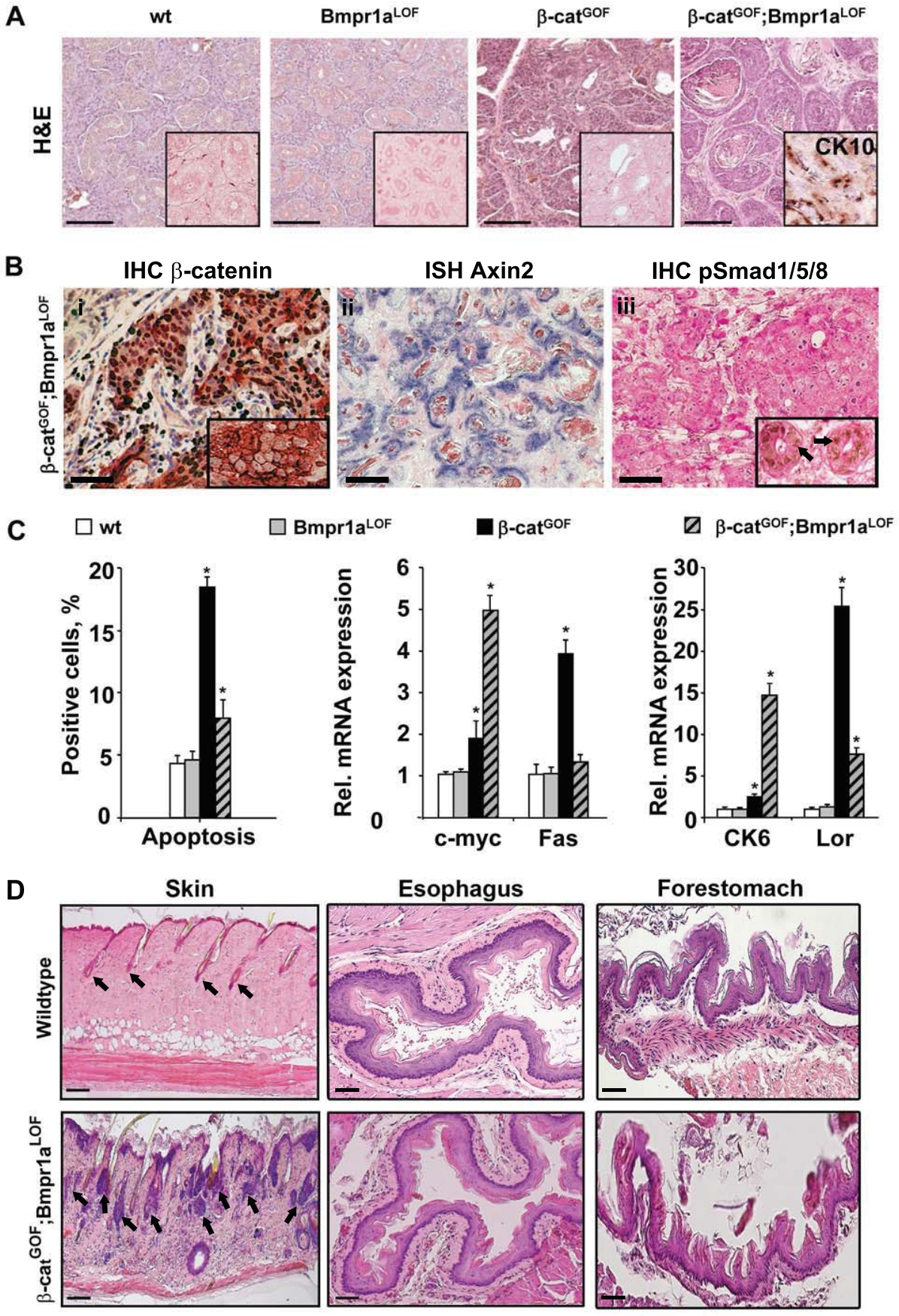

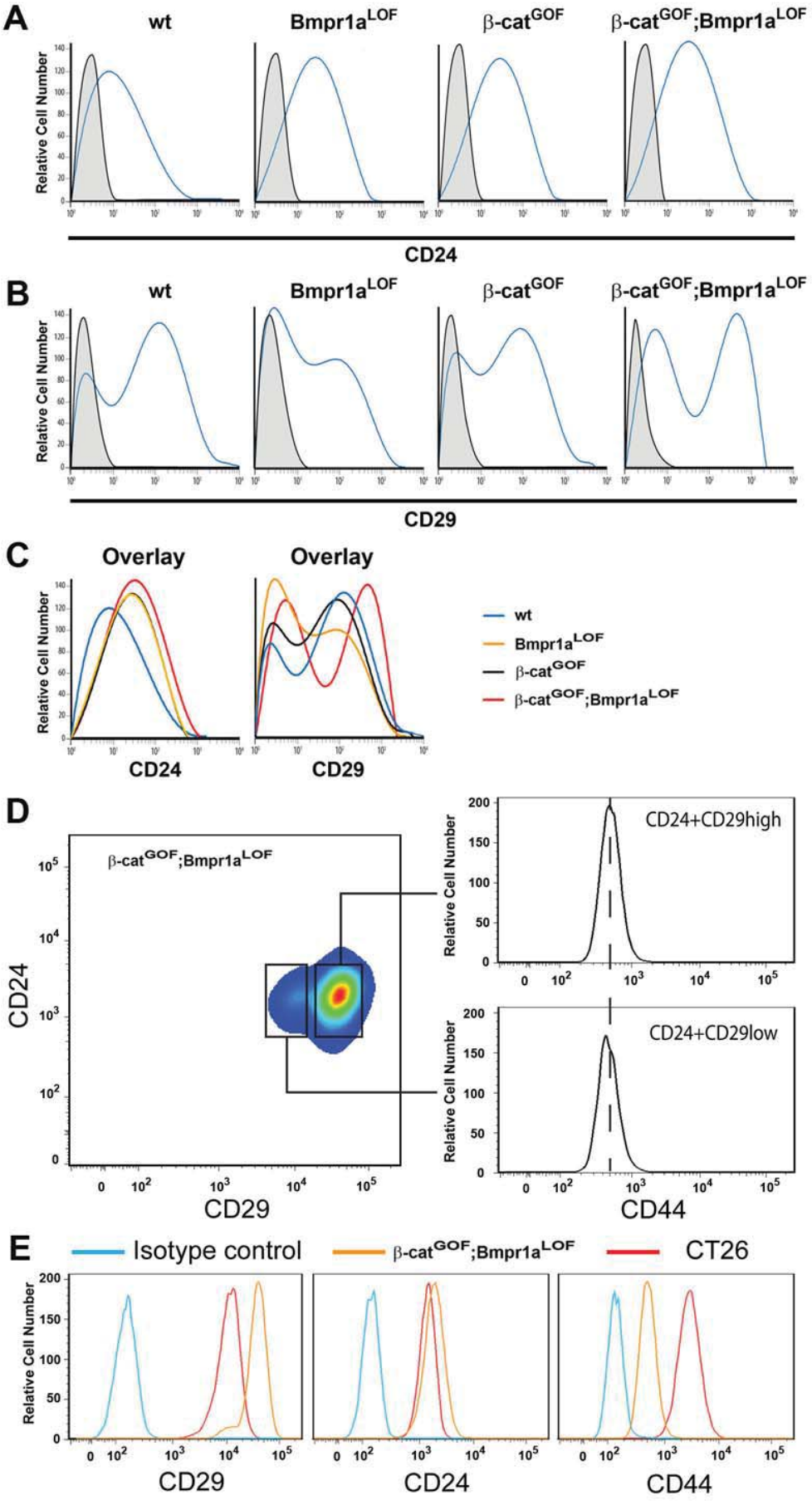
A
wt
Bmpr1a^LOF
β-cat^GOF
β-cat^GOF;Bmpr1a^LOF
Relative Cell Number
CD24
B
wt
Bmpr1a^LOF
β-cat^GOF
β-cat^GOF;Bmpr1a^LOF
Relative Cell Number
CD29
C
Overlay
Overlay
Relative Cell Number
CD24
CD29
wt
Bmpr1a^LOF
β-cat^GOF
β-cat^GOF;Bmpr1a^LOF
D
β-cat^GOF;Bmpr1a^LOF
CD24
CD29
CD24+CD29high
CD24+CD29low
Relative Cell Number
CD44
E
Isotype control
β-cat^GOF;Bmpr1a^LOF
CT26
Relative Cell Number
CD29
CD24
CD44

# Wend *et al.*, Suppl. Fig. 4

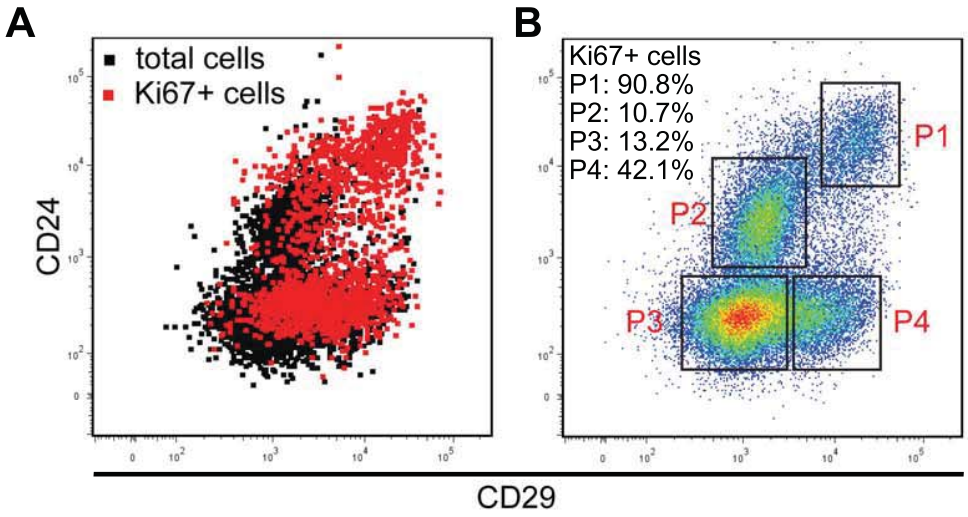


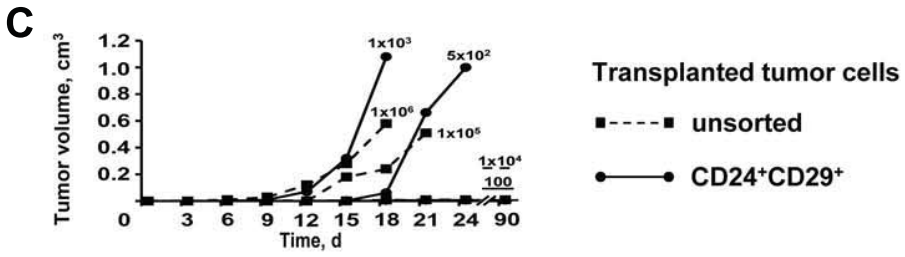


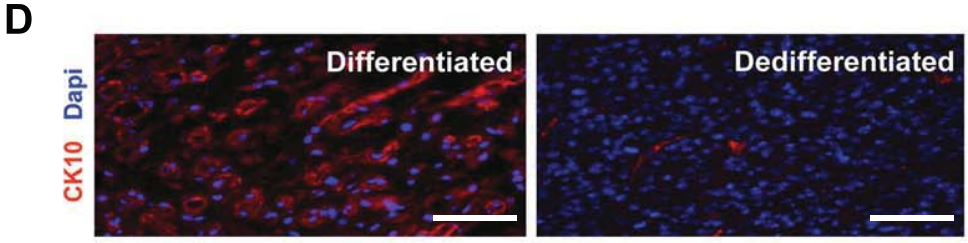


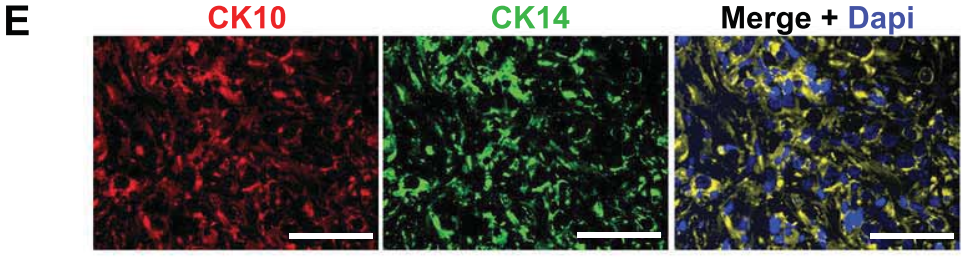


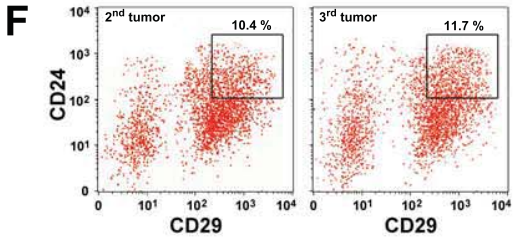


G

| Tumor | Transplanted cells | Tumor formation capacity | |
|---|---|---|---|
| | | Unsorted | $CD24^+CD29^+$ |
| 2nd | 100,000 | 1/3 | 3/3 |
| 2nd | 500 | 0/3 | 2/3 |
| 3rd | 100,000 | 2/3 | 3/3 |
| 3rd | 500 | 0/3 | 3/3 |

# Wend *et al.*, Suppl. Fig. 5

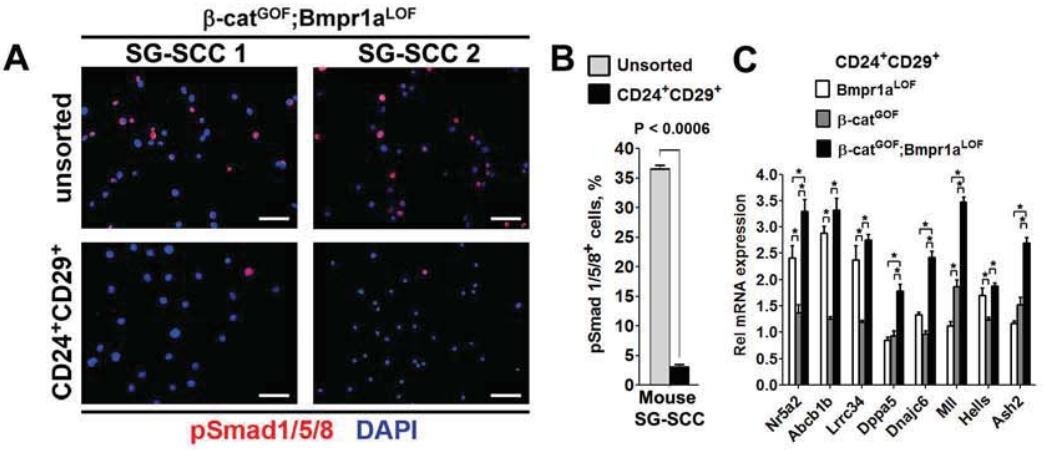


**D**

Affymetrix gene profiling of CD24$^{+}$CD29$^{+}$ salivary gland cells at P80.
Gene signature of CD24$^{+}$CD29$^{+}$ tumor propagating cells of the salivary gland.
[1] = Bmpr1a$^{LOF}$
[2] = β-cat$^{GOF}$
[3] =double mutant

| Symbol | fc [3] / [1] | p [3] / [1] | fc [3] / [2] | p [3] / [2] |
|---|---|---|---|---|
| Axin2 | 1,930 | 3,41E-04 | 1,898 | 8,07E-05 |
| Dnajc6 | 1,816 | 5,75E-04 | 2,491 | 2,97E-06 |
| Nr5a2 | 1,373 | 7,95E-05 | 2,409 | 3,09E-05 |
| Lrrc34 | 1,159 | 4,60E-04 | 2,309 | 1,19E-04 |
| Hells | 1,103 | 1,41E-05 | 1,515 | 6,14E-05 |
| Abcb1b | 1,075 | 5,07E-04 | 2,655 | 2,63E-05 |

Affymetrix gene profiling of salivary glands at P1.
[1] = β-cat$^{GOF}$
[2] =double mutant

| Symbol | fc [2]/[1] | p |
|---|---|---|
| Dppa5a | 2,139 | 1,99E-04 |
| Rnf2 | 1,626 | 2,80E-05 |
| Ash2 | 1,626 | 1,07E-05 |

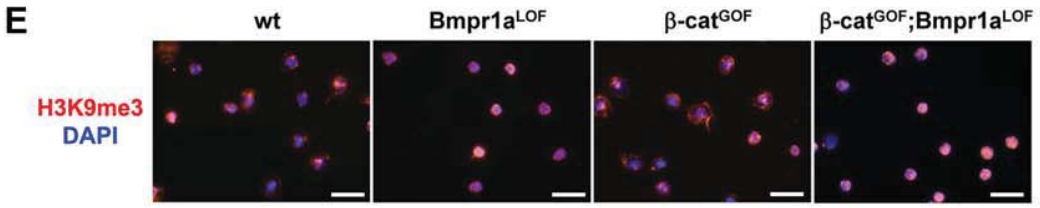


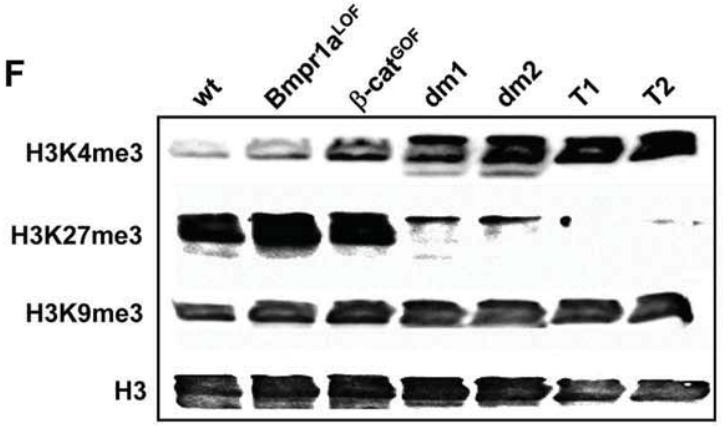


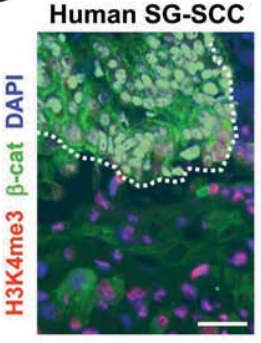

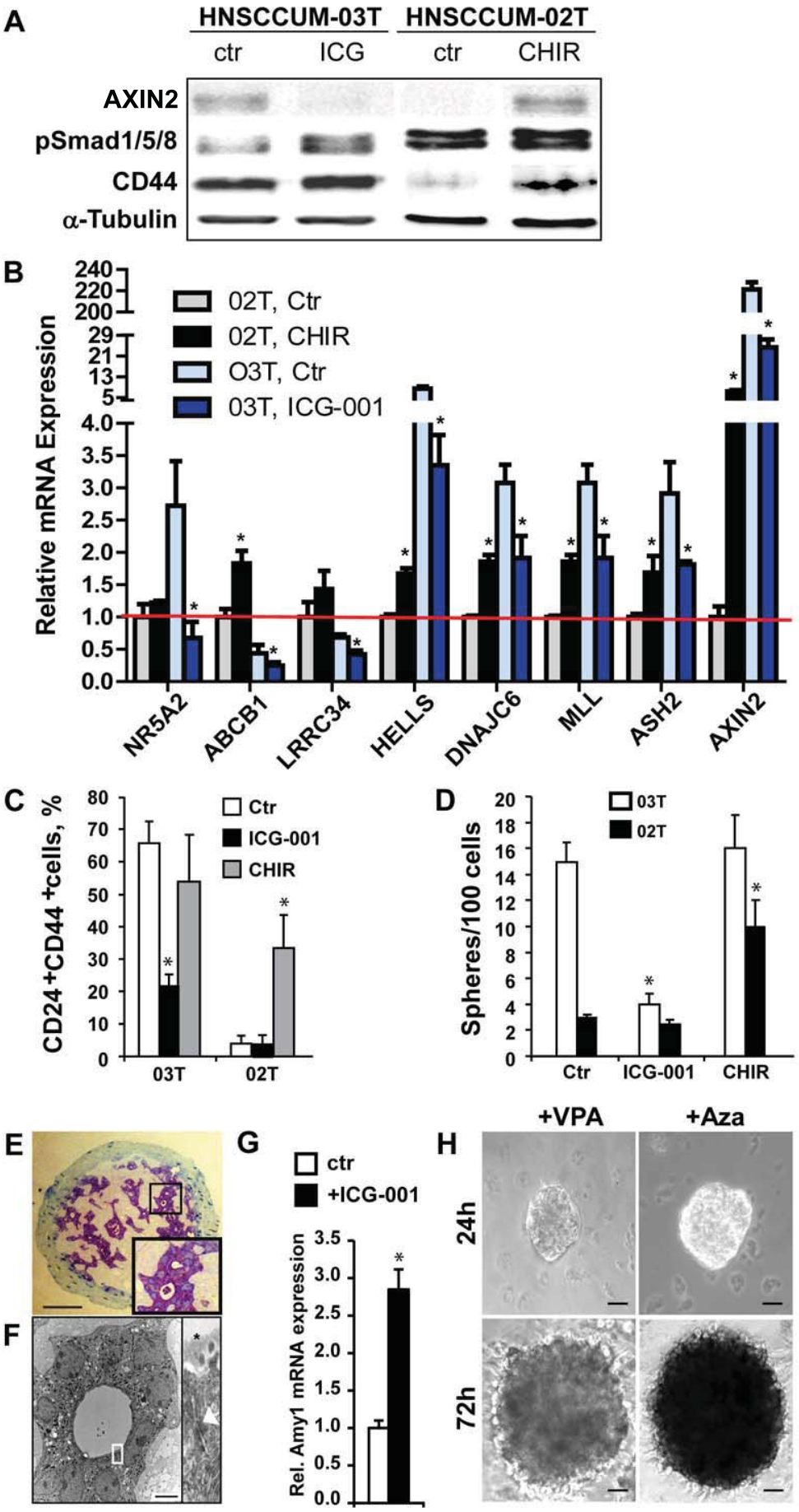
A
HNSCCUM-03T
HNSCCUM-02T
ctr
ICG
ctr
CHIR
AXIN2
pSmad1/5/8
CD44
α-Tubulin
B
Relative mRNA Expression
02T, Ctr
02T, CHIR
O3T, Ctr
03T, ICG-001
NR5A2
ABCB1
LRRC34
HELLS
DNAJC6
MLL
ASH2
AXIN2
C
CD24+CD44+cells, %
Ctr
ICG-001
CHIR
03T
02T
D
Spheres/100 cells
03T
02T
Ctr
ICG-001
CHIR
E
F
G
ctr
+ICG-001
Rel. Amy1 mRNA expression
H
+VPA
+Aza
24h
72h

**A**

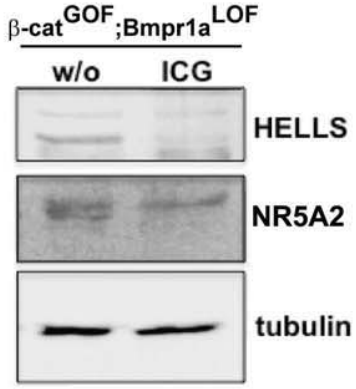


**B**

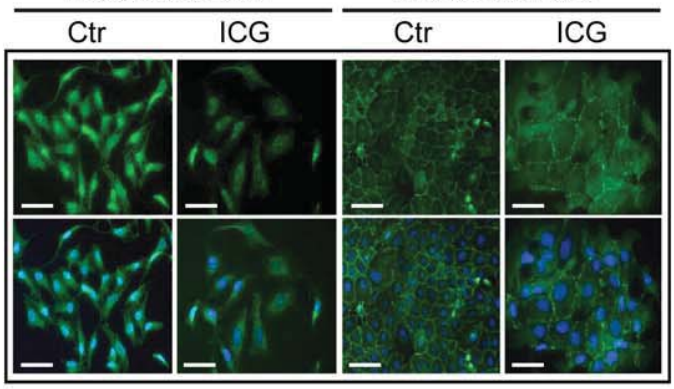


**C**

| Treatment | H3K4me3⁺ cells Mean (%) | SD (%) |
|---|---|---|
| siCtr | 97.6 | 5.9 |
| ICG-001 | 29.1 | 4.3 |
| siMll | 52.4 | 5.1 |
| siβ-catenin | 61.9 | 5.8 |
| siCBP | 63.2 | 4.7 |
| siAsh1 | 95.3 | 7.6 |

**D**

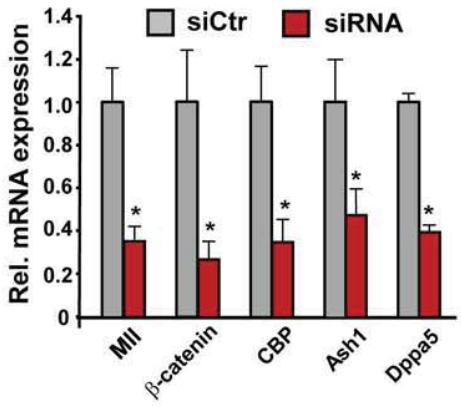


**E**

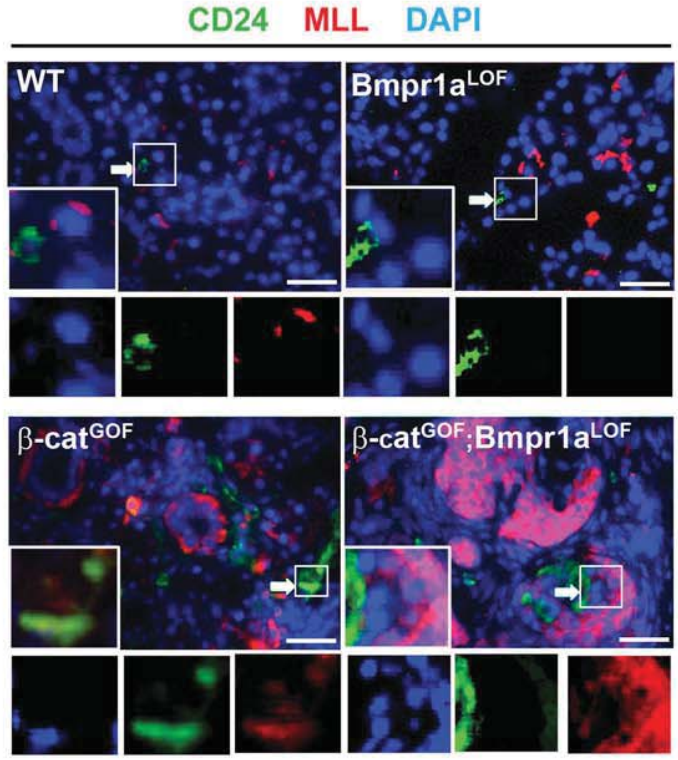


**F**

| Nuclear β-catenin | Nuclear MLL low | med | high | Total (n) (n) |
|---|---|---|---|---|
| low | 2 | 2 | 0 | 4 |
| med | 0 | 3 | 2 | 5 |
| high | 0 | 0 | 4 | 4 |
| Total (n) | 2 | 5 | 6 | 13 |

**G**

| | Marker expression | | | | | | Total (n) |
|---|---|---|---|---|---|---|---|
| | low | | medium | | high | | |
| Tumor Grade | β-cat | MLL | β-cat | MLL | β-cat | MLL | β-cat/MLL |
| 2 | 3 | 2 | 1 | 2 | 0 | 0 | 4/4 |
| 3 | 1 | 0 | 4 | 3 | 4 | 6 | 9/9 |
| Total (n) | 4 | 2 | 5 | 5 | 4 | 6 | 13/13 |

**H**

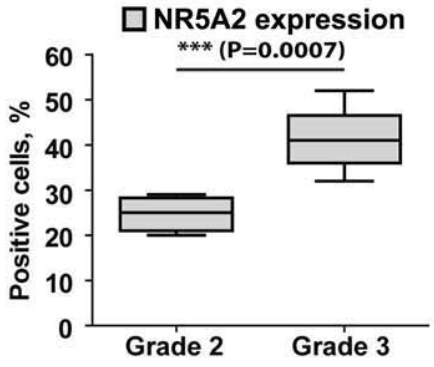

**Table S1: Characteristics of human salivary gland and head and neck SCCs.[1]**

| # | Origin | SG-SCC[2] # | Sex | Age at diagnosis (years) | Site | Grade | IHC β-catenin[3] | IHC pS1/5/8[3] | IHC MLL[3] |
|---|---|---|---|---|---|---|---|---|---|
| 1 | Ch Berlin[4] | 1 | M | 32 | parotid | 3 | n (n-high) | - | high |
| 2 | Ch Berlin | 2 | M | 55 | parotid | 2 | n (n-med) | - | med |
| 3 | Ch Berlin | 3 | F | 64 | parotid | 3 | n (n-med) | - | med |
| 4 | Ch Berlin | 4 | F | 71 | parotid | 3 | n (n-high) | - | high |
| 5 | Ch Berlin | 5 | F | 74 | parotid | 3 | n (n-med) | - | high |
| 6 | Ch Berlin | 6 | M | 76 | parotid | 3 | n (n-med) | - | high |
| 7 | Ch Berlin | 7 | F | 76 | parotid | 2 | m (n-low) | + | med |
| 8 | Ch Berlin | 8 | F | 76 | parotid | 3 | n (n-med) | - | med |
| 9 | Ch Berlin | 9 | M | 76 | parotid | 3 | n (n-high) | - | high |
| 10 | Ch Berlin | 10 | F | 79 | sublingual | 3 | m (n-low) | + | med |
| 11 | Ch Berlin | 11 | M | 80 | parotid | 3 | n (n-high) | - | high |
| 12 | Ch Berlin | 12 | F | 83 | parotid | 2 | m (n-low) | + | low |
| 13 | Ch Berlin | 13 | F | 94 | parotid | 2 | m (n-low) | + | low |
| 14 | UH Düss[5] | 14 | M | 61 | parotid | 2 | n | - | n.d. |
| 15 | UH Düss | 15 | F | 74 | parotid | 2 | m | + | n.d. |
| 16 | UH Düss | 16 | M | 76 | parotid | 2 | m | + | n.d. |
| 17 | UH Düss | 17 | M | 84 | parotid | 2 | m | + | n.d. |
| 18 | UH Düss | 18 | F | 90 | parotid | 3 | m | + | n.d. |
| | | | | Ø 73.4 ØF 78.1 ØM 67.5 | | | | | |
| | | HN-SCC[6] # | | | | | | | |
| 19 | UH Düss | 1 | M | 47 | mandible | 2 | n | - | n.d. |
| 20 | UH Düss | 2 | M | 49 | pharynx | 2 | m | + | n.d. |
| 21 | UH Düss | 3 | F | 49 | tongue | 2 | n | - | n.d. |
| 22 | UH Düss | 4 | M | 51 | tongue | 3 | n | - | n.d. |
| 23 | UH Düss | 5 | F | 52 | larynx | 3 | m | + | n.d. |
| 24 | UH Düss | 6 | M | 54 | mouth floor | 3 | n | - | n.d. |
| 25 | UH Düss | 7 | M | 57 | glottis | 2 | n | - | n.d. |
| 26 | UH Düss | 8 | M | 58 | pharynx | 1 | m | + | n.d. |
| 27 | UH Düss | 9 | M | 58 | pharynx | 2 | m | + | n.d. |
| 28 | UH Düss | 10 | M | 58 | tonsil | 2 | m | + | n.d. |
| 29 | UH Düss | 11 | M | 59 | larynx | 2 | m | + | n.d. |
| 30 | UH Düss | 12 | M | 59 | larynx | 2 | n | - | n.d. |
| 31 | UH Düss | 13 | M | 60 | pharynx | 2 | n | - | n.d. |
| 32 | UH Düss | 14 | F | 60 | pharynx | 2 | m | + | n.d. |
| 33 | UH Düss | 15 | M | 61 | pharynx | 2 | n | - | n.d. |
| 34 | UH Düss | 16 | M | 61 | tongue | 2 | m | + | n.d. |
| 35 | UH Düss | 17 | M | 65 | larynx | 1 | m | - | n.d. |
| 36 | UH Düss | 18 | M | 65 | mouth floor | 2 | m | + | n.d. |
| 37 | UH Düss | 19 | M | 66 | larynx | 2 | m | + | n.d. |
| 38 | UH Düss | 20 | M | 68 | pharynx | 2 | n | - | n.d. |
| 39 | UH Düss | 21 | M | 68 | mouth floor/tongue | 2 | n | - | n.d. |
| 40 | UH Düss | 22 | M | 71 | pharynx | 2 | m | + | n.d. |
| 41 | UH Düss | 23 | M | 73 | tonsil | 2 | m | + | n.d. |
| 42 | UH Düss | 24 | M | 73 | larynx | 2 | m | + | n.d. |
| 43 | UH Düss | 25 | M | 73 | tongue | 2 | m | + | n.d. |
| 44 | UH Düss | 26 | M | 74 | glottis/larynx | 2 | n | - | n.d. |
| 45 | UH Düss | 27 | M | 77 | pharynx | 2 | m | + | n.d. |
| 46 | UH Düss | 28 | M | 78 | pharynx | 2 | m | + | n.d. |
| 47 | UH Düss | 29 | M | 80 | glottis | 2 | m | - | n.d. |
| | | | | Ø 62.9 ØF 53.7 ØM 64.0 | | | | | |

[1]Tumor specimens from 47 patients with primary salivary gland and head and neck squamous cell carcinoma (SCC) were evaluated. Cases with possible metastatic origin were stringently excluded. Tumour staging and grading was performed according to current clinical and pathological classifications (Barnes et al, 2005).

[2]SG-SCC, salivary gland squamous cell carcinoma. Tumors with mucoepidermoid or adenoid origin were stringently excluded by our collaborating pathologists.
[3]Scoring was based on intensity and percentage of positively stained cells by immunohistochemistry (IHC) for β-catenin (intracellular localization as analyzed for Fig. 1A: n, nuclear in ≥ 20% of the cells; m, membrane; cp, cytoplasmic. Nuclear score "n" [in brackets] as analyzed for Fig. 6F,G: low; ≤5%, medium; 5-25%, high; ≥25%), p-Smad 1/5/8 (as analyzed for Fig. 1A: -/detectable in ≤ 10% of the cells; +/detectable in ≥ 10% of the cells), and MLL (Nuclear score as analyzed for Fig. 6F,G: low; ≤5%, medium; 5-20%, high; ≥20%). n.d.; not determined.
[4]Institute of Pathology, Charité University Medicine/UKBF, 12200 Berlin, Germany
[5]Department of Otorhinolaryngology, University Hospital Düsseldorf, 40225 Düsseldorf, Germany
[6]HN-SCC, head and neck squamous cell carcinoma.

Reference:

Barnes L, Eveson JW, Reichart P, Sidransky D (2005) World Health Organization Classification of Tumours, Pathology & Genetics of Head and Neck Tumours. *IARC Press, Lyon*

## Suppl. Table 2: Affymetrix gene profiling of salivary glands at P1.*

**[1] = β-cat$^{GOF}$**
**[2] =double mutant**

| Probe ID | Symbol/Description | fc [2]/[1] | p |
|---|---|---|---|
| 1420347_at | palate, lung, and nasal epithelium carcinoma associated | 66.667 | 8.22E-06 |
| 1447360_at | TSC22-related inducible leucine zipper 1b (Tilz1b) | 35.211 | 6.87E-05 |
| 1425447_at | dickkopf homolog 4 (Xenopus laevis) | 16.807 | 3.02E-06 |
| 1441172_at | AF4/FMR2 family, member 3 (Aff3), mRNA | 12.594 | 5.09E-04 |
| 1437894_at | prospero-related homeobox 1 | 6.024 | 2.93E-04 |
| 1429856_at | tetraspanin 18 | 5.464 | 3.94E-04 |
| 1450781_at | high mobility group AT-hook 2 | 5.291 | 2.06E-04 |
| 1446269_at | high mobility group box transcription factor 1 | 5.291 | 6.53E-06 |
| 1423635_at | bone morphogenetic protein 2 | 4.505 | 4.22E-05 |
| 1422833_at | forkhead box A2 | 4.484 | 2.23E-04 |
| 1422912_at | bone morphogenetic protein 4 | 3.968 | 3.32E-07 |
| 1428816_a_at | GATA binding protein 2 | 3.953 | 2.18E-04 |
| 1416693_at | forkhead box C2 | 3.817 | 6.93E-05 |
| 1441165_s_at | calsyntenin 2 | 3.717 | 4.91E-05 |
| 1420085_at | fibroblast growth factor 4 | 3.717 | 5.74E-05 |
| 1448877_at | distal-less homeobox 2 | 3.676 | 6.14E-06 |
| 1427489_at | integrin alpha 8 | 3.676 | 4.72E-04 |
| 1417278_a_at | naked cuticle 1 homolog (Drosophila) | 3.676 | 3.60E-05 |
| 1421299_a_at | lymphoid enhancer binding factor 1 | 3.623 | 1.99E-05 |
| 1416101_a_at | histone 1, H1c | 3.584 | 5.13E-07 |
| 1445123_at | Chromobox homolog 1 (Drosophila HP1 beta) (Cbx1), mRNA | 3.460 | 2.56E-05 |
| 1419735_at | casein kappa | 3.425 | 6.93E-05 |
| 1435950_at | hairless | 3.390 | 3.00E-04 |
| 1439663_at | Patched homolog 1 (Ptch1), mRNA | 3.390 | 1.22E-04 |
| 1420017_at | tetraspanin 8 | 3.390 | 6.35E-05 |
| 1449559_at | homeo box, msh-like 2 | 3.289 | 9.60E-05 |
| 1418471_at | placental growth factor | 3.257 | 1.94E-04 |
| 1452240_at | bruno-like 4, RNA binding protein (Drosophila) | 3.165 | 8.21E-05 |
| 1431166_at | chromodomain helicase DNA binding protein 1 | 3.058 | 5.07E-05 |
| 1416003_at | claudin 11 | 2.950 | 3.31E-06 |
| 1425425_a_at | Wnt inhibitory factor 1 | 2.874 | 4.74E-05 |
| 1422914_at | trans-acting transcription factor 5 | 2.865 | 2.56E-04 |
| 1449470_at | distal-less homeobox 1 | 2.857 | 3.92E-07 |
| 1435790_at | olfactomedin 2 | 2.817 | 3.11E-04 |
| 1449863_a_at | distal-less homeobox 5 | 2.725 | 1.43E-04 |
| 1437060_at | olfactomedin 4 | 2.674 | 5.24E-04 |
| 1453131_at | CD300 antigen like family member G | 2.591 | 5.74E-05 |
| 1443227_at | basic leucine zipper and W2 domains 2 | 2.584 | 7.53E-05 |
| 1421677_at | fibroblast growth factor 20 | 2.558 | 1.01E-05 |
| 1422655_at | patched homolog 2 | 2.532 | 5.69E-06 |
| 1451629_at | limb-bud and heart | 2.494 | 1.07E-06 |
| 1437419_at | BMP2 inducible kinase | 2.469 | 3.54E-04 |
| 1423671_at | delta/notch-like EGF-related receptor | 2.421 | 5.97E-05 |
| 1441350_at | fibroblast growth factor 3 | 2.410 | 1.66E-06 |
| 1434559_at | syntaxin 3 | 2.398 | 5.66E-05 |
| 1450135_at | frizzled homolog 3 (Drosophila) | 2.387 | 3.41E-05 |
| 1440274_at | CAMP-GEFII | 2.370 | 9.77E-06 |
| 1449049_at | toll-like receptor 1 | 2.364 | 1.60E-04 |
| 1459720_x_at | Timeless interacting protein (Tipin), mRNA | 2.353 | 2.61E-06 |
| 1443087_at | CDC23 (cell division cycle 23, yeast, homolog) | 2.304 | 5.15E-06 |
| 1450475_at | distal-less homeobox 3 | 2.304 | 6.01E-04 |
| 1422985_at | frizzled homolog 1 (Drosophila) | 2.273 | 3.29E-07 |
| 1424446_at | armadillo repeat containing 7 | 2.257 | 1.73E-04 |

| | | | |
|---|---|---|---|
| 1435521_at | Musashi homolog 2 (Drosophila) | 2.252 | 3.75E-04 |
| 1433471_at | transcription factor 7, T-cell specific | 2.252 | 1.68E-07 |
| 1422537_a_at | inhibitor of DNA binding 2 | 2.227 | 6.08E-04 |
| 1427328_a_at | CLIP associating protein 2 | 2.217 | 1.42E-04 |
| 1456746_a_at | Cd99 antigen-like 2 | 2.203 | 1.91E-05 |
| 1428014_at | histone 1, H4h | 2.203 | 1.38E-04 |
| 1423259_at | inhibitor of DNA binding 4 | 2.193 | 6.03E-05 |
| 1431053_at | M-phase phosphoprotein 9 | 2.169 | 1.04E-04 |
| 1454086_a_at | LIM domain only 2 | 2.160 | 1.16E-05 |
| 1448886_at | GATA binding protein 3 | 2.151 | 8.15E-05 |
| 1416552_at | Dppa5a, developmental pluripotency associated 5A, Esg1, ecat2 | 2.139 | 1.99E-04 |
| 1428424_at | polycomb group ring finger 3 | 2.137 | 1.25E-04 |
| 1434593_at | eukaryotic translation initiation factor 5A2 | 2.128 | 1.26E-04 |
| 1456341_a_at | Kruppel-like factor 9 | 2.128 | 4.53E-04 |
| 1441339_at | chromodomain helicase DNA binding protein 9 | 2.123 | 2.81E-06 |
| 1421341_at | axin2 | 2.114 | 1.81E-05 |
| 1425611_a_at | cut-like 1 (Drosophila) | 2.105 | 1.48E-04 |
| 1429217_at | zinc finger protein 655 | 2.075 | 4.04E-04 |
| 1450082_s_at | ets variant gene 5 | 2.066 | 1.33E-05 |
| 1436218_at | leucine-rich repeat-containing G protein-coupled receptor 6 | 2.066 | 4.98E-06 |
| 1445315_at | WNK lysine deficient protein kinase 2 | 2.066 | 6.16E-04 |
| 1430216_at | zinc finger protein 292 | 2.058 | 9.40E-05 |
| 1449317_at | CASP8 and FADD-like apoptosis regulator | 2.053 | 4.70E-05 |
| 1427540_at | ZW10 interactor | 2.045 | 9.09E-06 |
| 1448925_at | twist homolog 2 (Drosophila) | 2.033 | 3.61E-04 |
| 1419380_at | zinc finger protein 423 | 2.024 | 3.69E-06 |
| 1441938_x_at | Cdk5 and Abl enzyme substrate 1 | 2.020 | 4.31E-05 |
| 1455280_at | Fras1 related extracellular matrix protein 1 | 2.016 | 2.64E-05 |
| 1440086_at | ring finger protein 182 | 2.000 | 4.71E-04 |
| 1437904_at | developmentally regulated RNA binding protein 1 | 1.965 | 4.06E-04 |
| 1446259_at | CD180 antigen (Cd180), mRNA | 1.961 | 3.54E-05 |
| 1437395_at | zinc finger, CCHC domain containing 11 | 1.961 | 1.08E-04 |
| 1427526_at | FGFR1 oncogene partner 2 | 1.949 | 1.02E-04 |
| 1455823_at | Bardet-Biedl syndrome 4 homolog (human) | 1.942 | 2.27E-04 |
| 1438815_at | histone 2, H2aa2 | 1.927 | 5.80E-04 |
| 1419848_x_at | toll-like receptor 7 | 1.927 | 3.30E-06 |
| 1460725_at | xeroderma pigmentosum, complementation group A | 1.927 | 5.50E-05 |
| 1448158_at | syndecan 1 | 1.923 | 5.95E-06 |
| 1416129_at | ERBB receptor feedback inhibitor 1 | 1.919 | 1.82E-05 |
| 1448742_at | snail homolog 1 (Drosophila) | 1.916 | 6.53E-05 |
| 1443962_at | transcription factor Dp 2 | 1.916 | 2.60E-04 |
| 1452021_a_at | hairy and enhancer of split 6 (Drosophila) | 1.908 | 4.75E-06 |
| 1425895_a_at | inhibitor of DNA binding 1 | 1.905 | 5.82E-04 |
| 1457276_at | SNF1-like kinase 2 | 1.894 | 4.21E-06 |
| 1453688_at | CWF19-like 2, cell cycle control (S. pombe) | 1.890 | 1.17E-04 |
| 1457586_at | RAS p21 protein activator 2 (Rasa2), mRNA | 1.873 | 5.35E-05 |
| 1436469_at | Bromodomain containing 7 (Brd7), mRNA | 1.862 | 4.86E-04 |
| 1434196_at | DnaJ (Hsp40) homolog, subfamily A, member 4 | 1.862 | 4.81E-05 |
| 1455717_s_at | dishevelled associated activator of morphogenesis 2 | 1.859 | 1.78E-04 |
| 1416451_s_at | taube nuss | 1.859 | 1.94E-05 |
| 1437162_at | GPI-anchored membrane protein 1 (Gpiap1), mRNA | 1.855 | 2.13E-05 |
| 1445314_at | ets variant gene 1 | 1.852 | 2.01E-04 |
| 1459910_at | tankyrase, TRF1-interacting ankyrin-related ADP-ribose polymerase | 1.845 | 3.65E-05 |
| 1416630_at | inhibitor of DNA binding 3 | 1.825 | 2.65E-05 |
| 1424614_at | FGF receptor activating protein 1 | 1.818 | 4.43E-05 |
| 1429634_at | zinc finger protein 580 | 1.815 | 1.05E-04 |
| 1443002_at | zinc finger RNA binding protein | 1.805 | 2.92E-04 |
| 1429962_at | CCAAT/enhancer binding protein zeta | 1.799 | 5.56E-05 |
| 1457327_at | SNF2 histone linker PHD RING helicase | 1.786 | 7.95E-07 |
| 1457038_at | Fras1 related extracellular matrix protein 2 | 1.783 | 2.94E-05 |
| 1443471_at | zinc finger and BTB domain containing 20 | 1.783 | 2.02E-04 |
| 1425107_a_at | leukemia inhibitory factor receptor | 1.779 | 2.04E-05 |

| | | | |
|---|---|---|---|
| 1451281_at | zinc finger protein 96 | 1.779 | 2.41E-05 |
| 1422031_a_at | zinc finger, A20 domain containing 3 | 1.779 | 2.10E-04 |
| 1422470_at | BCL2/adenovirus E1B 19kDa-interacting protein 1, NIP3 | 1.776 | 2.68E-06 |
| 1419816_s_at | ERBB receptor feedback inhibitor 1 | 1.776 | 1.02E-04 |
| 1428574_a_at | chimerin (chimaerin) 2 | 1.770 | 3.75E-04 |
| 1424074_at | basic transcription factor 3-like 4 | 1.767 | 7.20E-08 |
| 1419716_a_at | POU domain, class 2, transcription factor 1 | 1.764 | 2.12E-04 |
| 1456351_at | bromodomain containing 8 | 1.761 | 2.27E-04 |
| 1448662_at | frizzled homolog 6 (Drosophila) | 1.754 | 3.08E-04 |
| 1425464_at | GATA binding protein 6 | 1.751 | 2.84E-04 |
| 1418176_at | vitamin D receptor | 1.748 | 8.72E-07 |
| 1429399_at | ring finger protein 125 | 1.745 | 4.02E-05 |
| 1441467_at | Tetraspanin 5 (Tspan5), mRNA | 1.730 | 9.28E-05 |
| 1417958_at | tetraspan 1 | 1.727 | 2.04E-07 |
| 1455188_at | Eph receptor B1 | 1.724 | 3.03E-05 |
| 1443240_at | Glypican 3, mRNA (cDNA clone MGC:35964 IMAGE:4973409) | 1.724 | 3.22E-04 |
| 1423040_at | basic leucine zipper and W2 domains 1 | 1.721 | 1.81E-04 |
| 1428253_at | chromatin modifying protein 2B | 1.715 | 2.73E-05 |
| 1419144_at | CD163 antigen | 1.712 | 1.82E-06 |
| 1440341_at | Colony stimulating factor 1 receptor (Csf1r), mRNA | 1.712 | 3.25E-04 |
| 1434033_at | transducin-like enhancer of split 1, homolog of Drosophila E(spl) | 1.712 | 2.02E-05 |
| 1427300_at | LIM homeobox protein 8 | 1.706 | 9.39E-06 |
| 1427200_at | zinc finger, RAN-binding domain containing 1 | 1.698 | 3.45E-06 |
| 1449314_at | zinc finger protein, multitype 2 | 1.678 | 1.32E-05 |
| 1444667_at | bromodomain, testis-specific | 1.675 | 9.94E-05 |
| 1448789_at | aldehyde dehydrogenase family 1, subfamily A3 | 1.667 | 2.33E-05 |
| 1417182_at | DnaJ (Hsp40) homolog, subfamily A, member 2 | 1.664 | 3.22E-04 |
| 1438239_at | midline 1 | 1.661 | 1.63E-05 |
| 1448147_at | tumor necrosis factor receptor superfamily, member 19 | 1.661 | 6.21E-05 |
| 1428396_at | SMAD specific E3 ubiquitin protein ligase 1 | 1.658 | 1.14E-04 |
| 1447944_at | zinc finger with KRAB and SCAN domains 1 | 1.658 | 2.19E-04 |
| 1419368_a_at | ring finger protein 138 | 1.656 | 1.03E-04 |
| 1457441_at | early B-cell factor 1 | 1.647 | 3.28E-06 |
| 1426152_a_at | kit ligand | 1.647 | 7.29E-07 |
| 1451191_at | cellular retinoic acid binding protein II | 1.639 | 1.13E-04 |
| 1418147_at | transcription factor AP-2, gamma | 1.639 | 7.92E-08 |
| 1426151_a_at | syntaxin 3 | 1.634 | 5.37E-05 |
| 1448042_s_at | Rnf2, ring finger protein 2 AI326319, AI450156, AU019207, Ring1B | 1.626 | 2.80E-05 |
| 1441042_at | fibroblast growth factor 1 | 1.626 | 2.01E-04 |
| 1421412_at | goosecoid | 1.626 | 6.17E-06 |
| 1420615_at | ash2 (absent, small, or homeotic)-like (Drosophila) | 1.626 | 1.07E-05 |
| 1458450_at | zinc finger RNA binding protein | 1.623 | 1.21E-05 |
| 1423702_at | H1 histone family, member 0 | 1.621 | 5.80E-06 |
| 1422932_a_at | vav 1 oncogene | 1.621 | 5.27E-07 |
| 1418671_at | calpain 5 | 1.616 | 4.40E-04 |
| 1422021_at | sprouty homolog 4 (Drosophila) | 1.613 | 5.05E-05 |
| 1448366_at | syntaxin 1A (brain) | 1.613 | 6.67E-06 |
| 1440585_at | syntaxin 6 | 1.613 | 1.76E-04 |
| 1460441_at | zinc finger, X-linked, duplicated A | 1.613 | 6.27E-06 |
| 1434949_at | armadillo repeat containing 8 | 1.608 | 6.70E-05 |
| 1427956_at | polycomb group ring finger 1 | 1.608 | 1.37E-04 |
| 1416111_at | CD83 antigen | 1.603 | 6.06E-07 |
| 1427941_at | Dicer1, Dcr-1 homolog (Drosophila) | 1.603 | 1.48E-06 |
| 1427454_at | homeo box C6 | 1.603 | 7.72E-05 |
| 1451739_at | Kruppel-like factor 5 | 1.603 | 5.55E-08 |
| 1417839_at | claudin 5 | 1.600 | 3.16E-04 |
| 1425555_at | CDC2-related kinase 7 | 1.597 | 8.02E-06 |
| 1441544_at | Cyclin M3 (Cnnm3), mRNA | 1.597 | 2.81E-07 |
| 1421298_a_at | homeodomain interacting protein kinase 1 | 1.597 | 1.29E-04 |
| 1446349_at | zinc finger protein 78 | 1.597 | 4.09E-06 |
| 1421943_at | transforming growth factor alpha | 1.595 | 2.78E-06 |
| 1446048_at | Cadherin 11 (Cdh11), mRNA | 1.592 | 5.51E-05 |

| | | | |
|---|---|---|---|
| 1427618_at | cadherin 9 | 1.592 | 2.44E-06 |
| 1435903_at | CD300A antigen | 1.592 | 1.17E-05 |
| 1416895_at | ephrin A1 | 1.592 | 7.44E-06 |
| 1454880_s_at | Bcl2 modifying factor | 1.590 | 1.52E-04 |
| 1451156_s_at | very low density lipoprotein receptor | 1.590 | 2.75E-04 |
| 1423528_at | breast carcinoma amplified sequence 3 | 1.585 | 4.32E-05 |
| 1429086_at | grainyhead-like 2 (Drosophila) | 1.585 | 6.98E-05 |
| 1419126_at | homeo box D9 | 1.585 | 2.65E-04 |
| 1418213_at | keratin complex 1, acidic, gene 23 | 1.585 | 2.44E-07 |
| 1419356_at | Kruppel-like factor 7 (ubiquitous) | 1.582 | 1.14E-04 |
| 1420376_a_at | H3 histone, family 3B | 1.580 | 2.89E-05 |
| 1438495_at | topoisomerase (DNA) I | 1.580 | 1.27E-04 |
| 1425693_at | Braf transforming gene | 1.577 | 4.40E-06 |
| 1442757_at | leucine-rich repeats and calponin homology (CH) domain containing 1 | 1.577 | 1.37E-06 |
| 1449732_at | zinc finger proliferation 1 | 1.575 | 9.62E-05 |
| 1434234_at | zinc finger protein 341 | 1.575 | 3.62E-06 |
| 1444328_at | clathrin, light polypeptide (Lca) | 1.572 | 6.46E-06 |
| 1424355_a_at | transcriptional regulator, SIN3B (yeast) | 1.570 | 2.90E-06 |
| 1421151_a_at | Eph receptor A2 | 1.567 | 2.96E-04 |
| 1439638_at | Erbb2 interacting protein | 1.567 | 2.09E-06 |
| 1419874_x_at | zinc finger and BTB domain containing 16 | 1.567 | 9.97E-05 |
| 1426753_at | PHD finger protein 17 | 1.565 | 1.66E-06 |
| 1453247_at | zinc fingerprotein 618 | 1.565 | 9.53E-06 |
| 1416511_a_at | CDC42 effector protein (Rho GTPase binding) 4 | 1.563 | 2.55E-04 |
| 1418285_at | ephrin B1 | 1.563 | 2.82E-05 |
| 1417394_at | Kruppel-like factor 4 (gut) | 1.563 | 1.25E-05 |
| 1455658_at | CGG triplet repeat binding protein 1 | 1.560 | 3.24E-05 |
| 1452718_at | E3 ubiquitin protein ligase, HECT domain containing, 1 | 1.560 | 8.96E-05 |
| 1426332_a_at | claudin 3 | 1.558 | 6.84E-04 |
| 1439079_a_at | Erbb2 interacting protein | 1.558 | 3.88E-06 |
| 1448765_at | Fyn proto-oncogene | 1.555 | 1.46E-05 |
| 1418478_at | LIM domain only 1 | 1.555 | 2.93E-06 |
| 1426981_at | proprotein convertase subtilisin/kexin type 6 | 1.550 | 4.61E-06 |
| 1428034_a_at | tumor necrosis factor receptor superfamily, member 9 | 1.548 | 7.45E-06 |
| 1424298_at | zinc finger protein 282 | 1.548 | 4.77E-06 |
| 1419474_a_at | ets homologous factor | 1.546 | 2.94E-07 |
| 1424638_at | cyclin-dependent kinase inhibitor 1A (P21) | 1.543 | 4.10E-04 |
| 1434370_s_at | Fas-associated factor 1 | 1.543 | 4.14E-07 |
| 1418581_a_at | LIM motif-containing protein kinase 2 | 1.543 | 9.36E-05 |
| 1437657_at | zinc finger protein 291 | 1.543 | 7.10E-06 |
| 1454305_at | chromobox homolog 3 (Drosophila HP1 gamma) | 1.541 | 7.20E-04 |
| 1455368_at | zinc finger, DHHC domain containing 3 | 1.541 | 4.87E-05 |
| 1423805_at | disabled homolog 2 (Drosophila) | 1.538 | 5.69E-07 |
| 1453848_s_at | zinc finger, BED domain containing 3 | 1.538 | 6.44E-06 |
| 1421005_at | centrosomal protein 1 | 1.536 | 1.13E-05 |
| 1457577_at | Ephrin B2 (Efnb2), mRNA | 1.536 | 7.94E-05 |
| 1424127_at | eyes absent 2 homolog (Drosophila) | 1.536 | 2.93E-06 |
| 1441635_at | Germ cell nuclear factor protein (Nr6a1) | 1.536 | 2.42E-05 |
| 1455725_a_at | H3 histone, family 3B | 1.536 | 5.76E-05 |
| 1419654_at | transducin-like enhancer of split 3, homolog of Drosophila E(spl) | 1.536 | 3.29E-05 |
| 1428634_at | TWIST neighbor | 1.536 | 1.89E-04 |
| 1456639_at | zinc finger protein 398 | 1.536 | 1.56E-05 |
| 1451696_at | zinc finger protein 64 | 1.536 | 2.78E-08 |
| 1449126_at | zinc finger protein 90 | 1.536 | 1.66E-06 |
| 1425092_at | cadherin 10 | 1.534 | 3.09E-05 |
| 1439019_at | Fraser syndrome 1 homolog (human) | 1.531 | 1.02E-05 |
| 1431993_a_at | ring finger protein 38 | 1.531 | 1.60E-04 |
| 1444246_at | chromodomain helicase DNA binding protein 2 | 1.527 | 9.26E-07 |
| 1433507_a_at | high mobility group nucleosomal binding domain 2 | 1.527 | 2.05E-07 |
| 1450267_at | toll-like receptor 8 | 1.527 | 2.62E-05 |
| 1428378_at | zinc finger CCCH type, antiviral 1 | 1.527 | 7.87E-06 |
| 1452504_s_at | chitobiase, di-N-acetyl- | 1.524 | 2.97E-05 |

| | | | |
|---|---|---|---|
| 1426124_a_at | CDC-like kinase 1 | 1.522 | 4.48E-04 |
| 1423203_a_at | centrin 1 | 1.520 | 3.93E-05 |
| 1453415_at | zinc finger CCCH type containing 6 | 1.520 | 3.85E-05 |
| 1419307_at | tumor necrosis factor receptor superfamily, member 13c | 1.517 | 1.26E-05 |
| 1435071_at | zinc finger, FYVE domain containing 1 | 1.517 | 5.08E-05 |
| 1439080_at | Erbb2 interacting protein | 1.515 | 2.55E-04 |
| 1435608_at | zinc and ring finger 3 | 1.515 | 7.58E-06 |
| 1434236_at | zinc finger, DHHC domain containing 20 | 1.515 | 3.33E-06 |
| 1437201_at | leucine rich repeat containing 4C | 1.513 | 1.23E-06 |
| 1419369_at | ring finger protein 138 | 1.513 | 6.77E-05 |
| 1456912_at | zinc finger protein 691 | 1.513 | 2.30E-05 |
| 1420745_a_at | cyclin D-type binding-protein 1 | 1.511 | 3.78E-04 |
| 1445635_at | Eph receptor A7, mRNA (cDNA clone MGC:14056 IMAGE:3991628) | 1.508 | 4.73E-07 |
| 1449295_at | transcriptional regulator protein | 1.508 | 2.84E-05 |
| 1434651_a_at | claudin 3 | 1.506 | 6.78E-05 |
| 1421604_a_at | Kruppel-like factor 3 (basic) | 1.506 | 1.12E-05 |
| 1425635_at | tyrosine kinase, non-receptor, 1 | 1.506 | 3.03E-04 |
| 1420675_at | zinc finger protein 113 | 0.664 | 3.65E-04 |
| 1429111_at | talin 2 | 0.663 | 1.39E-06 |
| 1448837_at | villin 1 | 0.663 | 8.08E-06 |
| 1416757_at | Zwilch, kinetochore associated, homolog (Drosophila) | 0.663 | 1.95E-04 |
| 1459009_at | Utrophin | 0.662 | 3.35E-07 |
| 1424789_at | GLI-Kruppel family member HKR2 | 0.661 | 3.29E-04 |
| 1434824_at | bromodomain adjacent to zinc finger domain, 1B | 0.661 | 4.18E-04 |
| 1459589_at | crystallin, lamda 1 | 0.658 | 4.71E-04 |
| 1419979_s_at | cAMP responsive element binding protein 3 | 0.657 | 4.54E-04 |
| 1433592_at | calmodulin 1 | 0.657 | 1.00E-06 |
| 1419573_a_at | lectin, galactose binding, soluble 1 | 0.656 | 4.00E-05 |
| 1445534_at | Filamin, beta, mRNA (cDNA clone IMAGE:3488025) | 0.655 | 8.48E-05 |
| 1438861_at | basonuclin 2 | 0.654 | 1.49E-07 |
| 1420631_a_at | bladder cancer associated protein homolog (human) | 0.654 | 3.66E-05 |
| 1449233_at | basic helix-loop-helix domain containing, class B, 8 | 0.652 | 3.29E-04 |
| 1438498_at | zinc finger, MYND domain containing 15 | 0.652 | 3.31E-04 |
| 1423505_at | transgelin | 0.651 | 2.61E-05 |
| 1451537_at | chitinase 3-like 1 | 0.651 | 3.94E-06 |
| 1452968_at | collagen triple helix repeat containing 1 | 0.650 | 1.38E-04 |
| 1448594_at | WNT1 inducible signaling pathway protein 1 | 0.648 | 8.58E-06 |
| 1417067_s_at | chaperone, ABC1 activity of bc1 complex like (S. pombe) | 0.648 | 7.80E-06 |
| 1422748_at | zinc finger homeobox 1b | 0.647 | 2.61E-06 |
| 1441198_at | zinc finger protein 39 | 0.647 | 2.92E-05 |
| 1458141_at | CAMP specific phosphodiesterase 7B (PDE7B gene) | 0.646 | 7.38E-05 |
| 1416246_a_at | coronin, actin binding protein 1A | 0.646 | 4.05E-06 |
| 1421251_at | zinc finger protein 40 | 0.646 | 2.28E-04 |
| 1456405_at | death inducer-obliterator 1 | 0.645 | 3.87E-05 |
| 1450416_at | chromobox homolog 5 (Drosophila HP1a) | 0.641 | 1.26E-04 |
| 1452265_at | CLIP associating protein 1 | 0.641 | 8.21E-06 |
| 1417457_at | CDC28 protein kinase regulatory subunit 2 | 0.641 | 8.39E-05 |
| 1422308_a_at | lectin, galactose binding, soluble 7 | 0.641 | 1.36E-04 |
| 1438817_at | DNA2 DNA replication helicase 2-like (yeast) | 0.640 | 3.07E-06 |
| 1426808_at | lectin, galactose binding, soluble 3 | 0.640 | 3.30E-05 |
| 1424698_s_at | grancalcin | 0.639 | 4.38E-04 |
| 1438833_at | cancer susceptibility candidate 5 | 0.638 | 7.64E-07 |
| 1437643_at | centromere protein J | 0.638 | 1.63E-04 |
| 1428460_at | synapsin II | 0.637 | 3.34E-05 |
| 1416265_at | calpain 10 | 0.637 | 1.61E-04 |
| 1448289_at | collapsin response mediator protein 1 | 0.637 | 6.31E-05 |
| 1420863_at | dynactin 4 | 0.637 | 4.92E-05 |
| 1423691_x_at | keratin complex 2, basic, gene 8 | 0.637 | 1.20E-05 |
| 1427884_at | procollagen, type III, alpha 1 | 0.635 | 6.14E-06 |
| 1435781_at | cullin associated and neddylation disassociated 1 | 0.632 | 1.20E-06 |
| 1456483_at | zinc finger protein 9 | 0.629 | 4.69E-04 |
| 1424629_at | breast cancer 1 | 0.627 | 1.67E-05 |

| | | | |
|---|---|---|---|
| 1430139_at | helicase, lymphoid specific | 0.627 | 5.52E-06 |
| 1439436_x_at | inner centromere protein | 0.626 | 2.64E-05 |
| 1439945_at | zinc finger protein 449 | 0.626 | 2.08E-05 |
| 1418133_at | B-cell leukemia/lymphoma 3 | 0.626 | 4.41E-05 |
| 1441375_at | Leucine-rich repeats and immunoglobulin-like domains 1 (Lrig1), mRNA | 0.623 | 7.33E-05 |
| 1422279_at | Friend virus susceptibility 1 | 0.622 | 2.81E-06 |
| 1418495_at | zinc finger CCCH type containing 8 | 0.620 | 3.50E-06 |
| 1433623_at | zinc finger protein 367 | 0.620 | 1.09E-04 |
| 1422481_at | keratin complex 2, basic, gene 1 | 0.620 | 1.36E-07 |
| 1454849_x_at | clusterin | 0.618 | 4.51E-05 |
| 1427290_at | keratin complex 2, basic, gene 19 | 0.614 | 5.50E-05 |
| 1434201_at | Chordin-like 1 (Chrdl1), mRNA | 0.612 | 1.76E-07 |
| 1450536_s_at | keratin associated protein 12-1 | 0.612 | 4.51E-06 |
| 1425356_at | zinc finger protein 142 | 0.612 | 2.80E-05 |
| 1439407_x_at | transgelin 2 | 0.611 | 8.05E-07 |
| 1437788_at | trans-acting transcription factor 6 | 0.609 | 2.49E-04 |
| 1439631_at | zinc finger, CCHC domain containing 11 | 0.608 | 1.70E-05 |
| 1450842_a_at | centromere autoantigen A | 0.604 | 9.42E-05 |
| 1439030_at | GDP-mannose pyrophosphorylase B | 0.604 | 1.01E-05 |
| 1428503_a_at | NFKB inhibitor interacting Ras-like protein 1 | 0.598 | 1.20E-04 |
| 1416083_at | zinc finger, A20 domain containing 2 | 0.597 | 1.56E-05 |
| 1418735_at | keratin complex 2, basic, gene 4 | 0.597 | 6.76E-05 |
| 1436095_at | chromodomain helicase DNA binding protein 5 | 0.596 | 7.68E-05 |
| 1428650_at | tensin 1 | 0.596 | 1.99E-04 |
| 1448467_a_at | tangerin | 0.595 | 8.37E-07 |
| 1421460_at | desmocollin 1 | 0.593 | 1.00E-04 |
| 1427366_at | keratin associated protein 3-1 | 0.593 | 1.01E-05 |
| 1437355_at | zinc finger, CCHC domain containing 5 | 0.592 | 1.31E-04 |
| 1451484_a_at | synapsin I | 0.585 | 4.82E-06 |
| 1437685_x_at | fibromodulin | 0.580 | 1.25E-06 |
| 1451637_a_at | mucin 10, submandibular gland salivary mucin | 0.579 | 1.02E-04 |
| 1451997_at | zinc finger protein 426 | 0.578 | 3.35E-06 |
| 1455187_at | zinc finger and BTB domain containing 40 | 0.576 | 8.66E-06 |
| 1444043_at | GLI-Kruppel family member GLI3 (Gli3), mRNA | 0.569 | 6.45E-06 |
| 1418608_at | calmodulin-like 3 | 0.567 | 8.83E-05 |
| 1455113_at | armadillo repeat containing 8 | 0.562 | 9.25E-07 |
| 1427348_at | zinc finger CCCH type containing 12A | 0.562 | 1.07E-04 |
| 1417878_at | E2F transcription factor 1 | 0.561 | 2.93E-05 |
| 1429347_at | Bcl2-like 14 (apoptosis facilitator) | 0.558 | 2.01E-05 |
| 1426471_at | zinc finger protein 52 | 0.557 | 1.19E-04 |
| 1424407_s_at | chromobox homolog 6 | 0.555 | 2.19E-05 |
| 1417917_at | calponin 1 | 0.554 | 9.53E-06 |
| 1425705_a_at | ERO1-like beta (S. cerevisiae) | 0.554 | 1.60E-05 |
| 1418091_at | transcription factor CP2-like 1 | 0.553 | 5.57E-05 |
| 1415948_at | cellular repressor of E1A-stimulated genes 1 | 0.549 | 1.78E-04 |
| 1439040_at | centromere protein E | 0.549 | 3.95E-06 |
| 1430669_at | keratin associated protein 4-7 | 0.547 | 5.97E-05 |
| 1457571_at | zinc finger protein 68 | 0.546 | 3.41E-07 |
| 1447812_x_at | filamin C, gamma (actin binding protein 280) | 0.544 | 1.82E-05 |
| 1423809_at | transcription factor 19 | 0.542 | 2.08E-05 |
| 1417552_at | fibroblast activation protein | 0.540 | 1.44E-04 |
| 1422747_at | CHK2 checkpoint homolog (S. pombe) | 0.536 | 5.71E-07 |
| 1448788_at | Cd200 antigen | 0.532 | 4.32E-04 |
| 1433862_at | extra spindle poles-like 1 (S. cerevisiae) | 0.532 | 6.56E-08 |
| 1427179_at | keratin complex 1, acidic, gene 3 | 0.528 | 4.73E-06 |
| 1451611_at | HRAS like suppressor 3 | 0.526 | 9.14E-07 |
| 1422582_at | leptin | 0.525 | 3.82E-04 |
| 1452166_a_at | keratin complex 1, acidic, gene 10 | 0.519 | 1.51E-04 |
| 1455642_a_at | tetraspanin 17 | 0.519 | 3.56E-06 |
| 1424218_a_at | cAMP responsive element binding protein 3-like 4 | 0.518 | 9.73E-06 |
| 1419295_at | cAMP responsive element binding protein 3-like 1 | 0.517 | 6.05E-06 |
| 1418063_at | keratocan | 0.515 | 7.97E-05 |

| | | | |
|---|---|---|---|
| 1436186_at | E2F transcription factor 8 | 0.515 | 2.98E-06 |
| 1433681_x_at | calpain 3 | 0.515 | 2.94E-05 |
| 1460082_at | inhibitor of growth family, member 3 | 0.512 | 9.59E-05 |
| 1448835_at | E2F transcription factor 6 | 0.505 | 1.37E-05 |
| 1457275_at | desmuslin | 0.501 | 3.13E-04 |
| 1442140_at | tenascin N | 0.500 | 1.10E-05 |
| 1418440_at | procollagen, type VIII, alpha 1 | 0.499 | 4.76E-07 |
| 1422954_at | zinc finger protein 60 | 0.497 | 5.33E-06 |
| 1440770_at | B-cell leukemia/lymphoma 2 | 0.494 | 2.40E-05 |
| 1434573_at | TRAF3 interacting protein 3 | 0.494 | 1.51E-05 |
| 1442542_at | eyes absent 4 homolog (Drosophila) | 0.493 | 2.16E-04 |
| 1446636_at | tensin 3 | 0.492 | 2.19E-05 |
| 1418804_at | succinate receptor 1 | 0.491 | 1.27E-06 |
| 1424567_at | tetraspan 2 | 0.490 | 2.87E-05 |
| 1427161_at | centromere autoantigen F | 0.480 | 2.36E-05 |
| 1443931_at | Zinc finger protein 617 (Zfp617), mRNA | 0.478 | 8.22E-07 |
| 1418093_a_at | epidermal growth factor | 0.473 | 1.73E-04 |
| 1425262_at | CCAAT/enhancer binding protein (C/EBP), gamma | 0.469 | 2.45E-04 |
| 1417268_at | CD14 antigen | 0.469 | 5.95E-04 |
| 1419521_at | zinc finger protein 94 | 0.464 | 4.15E-04 |
| 1431035_at | dishevelled associated activator of morphogenesis 1 | 0.464 | 1.75E-05 |
| 1417644_at | sarcospan | 0.464 | 6.85E-05 |
| 1457424_at | eyes absent 1 homolog (Drosophila) | 0.462 | 3.80E-05 |
| 1426180_a_at | submaxillary gland androgen regulated protein 2 | 0.462 | 5.01E-08 |
| 1445256_at | Vinculin, mRNA (cDNA clone MGC:6134 IMAGE:3495710) | 0.460 | 6.82E-06 |
| 1421355_at | transglutaminase 3, E polypeptide | 0.456 | 5.05E-05 |
| 1429067_at | calpain, small subunit 2 | 0.444 | 3.33E-04 |
| 1428052_a_at | zinc finger, MYM domain containing 1 | 0.444 | 4.19E-05 |
| 1437095_at | tetraspanin 18 | 0.442 | 3.24E-06 |
| 1454884_at | BTB (POZ) domain containing 4 | 0.439 | 4.01E-04 |
| 1435005_at | centromere protein E | 0.433 | 5.74E-06 |
| 1425237_at | keratin associated protein 16-8 | 0.421 | 2.05E-05 |
| 1420358_at | keratin associated protein 13 | 0.418 | 2.25E-08 |
| 1445032_at | Death associated protein kinase 1 (Dapk1), mRNA | 0.418 | 3.63E-05 |
| 1416025_at | fibrinogen, gamma polypeptide | 0.416 | 9.41E-06 |
| 1431727_at | submandibular gland protein C | 0.411 | 1.39E-05 |
| 1417686_at | lectin, galactose binding, soluble 12 | 0.407 | 3.79E-04 |
| 1422814_at | asp (abnormal spindle)-like, microcephaly associated (Drosophila) | 0.404 | 2.19E-05 |
| 1456228_x_at | myelin basic protein | 0.404 | 7.48E-05 |
| 1416658_at | frizzled-related protein | 0.401 | 1.78E-04 |
| 1460218_at | CD52 antigen | 0.397 | 3.00E-05 |
| 1416342_at | tenascin C | 0.391 | 1.18E-04 |
| 1449919_at | keratin associated protein 6-2 | 0.382 | 6.36E-06 |
| 1455519_at | desmoglein 1 beta | 0.375 | 1.56E-06 |
| 1423010_at | sacsin | 0.358 | 2.16E-04 |
| 1421691_at | keratin associated protein 16-7 | 0.357 | 9.29E-07 |
| 1420466_at | salivary protein 2 | 0.351 | 1.37E-05 |
| 1424528_at | cell growth regulator with EF hand domain 1 | 0.347 | 1.28E-05 |
| 1421855_at | fibrinogen-like protein 2 | 0.342 | 7.62E-05 |
| 1450633_at | calmodulin 4 | 0.342 | 9.47E-06 |
| 1429540_at | cornifelin | 0.339 | 2.71E-06 |
| 1430731_at | keratin associated protein 2-4 | 0.336 | 5.41E-07 |
| 1424531_a_at | transcription elongation factor A (SII), 3 | 0.331 | 3.45E-06 |
| 1449073_at | filamin C, gamma (actin binding protein 280) | 0.317 | 1.27E-06 |
| 1422640_at | protocadherin beta 9 | 0.315 | 6.16E-04 |
| 1459897_a_at | suprabasin | 0.313 | 2.81E-06 |
| 1424529_s_at | cell growth regulator with EF hand domain 1 | 0.309 | 1.40E-06 |
| 1422837_at | sciellin | 0.308 | 1.19E-04 |
| 1455900_x_at | transglutaminase 2, C polypeptide | 0.302 | 3.11E-06 |
| 1443745_s_at | dentin matrix protein 1 | 0.291 | 8.52E-06 |
| 1416455_a_at | crystallin, alpha B | 0.287 | 1.11E-05 |
| 1421589_at | keratin complex 1, acidic, gene 1 | 0.286 | 7.06E-08 |

| | | | |
|---|---|---|---|
| 1420183_at | Loricrin (Lor), mRNA | 0.273 | 4.86E-07 |
| 1431255_at | calreticulin 3 | 0.244 | 5.08E-05 |
| 1426043_a_at | calpain 3 | 0.218 | 3.23E-07 |
| 1418314_a_at | ataxin 2 binding protein 1 | 0.212 | 2.01E-04 |
| 1417979_at | tenomodulin | 0.207 | 1.70E-04 |
| 1435649_at | nexilin | 0.203 | 2.10E-08 |
| 1423253_at | myelin protein zero | 0.201 | 1.11E-04 |
| 1422588_at | keratin complex 2, basic, gene 6b | 0.198 | 5.57E-05 |
| 1458000_at | desmoglein 1 alpha | 0.197 | 6.25E-06 |
| 1422654_at | sarcoglycan, alpha (dystrophin-associated glycoprotein) | 0.186 | 2.34E-05 |
| 1445824_at | zinc finger protein 458 | 0.186 | 8.34E-06 |
| 1416776_at | crystallin, mu | 0.180 | 3.79E-05 |
| 1420751_at | keratin associated protein 6-1 | 0.180 | 2.99E-07 |
| 1422529_s_at | calsequestrin 2 | 0.167 | 1.99E-05 |
| 1448168_a_at | salivary protein 1 | 0.164 | 9.03E-05 |
| 1427735_a_at | actin, alpha 1, skeletal muscle | 0.162 | 2.09E-07 |
| 1418413_at | caveolin 3 | 0.157 | 1.55E-06 |
| 1459266_at | ARP3 actin-related protein 3 homolog (yeast) (Actr3), mRNA | 0.130 | 1.94E-04 |
| 1418951_at | taxilin beta | 0.129 | 9.86E-07 |
| 1427211_at | keratin associated protein 8-1 | 0.128 | 1.06E-04 |
| 1436867_at | sarcalumenin | 0.122 | 7.54E-06 |
| 1448745_s_at | loricrin | 0.110 | 1.13E-04 |
| 1423238_at | integrin beta 1 binding protein 2 | 0.109 | 8.05E-06 |
| 1448932_at | keratin complex 1, acidic, gene 16 | 0.109 | 4.43E-06 |
| 1435191_at | corneodesmosin | 0.108 | 5.84E-04 |
| 1460185_at | keratin complex 2, basic, gene 18 | 0.104 | 2.37E-06 |
| 1418742_at | keratin complex 1, acidic, gene 4 | 0.104 | 9.74E-05 |
| 1428007_at | keratin associated protein 13-1 | 0.099 | 2.53E-06 |
| 1422598_at | calsequestrin 1 | 0.098 | 2.19E-04 |
| 1420409_at | keratin complex 1, acidic, gene 24 | 0.093 | 2.35E-08 |
| 1420884_at | sarcolipin | 0.077 | 3.79E-06 |
| 1448327_at | actinin alpha 2 | 0.070 | 3.40E-05 |
| 1425382_a_at | aquaporin 4 | 0.068 | 2.93E-04 |
| 1418677_at | actinin alpha 3 | 0.067 | 1.57E-04 |
| 1427751_a_at | keratin complex 1, acidic, gene 5 | 0.054 | 4.32E-05 |
| 1447456_x_at | demilune cell and parotid protein ; cDNA sequence BC005655 | 0.050 | 9.98E-06 |
| 1435585_at | transcription elongation factor A (SII)-like 7 | 0.049 | 4.59E-06 |
| 1451551_at | keratin complex 2, basic, gene 16 | 0.049 | 4.73E-05 |
| 1452957_at | keratin associated protein 3-3 | 0.041 | 9.06E-06 |

*List of differentially expressed genes that distinguish between salivary gland tissue from double mutant mice and single mutant β-cat$^{GOF}$ mice according to gene chip analysis. Affymetrix probe set ID (Probe ID), gene description, fold change (fc), and p-value (p) are shown. Grey-marked genes were specifically discussed in the text.

**Wend *et al.***

**Table S3: Gene set enrichment analysis (GSEA)[1]**

| **Double-mutant salivary glands *vs.* single mutant beta-catenin glands at P1** | | | | | | |
|---|---|---|---|---|---|---|
| **Gene Set name** | | **Size** | **ES** | **NES** | **FDR (q-val)** | **Gene Set Description** |
| Wnt target gene sets | WNT_TARGETS | 17 | -0.79 | -2.19 | 0.0035 | Wnt up-regulated genes in Wnt homepage (Nusse lab) |
| | WNT_Signaling | 45 | -0.36 | -1.99 | 0.0524 | Wnt target genes from literature (curated by GEArray) |
| | Sansom_APC_LOSS4_UP | 115 | -0.69 | -2.39 | 0.0013 | Up-regulated in the mouse small intestine 4 d after Apc loss |
| Cell Cycle-related | CELL_Cycle | 67 | -0.61 | -1.77 | 0.0019 | Cell cycle genes (defined by Broad Institute) |
| | BRENTANI_CELL_CYCLE | 73 | -0.62 | -1.98 | 0.0278 | Cancer-related genes involved in cell cycle |
| | G1_TO_S_CELL_CYCLE_REACTOME | 59 | -0.49 | -1.82 | 0.0675 | Genes involved in G1 to S progression of cell cycle |
| Apoptosis | REACTOME_APOPTOSIS | 102 | 0.59 | 1.62 | 0.0481 | Genes involved in Apoptosis |
| Differentiation | STRUCTURAL_MOLECULE_ACTIVITY | 243 | 0.36 | 1.89 | 0.0512 | Structural integrity of a complex or assembly within or outside a cell |
| **Double-mutant tumor-propagating CD24+CD29+ cells *vs.* single mutant beta-catenin CD24+CD29+ cells at P90** | | | | | | |
| **Gene Set name** | | **Size** | **ES** | **NES** | **FDR (q-val)** | **Gene Set Description** |
| MULTICELLULAR_ORGANISM_DEVELOPMENT | | 78 | -0.45 | -2.03 | 0.0751 | Early organism development |

[1]Table includes gene sets strongly enriched in double-mutant salivary glands at P1 and double-mutant tumor-propagating cells compared to single mutant beta-catenin glands at P90, as determined by gene set enrichment analysis (GSEA).
Gene sets were generated and published in the Molecular Signature Database (MsigDB; Broad Institute, http://www.broad.mit.edu/gsea/msigdb). Size indicates number of genes included in each gene set. Enrichment score (ES) and normalized enrichment score (NES) and FDR were calculated by GSEA. Negative ES, negative NES, and FDR<0.2 indicate significant enrichment of a specific gene set in double-mutant salivary glands compared to single mutant beta-catenin glands.

**Suppl Table 4: Affymetrix gene profiling of $CD24^{+}CD29^{+}$ salivary gland cells at P80***

**Salivary gland $CD24^{+}CD29^{+}$ tumor propagating cell-gene signature**

**[1] = $Bmpr1a^{LOF}$**

**[2] = $\beta$-$cat^{GOF}$**

**[3] =double mutant**

| Probe ID | Symbol | UniGene | fc [3] / [1] | Regulation [3] / [1] | p [3] / [1] | fc [3] / [2] | Regulation [3] / [2] | p [3] / [2] |
|---|---|---|---|---|---|---|---|---|
| 1425642_at | Cep290 | Mm.229114 | 3.891 | up | 8.30E-05 | 5.098 | up | 6.83E-04 |
| 1420411_a_at | Pi4k2b | Mm.248647 | 3.571 | up | 3.82E-04 | 2.638 | up | 1.60E-05 |
| 1420330_at | Clec4e | Mm.248327 | 3.369 | up | 3.82E-06 | 1.580 | up | 1.32E-05 |
| 1437689_x_at | Clu | Mm.200608 | 2.663 | up | 3.27E-04 | 2.354 | up | 1.36E-05 |
| 1451798_at | Il1rn | Mm.882 | 2.310 | up | 3.76E-04 | 1.584 | up | 1.73E-06 |
| 1447084_at | Nfatc1 | Mm.329560 | 2.216 | up | 8.39E-04 | 1.026 | up | 1.42E-06 |
| 1449254_at | Spp1 | Mm.288474 | 2.184 | up | 2.37E-04 | 1.306 | up | 5.46E-05 |
| 1421473_at | Il1a | Mm.15534 | 2.155 | up | 1.10E-04 | 1.549 | up | 2.78E-07 |
| 1447669_s_at | Gng4 | Mm.215394 | 2.066 | up | 9.23E-05 | 1.533 | up | 1.68E-04 |
| 1449984_at | Cxcl2 | Mm.4979 | 2.050 | up | 3.79E-04 | 1.130 | up | 1.34E-04 |
| 1442376_at | Ablim1 | Mm.217161 | 1.967 | up | 2.93E-06 | 2.951 | up | 3.42E-07 |
| 1421341_at | Axin2 | Mm.71710 | 1.930 | up | 3.41E-04 | 1.898 | up | 8.07E-05 |
| 1436826_at | Tmtc3 | Mm.296805 | 1.824 | up | 4.05E-04 | 2.548 | up | 1.35E-05 |
| 1433596_at | Dnajc6 | Mm.76494 | 1.816 | up | 5.75E-04 | 2.491 | up | 2.97E-06 |
| 1421492_at | Ptgds2 | Mm.442454 | 1.663 | up | 9.28E-05 | 2.135 | up | 8.43E-06 |
| 1433966_x_at | Asns | Mm.2942 | 1.634 | up | 3.88E-08 | 2.939 | up | 1.37E-05 |
| 1428748_at | Zfp826 | Mm.100056 | 1.583 | up | 4.01E-04 | 2.229 | up | 7.11E-05 |
| 1420549_at | Gbp1 | Mm.457978 | 1.534 | up | 5.81E-05 | 2.697 | up | 1.51E-06 |
| 1448595_a_at | Bex1 | Mm.422943 | 1.513 | up | 2.37E-06 | 2.557 | up | 1.63E-04 |
| 1442282_at | Vmn2r84 | Mm.359168 | 1.407 | up | 1.64E-06 | 2.165 | up | 2.75E-04 |
| 1433781_a_at | Cldn12 | Mm.40132 | 1.381 | up | 8.04E-05 | 2.766 | up | 3.81E-05 |
| 1420410_at | Nr5a2 | Mm.16794 | 1.373 | up | 7.95E-05 | 2.409 | up | 3.09E-05 |
| 1425964_x_at | Hspb1 | Mm.13849 | 1.365 | up | 1.30E-05 | 2.023 | up | 4.61E-04 |
| 1425454_a_at | Il12a | Mm.103783 | 1.346 | up | 7.81E-04 | 2.685 | up | 6.30E-07 |
| 1460603_at | Samd9l | Mm.196013 | 1.331 | up | 1.29E-05 | 2.187 | up | 1.12E-04 |
| 1433374_at | Supt7l | Mm.164187 | 1.319 | up | 1.53E-05 | 2.698 | up | 6.33E-05 |
| 1423626_at | Dst | Mm.336625 | 1.296 | up | 2.29E-04 | 2.292 | up | 5.73E-05 |
| 1449211_at | Bpnt1 | Mm.227549 | 1.294 | up | 5.63E-05 | 2.281 | up | 4.04E-06 |
| 1430744_at | Napsa | Mm.383181 | 1.290 | up | 2.75E-04 | 2.072 | up | 9.02E-07 |
| 1436865_at | Slc26a11 | Mm.31869 | 1.239 | up | 8.74E-06 | 2.549 | up | 3.95E-06 |
| 1457769_at | H60a | Mm.387042 | 1.234 | up | 1.01E-05 | 2.969 | up | 7.54E-06 |
| 1422873_at | Prg2 | Mm.142727 | 1.198 | up | 7.80E-04 | 2.471 | up | 1.67E-06 |
| 1455521_at | Klf12 | Mm.458816 | 1.163 | up | 5.93E-07 | 2.049 | up | 1.06E-06 |
| 1429366_at | Lrrc34 | Mm.45373 | 1.159 | up | 4.60E-04 | 2.309 | up | 1.19E-04 |
| 1455164_at | Cdgap | Mm.370848 | 1.158 | up | 1.03E-04 | 9.923 | up | 9.34E-07 |
| 1435203_at | Man2a2 | Mm.269245 | 1.142 | up | 2.19E-04 | 2.153 | up | 5.46E-05 |
| 1425521_at | Paip1 | Mm.132584 | 1.125 | up | 3.54E-05 | 3.036 | up | 1.04E-05 |
| 1424748_at | Galnt11 | Mm.425232 | 1.121 | up | 5.39E-05 | 2.129 | up | 5.17E-05 |
| 1430139_at | Hells | Mm.57223 | 1.103 | up | 1.41E-05 | 1.515 | up | 6.14E-05 |
| 1459253_at | Arrdc3 | Mm.423137 | 1.086 | up | 8.80E-06 | 3.616 | up | 3.11E-05 |
| 1452855_at | Ly6k | Mm.273319 | 1.080 | up | 2.75E-07 | 2.204 | up | 4.84E-05 |
| 1418872_at | Abcb1b | Mm.146649 | 1.075 | up | 5.07E-04 | 2.655 | up | 2.63E-05 |
| 1418148_at | Abhd1 | Mm.389615 | 1.060 | up | 7.17E-05 | 2.775 | up | 1.36E-05 |
| 1418645_at | Hal | Mm.13000 | 1.060 | up | 5.56E-06 | 2.599 | up | 8.49E-05 |
| 1438239_at | Mid1 | Mm.34441 | 1.049 | up | 2.41E-04 | 3.717 | up | 3.42E-06 |
| 1457936_at | Mapk8 | Mm.21495 | 1.016 | up | 4.56E-05 | 6.864 | up | 4.96E-05 |
| 1450897_at | Arhgap5 | Mm.35059 | 1.015 | up | 2.78E-05 | 2.256 | up | 2.14E-06 |
| 1426753_at | Phf17 | Mm.286285 | 1.008 | up | 1.68E-04 | 2.227 | up | 1.80E-06 |
| 1451704_at | Abpd | Mm.389857 | 17.022 | down | 2.60E-07 | 1.026 | up | 1.35E-05 |
| 1427380_at | Klk1b3 | Mm.439740 | 12.599 | down | 6.00E-07 | 1.002 | up | 3.08E-06 |
| 1420770_at | Klk1b24 | Mm.444308 | 10.713 | down | 6.26E-04 | 1.082 | up | 9.67E-08 |
| 1421587_at | Klk1b27 | Mm.445911 | 9.346 | down | 7.61E-07 | 1.019 | up | 9.93E-05 |
| 1419675_at | Ngf | Mm.1259 | 3.273 | down | 6.00E-04 | 1.003 | up | 7.25E-07 |
| 1433769_at | Als2cl | Mm.86338 | 3.143 | down | 2.89E-04 | 1.201 | up | 6.35E-05 |
| 1451637_a_at | Muc10 | Mm.200411 | 2.670 | down | 1.60E-07 | 1.658 | up | 9.91E-06 |
| 1448962_at | Myh11 | Mm.250705 | 2.391 | down | 2.05E-04 | 1.134 | up | 6.04E-04 |
| 1420700_s_at | Folr4 | Mm.86738 | 2.353 | down | 4.08E-04 | 1.097 | up | 1.39E-04 |
| 1453568_at | Dapl1 | Mm.275769 | 2.275 | down | 1.51E-05 | 1.351 | up | 8.10E-07 |
| 1449191_at | Wfdc12 | Mm.6433 | 2.190 | down | 3.29E-04 | 1.581 | up | 4.55E-06 |
| 1426044_a_at | Prkcq | Mm.329993 | 2.122 | down | 2.05E-05 | 1.038 | up | 1.17E-05 |
| 1418353_at | Cd5 | Mm.779 | 2.116 | down | 7.78E-05 | 1.197 | up | 1.71E-05 |
| 1416454_s_at | Acta2 | Mm.213025 | 2.046 | down | 9.14E-06 | 1.047 | up | 2.54E-06 |
| 1418612_at | Slfn1 | Mm.10948 | 2.028 | down | 1.92E-04 | 1.202 | up | 2.66E-05 |
| 1427532_at | Trat1 | Mm.167298 | 2.023 | down | 2.63E-04 | 1.344 | up | 3.91E-06 |
| 1446675_at | Adk | Mm.188734 | 1.527 | down | 5.26E-05 | 2.049 | up | 1.29E-05 |
| 1439843_at | Camk4 | Mm.222329 | 1.455 | down | 3.83E-05 | 2.411 | up | 2.24E-04 |
| 1417459_at | Dcpp1 | Mm.371556 | 1.359 | down | 4.85E-04 | 3.931 | up | 7.87E-06 |
| 1435462_at | Plcxd2 | Mm.380993 | 1.221 | down | 2.98E-06 | 11.585 | up | 1.09E-08 |
| 1425764_a_at | Bcat2 | Mm.24210 | 1.202 | down | 1.22E-04 | 2.147 | up | 5.28E-06 |
| 1431708_a_at | Tia1 | Mm.423551 | 1.149 | down | 1.10E-04 | 2.069 | up | 3.77E-05 |
| 1452406_x_at | Erdr1 | Mm.391385 | 1.129 | down | 3.51E-04 | 2.299 | up | 1.83E-05 |

| | | | | | | | | |
|---|---|---|---|---|---|---|---|---|
| 1436796_at | Matr3 | Mm.215034 | 1.128 | down | 2.35E-07 | 2.333 | up | 7.21E-05 |
| 1447517_at | Skiv2l2 | Mm.291029 | 1.107 | down | 7.18E-07 | 23.144 | up | 2.06E-05 |
| 1421628_at | Il18r1 | Mm.253664 | 1.074 | down | 2.17E-04 | 2.775 | up | 1.98E-08 |
| 1437308_s_at | F2r | Mm.24816 | 1.037 | down | 5.36E-05 | 3.819 | up | 1.08E-05 |
| 1420505_a_at | Stxbp1 | Mm.278865 | 1.037 | down | 3.03E-05 | 2.911 | up | 8.93E-05 |
| 1448712_at | Chm | Mm.257316 | 1.036 | down | 1.98E-05 | 2.772 | up | 3.83E-05 |
| 1450837_at | Prp2 | Mm.333439 | 2.478 | up | 2.44E-04 | 1.141 | down | 9.62E-04 |
| 1449153_at | Mmp12 | Mm.2055 | 2.386 | up | 3.71E-06 | 1.013 | down | 1.82E-04 |
| 1431035_at | Daam1 | Mm.87417 | 2.128 | up | 1.46E-04 | 2.076 | down | 1.52E-04 |
| 1429443_at | Cpne4 | Mm.326240 | 2.047 | up | 7.83E-05 | 1.055 | down | 5.16E-07 |
| 1450680_at | Rag1 | Mm.828 | 1.524 | up | 2.77E-04 | 3.785 | down | 2.66E-05 |
| 1439426_x_at | Lyz1 | Mm.177539 | 1.265 | up | 6.09E-04 | 2.372 | down | 5.72E-05 |
| 1419394_s_at | S100a8 | Mm.21567 | 1.129 | up | 1.25E-05 | 3.532 | down | 8.09E-06 |
| 1423547_at | Lyz2 | Mm.45436 | 1.126 | up | 8.46E-05 | 2.102 | down | 1.75E-05 |
| 1424339_at | Oasl1 | Mm.95479 | 1.090 | up | 4.93E-05 | 2.018 | down | 9.74E-06 |
| 1445305_at | Slc10a7 | Mm.334631 | 1.074 | up | 5.25E-05 | 2.014 | down | 6.07E-05 |
| 1448756_at | S100a9 | Mm.2128 | 1.073 | up | 8.26E-04 | 2.582 | down | 5.41E-04 |
| 1441228_at | Apold1 | Mm.296104 | 1.011 | up | 4.04E-06 | 2.082 | down | 5.97E-04 |
| 1452592_at | Mgst2 | Mm.24679 | 1.011 | up | 6.31E-05 | 2.763 | down | 7.82E-08 |
| 1420398_at | Rgs18 | Mm.253927 | 1.006 | up | 1.31E-06 | 2.893 | down | 1.62E-07 |
| 1453644_at | Obp1a | Mm.430771 | 57.487 | down | 3.72E-05 | 1.137 | down | 4.07E-05 |
| 1437432_a_at | Trim12 | Mm.458309 | 24.627 | down | 3.56E-05 | 1.012 | down | 8.10E-06 |
| 1421803_at | Apbh | Mm.6205 | 21.606 | down | 1.19E-04 | 1.043 | down | 1.09E-04 |
| 1419090_x_at | Klk1b26 | Mm.439663 | 11.300 | down | 3.47E-06 | 3.415 | down | 1.88E-04 |
| 1420490_at | Klk1b16 | Mm.440887 | 9.701 | down | 4.05E-04 | 1.279 | down | 2.57E-06 |
| 1425144_at | Klk1b11 | Mm.443378 | 9.173 | down | 2.09E-05 | 2.075 | down | 5.38E-05 |
| 1418093_a_at | Egf | Mm.252481 | 8.961 | down | 7.72E-05 | 1.401 | down | 2.55E-04 |
| 1420701_at | Klk1b1 | Mm.447819 | 8.958 | down | 6.41E-05 | 1.387 | down | 1.54E-07 |
| 1449313_at | Klk1b5 | Mm.443373 | 7.628 | down | 1.38E-05 | 2.216 | down | 1.62E-04 |
| 1451607_at | Klk1b21 | Mm.443292 | 7.373 | down | 1.31E-04 | 1.387 | down | 1.86E-04 |
| 1421372_at | Klk1b4 | Mm.440886 | 7.294 | down | 4.40E-05 | 1.251 | down | 2.88E-04 |
| 1449463_at | Klk1b8 | Mm.435488 | 7.244 | down | 3.78E-06 | 1.403 | down | 4.35E-05 |
| 1449838_at | Crisp3 | Mm.14138 | 6.279 | down | 6.35E-05 | 1.537 | down | 1.15E-07 |
| 1416325_at | Crisp1 | Mm.16781 | 6.068 | down | 5.28E-05 | 2.469 | down | 5.72E-05 |
| 1421490_at | Prpmp5 | Mm.441627 | 5.010 | down | 3.26E-06 | 3.225 | down | 7.50E-05 |
| 1424592_a_at | Dnase1 | Mm.440565 | 4.112 | down | 2.73E-05 | 1.889 | down | 1.73E-07 |
| 1424857_a_at | Trim34 | Mm.326945 | 4.070 | down | 8.92E-05 | 1.371 | down | 2.05E-05 |
| 1449447_at | Cst10 | Mm.117117 | 3.625 | down | 5.36E-05 | 1.834 | down | 2.33E-04 |
| 1419595_a_at | Ggh | Mm.20461 | 3.237 | down | 2.09E-04 | 2.913 | down | 1.56E-04 |
| 1416456_a_at | Chia | Mm.46418 | 3.116 | down | 8.13E-04 | 1.284 | down | 3.00E-05 |
| 1420492_s_at | Smr3a | Mm.431303 | 3.069 | down | 7.04E-08 | 1.528 | down | 2.05E-06 |
| 1454608_x_at | Ttr | Mm.2108 | 2.790 | down | 4.79E-05 | 1.348 | down | 1.78E-04 |
| 1453752_at | Rpl17 | Mm.276337 | 2.611 | down | 9.84E-05 | 1.210 | down | 1.98E-05 |
| 1448626_at | Cdk5rap1 | Mm.289427 | 2.573 | down | 1.05E-05 | 2.330 | down | 3.05E-06 |
| 1417023_a_at | Fabp4 | Mm.582 | 2.559 | down | 3.43E-04 | 1.474 | down | 4.62E-06 |
| 1448998_at | Lpo | Mm.41236 | 2.549 | down | 5.32E-05 | 1.173 | down | 4.46E-05 |
| 1428010_at | Timm9 | Mm.207767 | 2.522 | down | 1.05E-06 | 1.766 | down | 8.99E-05 |
| 1437614_x_at | Zdhhc14 | Mm.476811 | 2.379 | down | 6.32E-05 | 3.162 | down | 4.49E-06 |
| 1425505_at | Mylk | Mm.33360 | 2.375 | down | 2.91E-04 | 1.139 | down | 4.14E-04 |
| 1450136_at | Cd38 | Mm.249873 | 2.358 | down | 2.88E-07 | 2.442 | down | 3.85E-06 |
| 1449526_a_at | Gdpd3 | Mm.246881 | 2.284 | down | 1.95E-04 | 2.029 | down | 1.26E-04 |
| 1449212_at | Pip | Mm.214755 | 2.270 | down | 1.09E-04 | 1.128 | down | 6.60E-05 |
| 1417765_a_at | Amy1 | Mm.439727 | 2.245 | down | 2.86E-04 | 1.252 | down | 1.30E-04 |
| 1430465_at | Raly | Mm.221440 | 2.219 | down | 1.58E-04 | 1.884 | down | 1.92E-04 |
| 1444322_at | Lcn11 | Mm.27838 | 2.211 | down | 8.38E-07 | 1.421 | down | 2.29E-06 |
| 1423450_a_at | Hs3st1 | Mm.12559 | 2.128 | down | 3.87E-05 | 3.962 | down | 2.70E-05 |
| 1428402_at | Zcchc3 | Mm.427626 | 2.111 | down | 1.34E-04 | 2.168 | down | 2.70E-04 |
| 1440582_at | Itch | Mm.208286 | 2.090 | down | 2.37E-07 | 2.001 | down | 1.45E-07 |
| 1423110_at | Col1a2 | Mm.277792 | 2.078 | down | 2.26E-05 | 1.570 | down | 1.02E-04 |
| 1415837_at | Klk1 | Mm.142722 | 2.064 | down | 1.70E-04 | 2.372 | down | 1.67E-05 |
| 1423608_at | Itm2a | Mm.193 | 2.029 | down | 2.39E-04 | 1.322 | down | 1.36E-04 |
| 1419814_s_at | S100a1 | Mm.24662 | 2.020 | down | 6.75E-06 | 1.132 | down | 1.07E-04 |
| 1444416_at | Cenpa | Mm.290563 | 2.012 | down | 2.98E-06 | 11.798 | down | 4.69E-05 |
| 1419764_at | Chi3l3 | Mm.387173 | 1.822 | down | 2.85E-05 | 4.038 | down | 8.12E-06 |
| 1426278_at | Ifi27 | Mm.271275 | 1.703 | down | 7.11E-06 | 3.049 | down | 5.01E-06 |
| 1418967_a_at | St7 | Mm.12051 | 1.699 | down | 6.33E-06 | 4.363 | down | 1.72E-06 |
| 1428820_at | Mapre1 | Mm.143877 | 1.593 | down | 4.95E-07 | 2.286 | down | 3.13E-04 |
| 1450753_at | Nkg7 | Mm.34613 | 1.513 | down | 4.39E-06 | 2.205 | down | 4.58E-05 |
| 1436107_at | Lsm8 | Mm.275158 | 1.512 | down | 2.60E-05 | 5.470 | down | 5.19E-06 |
| 1457458_at | Zc3h4 | Mm.333594 | 1.489 | down | 5.68E-05 | 2.534 | down | 5.98E-04 |
| 1450883_a_at | Cd36 | Mm.18628 | 1.485 | down | 8.83E-05 | 2.425 | down | 9.15E-06 |
| 1426166_at | Mup5 | Mm.445286 | 1.472 | down | 2.42E-05 | 2.399 | down | 7.27E-06 |
| 1460241_a_at | St3gal5 | Mm.38248 | 1.435 | down | 2.00E-04 | 2.156 | down | 1.27E-04 |
| 1434572_at | Hdac9 | Mm.310551 | 1.431 | down | 1.33E-04 | 2.116 | down | 5.97E-07 |
| 1436485_s_at | Whrn | Mm.300397 | 1.384 | down | 1.30E-05 | 2.210 | down | 1.98E-06 |
| 1449015_at | Retnla | Mm.441868 | 1.344 | down | 1.93E-04 | 3.434 | down | 3.70E-05 |
| 1427306_at | Ryr1 | Mm.439745 | 1.336 | down | 8.50E-06 | 2.035 | down | 1.85E-07 |
| 1422824_s_at | Eps8 | Mm.235346 | 1.310 | down | 4.58E-05 | 2.085 | down | 2.20E-04 |
| 1449465_at | Reln | Mm.425236 | 1.300 | down | 6.19E-05 | 3.672 | down | 4.72E-05 |
| 1418722_at | Ngp | Mm.236225 | 1.296 | down | 3.99E-07 | 5.603 | down | 7.82E-08 |
| 1432026_a_at | Herc5 | Mm.297393 | 1.293 | down | 6.54E-04 | 2.016 | down | 2.20E-05 |
| 1424775_at | Oas1a | Mm.14301 | 1.279 | down | 1.17E-07 | 2.827 | down | 2.65E-05 |
| 1428490_at | C1galt1 | Mm.102752 | 1.264 | down | 1.88E-04 | 2.100 | down | 2.44E-06 |
| 1442107_at | Flnb | Mm.475646 | 1.251 | down | 2.09E-05 | 4.390 | down | 2.60E-04 |
| 1429359_s_at | Rbpms | Mm.323997 | 1.211 | down | 4.58E-05 | 2.334 | down | 1.31E-05 |
| 1453196_a_at | Oasl2 | Mm.228363 | 1.205 | down | 4.08E-06 | 2.012 | down | 2.48E-05 |
| 1455359_at | Ptpn14 | Mm.4498 | 1.204 | down | 5.86E-06 | 2.062 | down | 1.15E-06 |
| 1419691_at | Camp | Mm.3834 | 1.189 | down | 7.69E-07 | 2.971 | down | 3.10E-05 |
| 1437874_s_at | Hexb | Mm.27816 | 1.133 | down | 3.19E-04 | 2.373 | down | 2.70E-04 |

| | | | | | | | | |
|---|---|---|---|---|---|---|---|---|
| 1425908_at | Gnb1 | Mm.2344 | 1.122 | down | 4.27E-06 | 9.115 | down | 5.58E-05 |
| 1423555_a_at | Ifi44 | Mm.30756 | 1.032 | down | 2.29E-06 | 2.300 | down | 5.93E-05 |

*List of differentially expressed genes that distinguish between $CD24^+CD29^+$ salivary gland tumor propagating cells of double mutant mice and $CD24^+CD29^+$ salivary gland cells of single mutant mice according to gene chip analysis. Affymetrix probe set ID (Probe ID), gene symbol (Symbol), Unigene ID, gene description, fold change (fc) and p-value (p) are shown. Grey-marked genes were specifically discussed in the text.

**Supplemental Table 5.** Oligo sequences used for quantitative Real-Time PCR.

| **Gene** | **Primer sequence** |
|---|---|
| m*c-myc* forward | 5'-TCCTGAAGCAGATCAGCAACAACC-3' |
| m*c-myc* reverse | 5'-TGCTTGAATGGACAGGATGTAGGC-3' |
| m*Fas* forward | 5'-AGTGCAAACCAGACTTCTACTGCG-3' |
| m*Fas* reverse | 5'-AAGGATGGTCAACAACCATAGGCG-3' |
| m*CK6* forward | 5'-AGAGAGGGGTCGCATGAACT-3' |
| m*CK6* reverse | 5'-TCATCTGTTAGACTGTCTGCCTT-3' |
| m*Loricrin* forward | 5'-TTGTGGAAAGACCTCTGGTGGAGG-3' |
| m*Loricrin* reverse | 5'-AACCACCTCCATAGGAACCACCG-3`; |
| m*Axin2* forward | 5'-AACTGAAACTGGAGCTGGAAAGCC-3' |
| m*Axin2* reverse | 5'-TTTGTGGGTCCTCTTCATAGCTGC-3' |
| m*Lef-1* forward | 5'-TGATGCCCAATATGAACAGCGACC-3' |
| m*Lef-1* reverse | 5'-TTGCTTGGAGTTGACATCTGACGG-3' |
| m*Bmp4* forward | 5'-AGAAGAATAAGAACTGCCGTCGCC-3' |
| m*Bmp4* reverse | 5'-ATGGCATGGTTGGTTGAGTTGAGG-3' |
| m*Msx2* forward | 5'-AAATCTGGTTCCAGAACCGAAGGG-3' |
| m*Msx2* reverse | 5'-CATGGTAGATGCCATATCCAACCG-3' |
| m*β-actin* forward | 5'-TCGTGCGTGACATCAAAGAGAAGC-3' |
| m*β-actin* reverse | 5'-ATGGATGCCACAGGATTCCATACC-3' |
| m*Dppa5* forward | 5'-GAAATATCTGTTTGGCCCACAGGG-3' |
| m*Dppa5* reverse | 5'-GCCATGGACTGAAGCATCCATTTAGC-3' |
| m*Dkk1* forward | 5'-TGTTGTGCAAGACACTTCTGGTCC-3' |
| m*Dkk1* reverse | 5'-TGTGGAGCCTAGAAGAATTGCTGG-3' |
| m*Nr5a2* forward | 5'-ACACAGAAGTCGCGTTCAACAACC-3' |
| m*Nr5a2* reverse | 5'-TAGTTGCAAACCGTGTAGTCCAGC-3' |
| m*Lrrc34* forward | 5'-TCAAGGGAATAAACCTGAACCGGC-3' |
| m*Lrrc34* reverse | 5'-ATTGCAGCTGACATCAAGGTAGCG-3' |
| m*Dnaja1* forward | 5'-TACAGCTGGTTGAAGCATTGTGCG-3' |
| m*Dnaja1* reverse | 5'-TCATATGGCCGACGGTATATTGGC-3' |
| m*Pdpn* forward | 5'-CACAGAGAACACGAGAGTACAACC-3' |
| m*Pdpn* reverse | 5'-ACGCCAACTATGATTCCAACCAGG-3' |
| m*Cdgap* forward | 5'-ATTGCCGGATTGGAAGAGAAAGCC-3' |
| m*Cdgap* reverse | 5'-ACGGTTGCTAAGTTCCAGTTGTGG-3' |
| m*Abcb1b* forward | 5'-TTATGCTGCTTGTTTCCGGTTCGG-3' |
| m*Abcb1b* reverse | 5'-TTTGGCTTTCGCATAGTCAGGAGC-3' |
| m*Geminin* forward | 5'-ATCTCAGACTTCAAGCTGTGGTCC-3' |
| m*Geminin* reverse | 5'-TTTATTCTCCTTTCTCAGGCGGGC-3' |
| m*Klf5* forward | 5'-ACGTCAATGAAACAGTTCCAGGGC-3' |
| m*Klf5* reverse | 5'-TTGGGTTGTGAATCGCCAGTTTGG-3' |
| m*Fgf5* forward | 5'-TCCTTGCTCTTCCTCATCTTCTGC-3' |
| m*Fgf5* reverse | 5'-ACTGGAAACTGCTATGTTCCGAGC-3' |
| m*Klk1b3* forward | 5'-ACCGATTTGTCAGCAAAGCCATCC-3' |
| m*Klk1b3* reverse | 5'-AATTTGGTGGGTGTAATGCTGCCC-3' |

| | |
|---|---|
| m*Dnajc6* forward | 5'-TCATTTGCCAGCAAACCTACCACC-3' |
| m*Dnajc6* reverse | 5'-AAGCTCACGTTGTAATTGGGTCGG-3' |
| m*Klf3* forward | 5'-GAA GCC CAA CAA ATA TGG GGT-3' |
| m*Klf3* reverse | 5'-GGA CGG GAA CTT CAG AGA GG-3' |
| m*Tbx6* forward | 5'-GGCAGCTCCATCTGTACCAT-3' |
| m*Tbx6* reverse | 5'-ACCGAGGCTCAGTACATTGG-3' |
| m*Trim2* forward | 5'-TGGACAGTTCAAAAGTCGTTTCG-3' |
| m*Trim2* reverse | 5'-AATGCTAACCCACTTGTTGTCAT-3' |
| m*Ctnnb1* forward | 5′-TGATTCGAAACCTTGCCCTTTGCC-3′ |
| m*Ctnnb1* reverse | 5′-TTACAATCCGGTTGTGAACGTCCC-3′ |
| m*Mll1* forward | 5′-AACAAGCATGGATCTCCCAATGCC-3′ |
| m*Mll1* reverse | 5′-ACATGTAGCAACCAATGCCCTTGC-3′ |
| m*Cbp* forward | 5′-ACCACAAGTCCATTTGGACAACCC-3′ |
| m*Cbp* reverse | 5′-TTCCCACTGATGTTTGCAACTGGG-3 |
| m*Ash1* forward | 5′-AGTTGAAGCTATGCAACGCCAAGC-3′ |
| m*Ash1* reverse | 5′-TTCAATTCCGGGCTGACAAACTGG-3′ |
| m*Ash2* forward | 5′-AAATGGTGTCAATCAGGGTGTGGC-3′ |
| m*Ash2* reverse | 5′-ACATCAGCCAGTGTGTGTTCTACC-3′ |
| m*Hells* forward | 5′-TTCGGAAATGTAATGGACAGC-3′ |
| m*Hells* reverse | 5′-GGGCCACATACAAGAAAAGG-3′ |
| m*Amy1* forward | 5′-ACATGTGGCCTGGAGACATAAAGG-3′ |
| m*Amy1* reverse | 5′-ATCCCACTTGCGCATAACTTTGCC-3′ |
| h*NR5A2* forward | 5'-TCATGGCCTATTTGCAGCAAGAGC-3' |
| h*NR5A2* reverse | 5'-ACCACTTGTCGGTAAATGTGGTCG-3' |
| h*ABCB1B* forward | 5'-AAGGCCTAATGCCGAACACATTGG-3' |
| h *ABCB1B* reverse | 5'-TTTGCCATCAAGCAGCACTTTCCC-3' |
| h*LRRC34* forward | 5'-TAATGATATTGGGCCCGAAGGTGG-3' |
| h*LRRC34* reverse | 5'-TTGCATTCCCAGATCACAGTCACC-3' |
| h*HELLS* forward | 5'-AAGGCATGGAATGGCTTAGGATGC-3' |
| h*HELLS* reverse | 5'-CCAGTTAGGAAGTGTAGACAAAGGGC-3` |
| h*DNAJC6* forward | 5'-ATCGAACTGCCAAGTTTCACAGCC-3' |
| h*DNAJC6* reverse | 5'-ACCAACCAGAATTGATGATGCCGC-3' |
| h*MLL1* forward | 5'-AGCAAGGTCATGGCAACAATCAGG-3' |
| h*MLL1* reverse | 5'-AGCTGCATTGGAAATCTGAGACGG-3' |
| h*ASH2* forward | 5'-ATGGTTCACGGCTGACACATTTGG-3' |
| h*ASH2* reverse | 5'-TTCGGATGTTCATCCTGTGTTCGG-3' |
| h*AXIN2* forward | 5'-TTCGGATGTTCATCCTGTGTTCGG-3' |
| h*AXIN2* reverse | 5'-TGGTGCAAAGACATAGCCAGAACC-3' |
| h*β-ACTIN* forward | 5'-TGGCACCACACCTTCTACAATGAGC-3' |
| h*β-ACTIN* reverse | 5'-GCACAGCTTCTCCTTAATGTCACGC-3' |

**Supplemental Table 6.** Oligonucleotide sequences used for transient RNAi.

| Gene | Oligo No. | Target Sequence |
|---|---|---|
| *β-catenin* | 1 | 5'-GCUGAAACAUGCAGUUGUAUU-3′ |
| | 2 | 5'-GAUAAAGGCUACUGUUGGAUU-3′ |
| | 3 | 5'-CCACUAAUGUCCAGCGUUUUU-3′ |
| | 4 | 5'-ACAAGUAGCUGAUAUUGAUUU-3′ |
| *Mll1* | 1 | 5'-CGCCAAAUGGAGCGAGUUU-3′ |
| | 2 | 5'-CCACCAAACCCACGAAGAA-3′ |
| | 3 | 5'-AGACAAAGCCCUCGAAGGA-3′ |
| | 4 | 5'-GCACAGUGGUCUCACGAUU-3′ |
| *Dppa5a* | 1 | 5'-GUUACAUCCUAGCAAGAUA-3′ |
| | 2 | 5'-AGUCGCUGGUGCUGAAAUA-3′ |
| | 3 | 5'-CCACAGGGAUCUCGAAUGU-3′ |
| | 4 | 5'-CGAAGAACUUAUCGAGGUC-3′ |
| *Crebbp* (CBP) | 1 | 5'-GGACAGCUGUUUACCAUGA-3′ |
| | 2 | 5'-GGAAUGAAGUCAAGGUUUG-3′ |
| | 3 | 5'-GAAAGCAGCUGUGUACAAU-3′ |
| | 4 | 5'-GCACAAGGAGGUAUUCUUU-3′ |
| *Ash1l* | 1 | 5'-GCGAAACAAUGGACAAUUA-3′ |
| | 2 | 5'-CAAGUAAGCUCGAGUCUGA-3′ |
| | 3 | 5'-GCUUAAGUAUUGAGUGUAA-3′ |
| | 4 | 5'-UAGUUGGACUGGUUAAUAA-3′ |
| Control | 1 | 5'-UGGUUUACAUGUCGACUAA-3′ |
| | 2 | 5'-UGGUUUACAUGUUGUGUGA-3′ |
| | 3 | 5'-UGGUUUACAUGUUUUCUGA-3′ |
| | 4 | 5'-UGGUUUACAUGUUUUCCUA-3′ |

**Supplemental Table 7.** Oligo sequences used for quantitative Real-Time PCR of ChIP samples.

| Gene | Primer sequence | Amplicon |
|---|---|---|
| m*Mll1* forward_I | 5'-ACATTCAATGGGAGAGTGCTTGCC-3' | chr9:44692191+44692323 |
| m*Mll1* reverse_I | 5'-AAAGAATCTCTCTCAGTGCCTCCC-3' | |
| m*Mll1* forward_II | 5'-AGCGTCGCCCAATTGATTCTATGC-3' | chr9:44689986+44690098 |
| m*Mll1* reverse_II | 5'-AAAGAGCTCCAAGCGTGAAGATGG-3' | |
| m*Mll1* forward_III | 5'-ACTGCCCTAGGAGTAACACATCTGC-3' | chr9:44688508+44688616 |
| m*Mll1* reverse_III | 5'-TTCACAGATTACCTCATCCGAGCC-3' | |
| m*Mll1* forward_IV | 5'-AGCACCAACTCCATGCAAGTAACC-3' | chr9:44686793+44686890 |
| m*Mll1* reverse_IV | 5'-TAAGCTGACAACACAGATCCCAGG-3' | |
| m*Hells* forward_I | 5'-AGCACCAGAATCAAAGGTGTGTGC-3' | chr19:39003188+39003313 |
| m*Hells* reverse_I | 5'-TGTTGGCCTCCAACTCAGAAATCC-3' | |
| m*Hells* forward_II | 5'-ACCTACCGAAAGGACAGGTATTGG-3' | chr19:39005106+39005195 |
| m*Hells* reverse_II | 5'-TAATGATGGTCCCGAGTTGTTCGG-3' | |
| m*Hells* forward_III | 5'-ACTTGAATCCCGTTCTGAAAGCCC-3' | chr19:39005840+39005941 |
| m*Hells* reverse_III | 5'-AGCATGGCTGGAGTAATCACCG-3' | |
| m*Hells* forward_IV | 5'-TGTGTGTGTGAGTGTGAGATGTCC-3' | chr19:39007011+39007138 |
| m*Hells* reverse_IV | 5'-TGCAGAGGTACCAGGTTTGTTTCC-3' | |
| m*Ash2* forward_I | 5'-ATAGCCATCACTTCATGGCACAGG-3' | chr8:26952740+26952888 |
| m*Ash2* reverse_I | 5'-ACGCAGAGATTGGTTAACTGTGGG-3' | |
| m*Ash2* forward_II | 5'-AAGCATATGGGTGGGCTCTAAACC-3' | chr8:26951979+26952076 |
| m*Ash2* reverse_II | 5'-TACATGCGCACACATCCGTAAAGC-3' | |
| m*Ash2* forward_III | 5'-AAGCAAGACAAATGTGTTCGCGGC-3' | chr8:26950689+26950787 |
| m*Ash2* reverse_III | 5'-CTTGCAATGCTTGGTCCTGAAAGC-3' | |
| m*Ash2* forward_IV | 5'-AACAGCAGCATGGAAGTGTAAGCC-3' | chr8:26948631+26948773 |
| m*Ash2* reverse_IV | 5'-ACCATAGCTAATGCAAGACCAGGG-3' | |
| m*Myc* forward | 5'-TGCCCAGTCAACATAACTGTACGACC-3' | chr15:61816229+61816317 |
| m*Myc* reverse | 5'-AGAGCCACTTAGGGATAAACAGCC-3' | |
| m*Gapdh* forward | 5'-ACGGCGGTTCATTCATTTCCTTCC-3' | chr6:125114819+125114915 |
| m*Gapdh* reverse | 5'-TGCATACCTTTGCGCATCATCTCC-3' | |
| h*MLL1* forward_I | 5'-TCTTCCTTCTTTCTGCTGCCTTGC-3' | chr11:118304931+118305068 |
| h*MLL1* reverse_I | 5'-TGTGTCAACAGATTTCTTCCCGCC-3' | |
| h*MLL1* forward_II | 5'-TTCGGGCTAACCCATCTTGTATCC-3' | chr11:118306634+118306727 |
| h*MLL1* reverse_II | 5'-AGAGCAGCTTCCAGTATAACGCGG-3' | |
| h*MLL1* forward_III | 5'-ACCTCCTTTCCCTCTGAAGATAACGG-3' | chr11:118309754+118309845 |
| h*MLL1* reverse_III | 5'-AGAAACTGTAGCCCTGTAAGACGG-3' | |
| h*MLL1* forward_IV | 5'-CCATGTAGTTGGAGAACCAAAGGC-3' | chr11:118309754+118309845 |
| h*MLL1* reverse_IV | 5'-CAACTCACATTTAAGCACCAACTCC-3' | |
| h*HELLS* forward_I | 5'-TAACTATCCTGTGAGATTGGGCGAGG-3' | chr10:96304154+96304293 |
| h*HELLS* reverse_I | 5'-ATTAGCCTGGAATGGGCTAATGTCCG-3' | |
| h*HELLS* forward_II | 5'-GGCGCCTTGCAAAGTATTAACAGC-3' | chr10:96305252+96305370 |
| h*HELLS* reverse_II | 5'-TAACTATCCTGTGAGATTGGGCGAGG-3' | |
| h*HELLS* forward_III | 5'-GGGAGAAAGGCTGTTTCTTGTTGG-3' | chr10:96306052+96306164 |

| | | |
|---|---|---|
| h*HELLS* reverse_III | 5'-AGTTGTTCAACCATTGCTGGAGCC-3' | |
| h*HELLS* forward_IV | 5'-TTGGGTGCCACAGTTGGTAAATGG-3' | chr10:96307516+96307632 |
| h*HELLS* reverse_IV | 5'-ACGGAAGGAGTATTACTGGAGTGG-3' | |
| h*ASH2* forward_I | 5'-TAGAAGCAAGTCACTGAGTCCAGC-3' | chr8:37960686+37960777 |
| h*ASH2* reverse_I | 5'-GATTACAGGAGTGAGCCATCATGC-3' | |
| h*ASH2* forward_II | 5'-ACCAGCTACTGTTGATGACTTCCC-3' | chr8:37962357+37962438 |
| h*ASH2* reverse_II | 5'-ATGTAGACAAGTTTGGTGCCCAGC-3' | |
| h*ASH2* forward_III | 5'-AAGCTGCAGGAGTATGAAGTTCGG-3' | chr8:37963787+37963923 |
| h*ASH2* reverse_III | 5'-ACCGCTTACATCGACCAAGTTTGC-3' | |
| h*ASH2* forward_IV | 5'-AATGGCAGGATCACAGCTTTCTGC-3' | chr8:37965508+37965626 |
| h*ASH2* reverse_IV | 5'-ATAAAGGAAAGCTGGGTGTGGTGG-3' | |
| h*MYC* forward | 5'-GCGCCCATTAATACCCTTCTTTCC-3' | chr8:128747818+128747989 |
| h*MYC* reverse | 5'-ATAAATCATCGCAGGCGGAACAGC-3' | |
| h*ACTIN* forward | 5'-TGCAGAAAGTGCAAAGAACACGGC-3' | chr7:5568420+5568576 |
| h*ACTIN* reverse | 5'-TGTGGGTGTAGGTACTAACACTGG-3' | |